Service through Science

DETERMINATION OF THERMODYNAMIC PROPERTIES OF AEROZINE-50

Final Report

by

JOSEPH P. COPELAND
JOHN A. SIMMONS

for

MANNED SPACECRAFT CENTER
NATIONAL AERONAUTICS AND SPACE ADMINISTRATION

Contract No.NAS9-6720

Atlantic Research Corporation
A Division of The Susquehanna Corporation
Shirley Highway at Edsall Road
Alexandria, Virginia, 22314

May 8, 1968

ATLANTIC RESEARCH

NASA CR 92463

DETERMINATION OF THERMODYNAMIC PROPERTIES OF AEROZINE-50

Final Report

by

JOSEPH P. COPELAND
JOHN A. SIMMONS

for

MANNED SPACECRAFT CENTER
NATIONAL AERONAUTICS AND SPACE ADMINISTRATION

Contract No.NAS9-6720

Atlantic Research Corporation
A Division of The Susquehanna Corporation
Shirley Highway at Edsall Road
Alexandria, Virginia, 22314

May 8, 1968

This report was prepared by the Atlantic Research Corporation a Division of The Susquehanna Corporation, under Contract No. NAS9-6720, entitled "Determination of Thermodynamic Properties of Aerozine-50", for the NASA Manned Spacecraft Center. The work was administered under the technical direction of the Auxiliary Propulsion and Pyrotechnics Branch with Mr. Julian Jones serving as technical monitor.

TABLE OF CONTENTS

TABLE OF CONTENTS (Continued)

LIST OF FIGURES

LIST OF FIGURES (Continued)

LIST OF TABLES

1.0 SUMMARY

This report describes the results of a program to determine the thermodynamic properties of the propellant, Aerozine-50 (assumed to be a 1:1 mixture of hydrazine and UDMH*) and presents charts and tables showing the corresponding values of enthalpy, entropy, phase composition, pressure, temperature and specific volume. Properties at pressures of 0.001 to 60 psia and at temperatures of -100 to 250°F were of primary interest.

The first phase of the program included:(1) a survey and evaluation of pertinent data reported in the literature, (2) selection of the most appropriate methods of correlating the data and calculating values of the thermodynamic properties, (3) determination of what data is lacking or unreliable, and must be measured, (4) delineation of the experiments and techniques to accomplish this, and (5) selection of the most appropriate means to present the derived thermodynamic properties. Phase II of this program consisted of the final design and construction of the required experimental apparatus, the performance of the measurements, correlation of the data and preparation of the charts and tables.

The establishment of the thermodynamic properties required several kinds of data. These included P-V-T data for the components, hydrazine and UDMH, and their mixtures, activity coefficients for the liquid phase, heats of phase transition, composition variations for phase transitions and thermodynamic functions for the components in the ideal gas state. Some of these data had been reported for Aerozine-50 in the literature, but all are not reliable.

From the results of the survey and analysis of the literature data it was apparent that additional data had to be measured in order to verify or correct suspect values and to obtain missing values. The types of data needed were the P-V-T properties of mixtures of UDMH and hydrazine vapors, P-T-x-y data for liquid-vapor phase equilibria, the vapor pressure of the

* Unsymmetrical dimethylhydrazine

freezing and eutectic mixtures, and the densities of liquid Aerozine-50 and hydrazine-rich mixtures. In order to minimize the number of measurements required for this, empirical and analytical correlations were selected to provide an accurate means of interpolation and extrapolation of data. These included the Redlich-Kwong equation of state (for P-V-T data) and a two constant correlation of solution activity coefficients which had the form of the van Laar equation.

Before assembly of the apparatus to obtain the needed experimental data, a series of tests were performed to determine the stability of hydrazine and UDMH in the presence of selected materials at high temperatures. The results indicated that decomposition would be negligible at temperatures up to 250°F in an apparatus constructed of the following materials:

304, 316 and 416 stainless steel,
Pyrex glass,
TFE-Teflon,
and 6061-T6 aluminum.

Apparatus for determining the P-V-T properties, the vapor pressure of the pure components, and liquid-vapor equilibria was a well-stirred, constant-volume pressure cell. Provision was made for withdrawing samples of the liquid for subsequent determination of composition by gas chromatography. Pressure was measured by a carefully calibrated diaphragm-type transducer. Temperature control was accomplished by immersing the cell in a constant temperature bath.

Pure samples of UDMH and hydrazine for the experiments were obtained by fractional distillation, at reduced pressure, of the commercially available materials.

The P-V-T experiments were performed at 242°F and at pressures up to about 2.5 atmospheres for various values of vapor composition. Analysis of the resulting data indicated that Wilson's modification of the Redlich-Kwong equation of state was adequate for UDMH-hydrazine vapor mixtures at temperatures up to 250°F and for pressures up to 3.0 atmospheres.

Measurements of the vapor pressure of pure components were made at various temperatures within the range from about 75° to 242°F. The data for both species were correlated by expressions of the form of the Clausius-Clapeyron equation.

Liquid-vapor equilibria were measured at temperatures of approximately 100°, 175° and 242°F. The temperature and pressure of the contents of the test cell and the composition of the equilibrium liquid phases were measured directly. The compositions of the equilibrium vapor phases were calculated from the resulting P-x data by means of the Gibbs-Duhem equation.

Densities of the pure liquids and their mixtures were determined pycnometrically at various temperatures. The data for the pure components agreed with correlations reported in the literature. The data for the mixtures agreed, to within 2 per cent, with values calculated from an ideal solution model.

The P-x-y data, the equation of state for the vapor, and the density correlations were used to calculate values of the activity coefficients for the components in solution. Next, the coefficients were correlated as functions of composition by means of the van Laar-type relationship, and in turn, the constants of these equations were expressed as functions of temperature by means of polynomials.

A pressure-temperature diagram for Aerozine-50 was constructed from data for the various phase boundaries, which were calculated from existing and newly obtained phase equilibria data, vapor pressure data for the pure components and equations of state for the vapor and condensed phases.

Calculated values of enthalpy and entropy for the boundaries and within the various two-phase regions of the phase diagram were tabulated as functions of temperature, pressure, and composition. In addition, skeletal temperature-entropy and pressure-enthalpy diagrams were prepared.

2.0 INTRODUCTION

The thermodynamic properties of Aerozine-50 are of major importance to research, development and design efforts concerning its use as a propellant or hydraulic working-fluid in space propulsion systems. Recent studies[2] have shown that upon exposure to a low-pressure environment, Aerozine-50 can undergo rapid evaporative cooling, and both composition and phase changes, including freezing. When used as a fuel in a rocket engine these phenomena can, in turn, produce severe and even extremely dangerous ignition irregularities, such as delayed and explosive ignition. Other studies[24] have demonstrated that Aerozine-50, when used as a hydraulic fluid for the actuation of propellant valves, can freeze upon leaking or intentional venting into a vacuum and thereby often cause severe malfunctions of the valve. Understanding these and other problems and predicting their extent requires knowledge of the thermodynamic properties of Aerozine-50.

On December 27, 1966, a program was undertaken to obtain the needed data and to prepare tables and charts of the desired thermodynamic properties, which would have sufficient accuracy for most engineering calculations. The program was divided into two phases. The purposes of the first phase were: (1) to accumulate and evaluate data, reported in the literature, for the thermal and physical properties of the pure components, hydrazine and UDMH*, and their mixtures; (2) to decide what remaining data needed to be determined by experiment; (3) to select appropriate techniques for correlating the various data in order to minimize the amount of experimentation. The second phase involved the needed experimentation, fitting the data to appropriate equations of state and other correlations, and finally, calculation and presentation of the properties derived from the data.

For the purposes of this work, Aerozine-50 was considered to be a 1:1 mixture of hydrazine and UDMH. The standard propellant grade of this

*Unsymmetrical dimethylhydrazine

material consists of 51.0±8 per cent hydrazine, 47.0 per cent (min) UDMH and 1.8 per cent (max) water. The range of properties considered were for pressures from 0.001 to 60 psia and for temperatures from -100° to 250°F.

This report summarizes the results of this program. The correlation of experimental data and techniques for calculating the thermodynamic properties from the data are described in Section 3.0. The portion of the data required for these calculations which have been reported in the literature together with the requirements for additional data are discussed in Section 4.0. The experimental apparatus and procedures used to obtain the missing data are described in Section 5.0. The analysis, correlation, and evaluation of the experimental data are presented in Section 6.0. The tables of computed properties and skeletal thermodynamic diagrams are discussed in Section 7.0. Recommendations for additional experimental and analytic work are made in Section 8.0.

3.0 PHASE DIAGRAM AND THERMODYNAMIC COMPUTATIONS

In this section, the phase diagram (P-T) for the system Aerozine-50 is described qualitatively. Then for each region of the diagram the basic equations and correlations which are appropriate for treating the thermophysical properties of hydrazine-UDMH mixtures are discussed.

3.1 PHASE DIAGRAM FOR AEROZINE-50

Figure 3-1 is a schematic pressure-temperature diagram for the system Aerozine-50. (Figure 7-1 is a quantitative, partial P-T diagram based on the data to be presented in subsequent sections.) The diagram consists of six single- or multi-phase regions. The condensed phases are separated from the vapor phase by a two-phase region bounded by bubble-point and dew-point curves. The reason for this is that a two-component system generally does not vaporize congruently. Thus, vapor in equilibrium (at the bubble point) with liquid Aerozine-50 does not have the same composition as the liquid, but will have a higher concentration of the more volatile component, UDMH. Similarly, the liquid in equilibrium (at the dew point) with vapor of Aerozine-50 composition is richer in the less volatile component, hydrazine. In between the bubble-point and dew-point curves, the liquid phase has compositions progressing from Aerozine-50 to that in equilibrium with gaseous Aerozine-50. An analogous statement holds for the compositions of the vapor.

At high temperatures and pressures the bubble-point and dew-point curves bend over towards each other and meet, forming a loop. The top of this loop corresponds to, or replaces, the critical point of one-component systems. However, the maximum temperature and maximum pressure for the existence of distinct vapor and liquid phases occur at separate points, the plait point and contact point, respectively. Analogous to the condition at the critical point of a single-component system, the enthalpy of vaporization (heat of vaporization) at the contact point is zero.

Aerozine-50 does not have a true triple point at which congruent freezing occurs. Instead a "quadruple point" (QP) and two "pseudo-triple-points" (PTP) exist. Following the vapor-pressure curve from PTP-I to QP, by

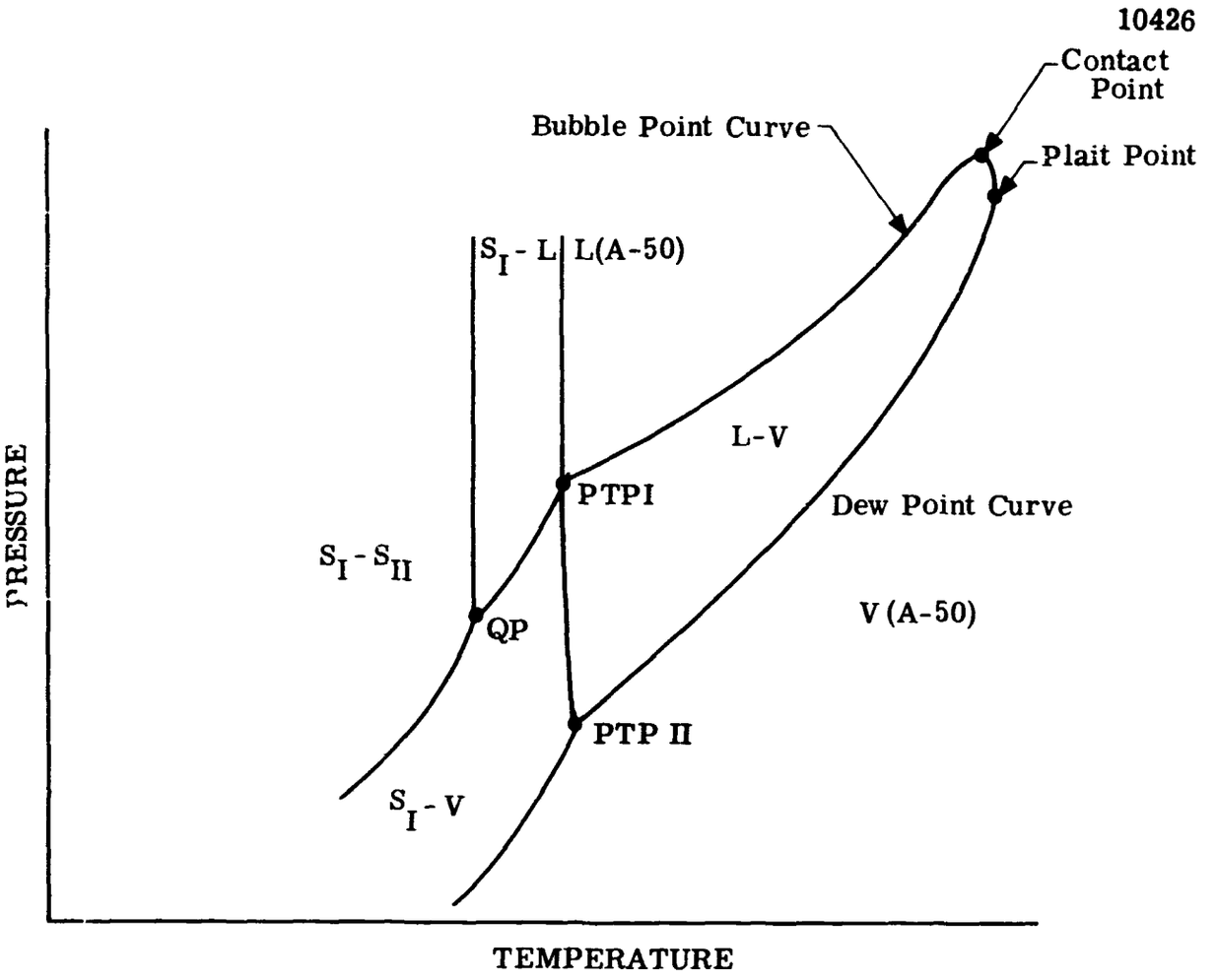

Key:

V - Vapor

L - Liquid

S_I - Solid Hydrazine

S_{II} - Eutectic (approximately 97% UDMH)

PTPI - Pseudo Triple Point I

PTPII - Pseudo Triple Point II

QP - Quadriple Point

Figure 3.1. Schematic Pressure - Temperature Diagram of the System Aerozine-50.

simultaneously lowering the temperature and pressure of the mixture, S_I (hydrazine) freezes as the liquid becomes enriched in UDMH. When QP is reached the liquid has the eutectic composition at which it freezes congruently.

3.2 CORRELATIONS AND THERMODYNAMIC COMPUTATIONS

3.2.1 Vapor Region

Wilson's modification[18] of the Redlich-Kwong equation of state has been shown to be well suited for correlating P-V-T data of the vapor phase (see Section 6.3). This equation is (see Table 3.1, page 3-4, for nomenclature):

$$\frac{PV}{RT} = \frac{V}{V-b} - f\left(\frac{T_c}{T},\omega\right)\frac{b}{V+b} \quad . \tag{3.1}$$

The constant, b, is independent of temperature and is evaluated from the composition of the vapor mixture and the critical properties of the pure components. Application to Aerozine-50 yields:

$$b_{mix} = 0.0865\ R\left[\left(\frac{yT_c}{P_c}\right)_h + \left(\frac{yT_c}{P_c}\right)_u\right] \tag{3.2}$$

The coefficient, $f\left(\frac{T_c}{T},\omega\right)$, is dependent on temperature and Pitzer's acentric factor[19], ω, defined as follows:

$$\omega_i \equiv \log P'_{Ri} - 1.000,$$

where P'_{Ri} is the reduced vapor pressure of the component at a reduced temperature of 0.7. For a mixture, f_{mix} is the molar average of the values for the pure components, which for a mixture of hydrazine and UDMH is

$$f_{mix} = y_h\, f\left(\frac{T_c}{T},\omega\right)_h + y_u\, f\left(\frac{T_c}{T},\omega\right)_u \quad . \tag{3.3}$$

For a pure component, f_i can be computed from the relation:

$$f\left(\frac{T_c}{T},\omega\right)_i = 4.934\ \left[1 + (1.57 + 1.62\omega_i)\left(\frac{T_{ci}}{T} - 1\right)\right] \quad . \tag{3.4}$$

TABLE 3.1

NOMENCLATURE

f	-	Fugacity, psia
G	-	Free energy, BTU/lb-mole
H_T	-	Enthalpy, Btu/lb-mole
H_T^{id}	-	Ideal gas enthalphy, Btu/lb-mole
P	-	Pressure, psia
P_c	-	Critical pressure, psia
P'	-	Vapor pressure, psia
R	-	Universal gas constant, 1.987 Btu/lb-mole °F
S_T	-	Entropy, Btu/lb-mole °F
S_T^{id}	-	Ideal gas entropy, Btu/lb-mole °F
T	-	Temperature, °F
T_c	-	Critical temperature, °F
y	-	Vapor composition, mole fraction
x	-	Liquid composition, mole fraction
V	-	Molar volume, cu. ft./mole
γ	-	Activity coefficient, defined by equation (3-15)

NOMENCLATURE (Continued)

Superscripts

id	-	ideal vapor
bar ($\bar{}$)		indicates partial molar quantity
L	-	liquid phase
V	-	vapor phase
'	-	vapor pressure
E	-	excess property of mixing

Superscripts

h	-	hydrazine
u	-	unsymmetrical dimethylhydrazine (UDMH)
H	-	enthalpy function
S	-	entropy function
s	-	solid phase

Enthalpy and entropy of the vapor phase of Aerozine-50 may be computed from the relations,

$$H_T = H_T^{id} + f_H(T,P) = H_T^{id} + PV - RT\int_{\infty}^{V}\left[P - T\left(\frac{\partial P}{\partial T}\right)_V\right]_T dV, \qquad (3.5)$$

and

$$S_T = S_T^{id} + f_S(T,P) = S_T^{id} + \int_0^P \left[\frac{R}{P} + \frac{\partial P}{\partial T}_V\right]_T dV, \qquad (3.6)$$

where the integrals are to be evaluated using the equation of state. (See Appendix C). The quantities, H_T^{id} and S_T^{id}, are the enthalpy and entropy of the ideal gas, respectively, for the vapor mixture and are calculated from the corresponding values for the pure components using the relationship,

$$H_T^{id} = y_h H_{T,h}^{id} + y_u H_{T,u}^{id} \quad , \qquad (3.7)$$

and

$$S_T^{id} = y_h (S_T^{id} - R \ln y)_h + y_u (S_T^{id} - R \ln y)_u. \qquad (3.8)$$

3.2.2 Liquid-Vapor Region

The calculation of enthalpy and entropy values in the liquid-vapor region (Figure 3.1) is a two-part process, since two phases exist in equilibrium. The thermodynamic properties for the vapor phase may be evaluated by the method discussed in the previous section, since the concentration dependency of the constants of the equation of state may be computed.

The thermodynamic properties of the equilibrium liquid phase may be evaluated from the partial properties by the relations:

$$H_{mix} = x_h \bar{H}_h + x_u \bar{H}_u, \qquad (3.9)$$

and

$$S_{mix} = x_h \overline{S}_h + x_u \overline{S}_u \ . \tag{3.10}$$

For a component in solution, the partial molal enthalpy and entropy are given by the equations:

$$\overline{H}_i = H^{id}(T)_i + f_{Hi}(T,P) - \Delta H_{vi} - \left(\Delta H_{mix}\right)_i \tag{3.11}$$

and

$$\overline{S}_i = S^{id}(T)_i + f_{Si}(T,P) - \frac{\Delta H_{vi}}{T} + \left(\Delta S_{mix}\right)_i \ , \tag{3.12}$$

respectively. The second terms in each of these equations are defined by equations (3.5) and (3.6), but, in this case, they apply to the pure components. The third terms are the enthalpy and entropy of vaporization of the pure components, and the fourth terms are the enthalpy and entropy of mixing.

Enthalpy and entropy of mixing are readily evaluated from composition and pressure measurements if the liquid phase is a regular solution. (Justification for this assumption is derived from the experimental data in Section 6.4). In this case the enthalpy of mixing for a component in solution is equal to the excess partial free energy and is given by the relation:

$$\left(\Delta H_{mix}\right)_i = RT \ln \gamma_i \ , \tag{3.13}$$

where γ_i is the activity coefficient of the component in solution. The entropy of mixing for a regular solution is the corresponding ideal solution value:

$$\left(\Delta S_{mix}\right)_i = -R \ln x_i \tag{3.14}$$

The activity coefficient for a component in solution may be defined:

$$\gamma_i^L = \frac{\hat{f}_i^V}{x_i f_i} \tag{3.15}$$

where $\hat{f}_i$ is the fugacity of the component in solution, and f_i is the fugacity of the pure component in the standard state (pure component at the pressure and temperature of the solution and in the same phase). For the case of an ideal vapor, equation 3.15 becomes:

$$\gamma_i^L = \frac{y_i P}{x_i P_i'} \tag{3.16}$$

Relationships for calculating values of γ_i^L from phase equilibria data together with the equation of state are derived in Appendix B.

The values of the activity coefficients thus obtained may be correlated as functions of temperature and composition to permit interpolation and extrapolation of the experimental data. A common technique for deriving such correlations is to assume one of the following functions for relating the excess free energy of mixing to the liquid composition at constant temperature:

$$\frac{\Delta G^E}{x_1 x_2 RT} = B+C(2x_1-1) + D(2x_1-1)^2 + \ldots \tag{3.17}$$

or

$$\frac{x_1 x_2 RT}{\Delta G^E} = B+C(2x_1-1) + D(2x_1-1)^2 + \ldots \tag{3.18}$$

Values of the quantities on the left hand sides of these relationships may be calculated from experimental γ-x data by use of the following equation for the binary mixture:

$$\frac{\Delta G^E}{RTx_1x_2} = \frac{x_1 \ln\gamma_1}{x_2} + \frac{x_2 \ln\gamma_2}{x_1} \quad . \tag{3.19}$$

As discussed in section 6, equation(3.18)proved to be the more convenient form for correlating the data obtained in this work, and that equation may be reduced to a linear equation in x_1, i.e.,

$$\frac{x_1x_2RT}{\Delta G^E} = B + C(2x_1 - 1) \tag{3.20}$$

Then the following relationships for ln γ_1 and ln $\gamma 2$ may be derived (see Section 6):

$$\ln \gamma_1 = \frac{x_2^2 \; I}{(Sx_1 + I)^2} \tag{3.21}$$

$$\ln \gamma_2 = \frac{x_1^2 \; (S + I)}{(Sx_1 + I)^2} \tag{3.22}$$

where S and I are temperature dependent only. (By rearranging these equations, it can be shown that they are equivalent in form to the famous van Laar equations). The coefficients S and I are functions of temperature alone, which may be determined empirically.

The results of this procedure are expressions for the activity coefficients as functions of temperature and composition. With these, the vapor compositions along the bubble point curve (liquid composition Aerozine-50) may be calculated directly. For the dew point curve, (vapor composition Aerozine-50) these expressions are used in an iterative procedure to compute the composition of the liquid.

3.2.3 Liquid Region

Activity coefficients for the components in liquid Aerozine-50 may be computed by the technique just described. Since the composition of

the liquid is invariant throughout this region, only the temperature dependency need be considered. The calculation of enthalpy and entropy may be accomplished by using equations (3.9) through (3.12).

3.2.4 Solid-Vapor Region

Within the solid-vapor region, the composition of the equilibrium vapor phase (if assumed ideal) may be computed from the total pressure and the vapor pressure of solid hydrazine according to:

$$y_u = 1 - P/P_h' \tag{3.23}$$

where y_u is the mole fraction of UDMH in the vapor and $P_{h,s}'$ is the vapor pressure of solid hydrazine. At the solid-vapor, vapor boundary, the vapor composition is that of Aerozine-50 (0.348 mole per cent UDMH and 0.652 mole per cent hydrazine). Substituting these data into equation (3.23) and rearranging yields the formula,

$$P = P_{h,s}'/0.652. \tag{3.24}$$

Therefore the dew point curve for this region can be calculated from the data for the vapor pressure of solid hydrazine, alone.

The pressure variation along the curves connecting points QP and PTPI and points PTPI and PTPII, in Figure 3.1, may be computed from the relationship.

$$P = \gamma_h P_h' x_h + \gamma_u P_u' x_u, \tag{3.25}$$

where γ_u and γ_h are given by equations (3.21) and (3.22), respectively. The required values of x_u and x_h had been determined previously (Section 4.2).

The curve extending downward and to the left of QP, in Figure 3.1, represents the sum of the vapor pressures of hydrazine (SI) and the eutectic (SII). Since the latter is 94 mole per cent UDMH, pressure variation along the curve is very nearly identical with the sum of the vapor pressures

of solid hydrazine and solid UDMH, i.e.,

$$P = P'_{u,s} + P'_{h,s} \tag{3.26}$$

The values for enthalpy and entropy of the vapor in this region may be computed by the techniques described in Section 3.1.1. The enthalpy and entropy of solid hydrazine may be calculated by means of similar formulas:

$$H_{h,s} = H_T^{id} - \Delta H_{sub,h} , \tag{3.27}$$

and

$$S_{h,s} = S_T^{id} - \frac{\Delta H_{sub,h}}{T} - R \ln P'_{h,s} , \tag{3.28}$$

where, again, the vapor is assumed to be ideal because of the low pressures involved.

3.2.5 Solid-Liquid

The solid phase in this region is hydrazine. Because of the low pressures being considered, the composition of the liquid phase may be assumed to depend on temperature alone. Thus the compositions within this region are defined by the compositions and their corresponding temperatures along the curve QP-PTPI. The enthalpy and entropy of the liquid phase may be computed from equations (3.9) through (3.12) according to the techniques discussed in Section 3.1.2. The corresponding values for the solid phase may be computed from equations (3.27) and (3.28).

3.2.6 Solid Region

Equation (3.26) establishes the boundary between this region and the solid-vapor region. Assuming that the solid phase is a 50-50 mixture by weight, then the enthalpy and entropy of the solid per unit mass of mixture may be calculated as follows:

$$H_s = .348 H_{u,s} + .652\ H_{h,s} \tag{3.29}$$

$$S_s = .348\ S_{u,s} + .652\ S_{h,s} \tag{3.30}$$

The values of $H_{h,s}$ and $S_{h,s}$ are calculated by means of equations (3.27) and (3.28), respectively. Equations of similar form may be used to calculate values of $H_{u,s}$ and $S_{u,s}$.

4.0 FUNDAMENTAL DATA

This section contains a discussion of the fundamental data which were required to construct the desired charts and tables. These constitute the data necessary for the application of the theory, correlations and calculational techniques discussed in Section 3.0. This section also presents a review and evaluation of such data that was available from the Literature. Further gaps and insufficiencies are identified which had to be filled by the acquisition, experimentally, of additional data.

4.1 DATA REQUIRED

The data required for the derivation of the values for the several properties, including enthalpy, entropy, density, pressure and phase composition, are as follows. In the vapor region, V(A-50) in Figure 3-1, P-V-T data to establish an equation of state for Aerozine-50 vapor and the ideal properties of the pure components are required.

For the liquid vapor region, L-V, the data required include:(1) the latent heats of vaporization and vapor pressure of the pure components, and (2) the heat of mixing, density, vapor pressure and composition of the equilibrium phases for the mixtures. As discussed in Section 3.2.2 the latter properties, except for phase densities, are related to the activity coefficients, which may be calculated from suitable, but limited vapor-liquid phase composition measurements in this region. In order to perform these calculations as well as to compute the enthalpy and entropy of the various compositions, P-V-T data for vapor mixtures other than Aerozine-50 are required.

Similar data are required for the solid-vapor region, S-V. However, in this case, property data are also required for the solid phases of the pure components. These include the heats of sublimation and fusion, density and vapor pressure.

In the condensed phase region, L(A-50), S_I-L and S_I-S_{II}, it may be assumed that the properties are independent of pressure over the range of interest (pressures less than 5 atm). Accordingly, the properties, enthalpy,

entropy, density and composition, are functions of temperature alone, and furthermore the values for these properties at the boundaries with the vapor regions are identical to the values within the interior of the condensed phase regions. Thus no additional data beyond that for the L-V and S-V regions are required.

The data for the latent heat of vaporization and sublimation must include the temperature variation. Generally this variation is not available, directly, but may be derived from the heat capacities of the condensed and vapor phases. This is the case for hydrazine and UDMH, and consequently the heat capacity of these materials constitute additional data that is required.

The data required for the construction of the desired charts and tables are summarized in Table 4.1.

4.2 EVALUATION OF DATA AVAILABLE

In general, all measurements of properties of hydrazine or UDMH made at high temperatures were suspect since both of these compounds are known to undergo spontaneous, thermal decomposition[1,3,4,5,6]. At lower temperatures, hydrazine is known to be susceptible to heterogeneous or catalyzed decomposition, particularly in the presence of certain metals (including mercury)[15,16]. Even silica will initiate decomposition at certain pressures and temperatures[1,17]. These phenomena are discussed further in Section 5.2.

In addition, the purity of the samples used in obtaining the measurements has an influence on the accuracy of the data. In some cases, there was little or no information given about the chemical purity or the preparation of the samples used.

In addition to the data required for the computations, Table 4.1 also summarizes the data which were available from previous work. These data are discussed in the following paragraphs. Table 4.2 lists the specific data which were used in the computations.

TABLE 4.1

Data Required for Calculation of
Thermodynamic Properties

Phase Region	Data Required	Data Available
Vapor	P-V-T, ideal-gas enthalpy and entropy.	Ideal-gas enthalpy and entropy.
Liquid-Vapor	Latent heat of vaporization, heat capacity and vapor pressure of pure components; density, P-V-T and activity coefficients for mixtures.	Latent heats of vaporization, heat capacity and vapor pressure (some) of pure components; density (some) and activity coefficients (some) for mixtures.
Solid-Vapor	Latent heats of fusion and sublimation, heat capacity and vapor pressure of the pure components (solid); composition, vapor pressure, density of the eutectic; activity coefficients and compositions of the freezing liquid mixtures.	Latent heats of fusion and sublimation, heat capacity and vapor pressure of the pure components (solid); compositions of the freezing liquid mixtures.
Condensed, Liquid, Solid-Liquid and Solid.	No additional data required for these regions.	

TABLE 4.2

Summary of Literature Data and Correlations
Used for Calculation of Thermodynamic Properties

Property	Value or Correlation	
	Hydrazine	UDMH
Molecular Weight	32.05	60.08
Critical Temperature (°K)	653	523
Critical Pressure (atm.)	145	53.6
Heat of Vaporization (Kcal/g-mole @ 25°C)	10.7	8.366
Heat of Fusion (Kcal/g-mole)	3.025 @ 274.69°K	2.407 @ 215.95°K
Ideal gas entropy (e.u. @ 25°C, 1 atm.)	56.97	72.30
Ideal gas heat capacity (cal/g-mole-°K)	$C_p^{id} = 3.750+3.134\times10^{-2}T - 1.395\times10^{-5}T^2$	$C_p^{id} = -.5791+9.334\times10^{-2}T - 5.129\times10^{5}T^2$
Heat capacity of liquid (cal/g-mole-°K)	$C_p^{L} = 22.79 - 9.458\times10^{-3}T + 4.113\times10^{-5}T^2$	$C_p^{L} = 28.88 + 3.536 \times 10^{-2}T - 2.421\times10^{-6}T^2$
Heat capacity of solid (cal/g-mole-°K)	$C_p^{S} = 3.955 + 4.080\times10^{-2}T + 1.992\times10^{-6}T^2$	$C_p^{S} = 13.09 - 1.585\times10^{-2}T + 2.742 \times 10^{-4}T^2$
Liquid density (g/cc @ t°C)	$\rho = 1.026-8.3406 \times 10^{-4}t - 1.2122\times10^{-6}t^2 + 3.1171 \times 10^{-9}t^3$	$\rho = 0.814 - 1.011 \times 10^{-3}t$

4.2.1 Pure Components

4.2.1.1 Unsymmetrical Dimethylhydrazine

Aston et al[8] have reported a value of the ideal-gas entropy of UDMH at 298.16°K equal to 72.82 ± 0.20 e.u, which was calculated from calorimetric data, and a value of 70.70 e. u. for the trans form and 72.30 e.u. for the gauche form, which were calculated from spectroscopic and molecular structure data. The authors stated that since the trans form has a higher energy than the gauche form, the trans form exists in negligible quantities at room temperature. Therefore, the agreement between the values of entropy calculated from the two sets of data is very good.

The same authors reported an experimental value of 8366 ± 16 cal./mole for the latent heat of vaporization of UDMH at 298.16°K based on calorimetric data and a value of 8353 cal./mole based on vapor pressure data. These agree within about 0.2%. Data for the heat capacity of solid and liquid UDMH were reported in the temperature range from 13° to 287°K. An experimental value of 2407.4 ± 1.50 cal./mole was reported for the heat of fusion at the triple point, 215.951 ± .005°K.

The vapor pressure of UDMH has been measured by Aston in the temperature range from 237° to 287.16°K,by Pannetier and Mignotte[10] in the range from + 35° to +65°C, and by Chang and Gokcen[9] in the range from -25°C to +35°C.

The data reported by Aston and coworkers (ideal-gas entropy, heat of vaporization, solid and liquid heat capacity, and vapor pressure) appear to be reliable. From the variation of triple-point temperature with the fraction of sample melted, the solid-insoluble, liquid-soluble impurity was computed to be only 0.01 mole per cent. Also, since the measurements were made at or below room temperature, the UDMH probably did not decompose thermally to a significant degree. There is a slight possibility that heterogenous or catalyzed decomposition did occur, however. The calorimeter and the resistance thermometer used for obtaining the data, from which the heat capacities were calculated, were made of platinum, and the vapor pressures were measured with a mercury

manometer. Both of these metals are known to catalyze the decomposition of hydrazine, and they similarly may cause decomposition of UDMH.

In general, the vapor pressure data in the range of -25°C to +35°C reported by Chang and Gokcen are higher than those reported by Aston and those for low temperatures reported by Pannetier and Mignotte, but are lower at higher temperatures. (Chang and Gokcen made this comparison by extrapolating each of the three sets of data to cover the temperature range from -25° to +75°C.) The reason given for differences in the three sets of data is that the test samples employed by Chang and Gokcen were of higher, initial chemical purity. However, they state that the UDMH vapor in their samples may have decomposed because of the presence of the mercury in their manometers.

Lawrence[25] has reported data for the vapor pressure in the range from 25°C up to the critical point (250°C, 53.5 atm), liquid density in the range from -65° to 245°C, and calculated values of the molar heat capacity of the ideal vapor in the temperature range from -23° to 227°C. The data for the critical constants, vapor densities, and for vapor pressures above one atmosphere and at the higher temperatures are suspect, since these measurements were made in an apparatus which used mercury (a material which reacts with UDMH) as a confining fluid. The data for the density of the liquid phase should be reasonably good, even though the same apparatus was used, because the concentration of decomposition products in the liquid phase is generally negligible.

4.2.1.2 Hydrazine

Scott et al[7] have reported experimental data for the heat capacity of solid and liquid hydrazine in the temperature range from 12° to 340°K, the vapor pressure for the solid at 0°C and for the liquid in the range from 0°C to 145°C, and the heat of fusion, 3025 cal./mole. The latent heat of vaporization, 10,700 ± 75 cal./mole, was calculated from the vapor pressure data. The ideal-gas entropy at 298.16°K and 1 atmosphere pressure calculated from the calorimetric data is 56.97 ± 0.30 e.u. The value of entropy calculated from spectroscopic and molecular structure data is 54.41 e.u.

Free energy, enthalpy, heat capacity, and entropy values were calculated from the spectral and structural data in the temperature range from 298° to 1500°K.

From a study of the melting point as a function of the fraction melted, these authors estimated that their samples used for the calorimetric measurements were 99.75 mole per cent hydrazine and that the major impurity was water. They estimate the maximum uncertainty of the values of heat capacity to be 0.3%, resulting primarily from the presence of water in the samples.

The small amount of water in the samples had a more significant effect on the vapor pressure measurements. The authors purified their hydrazine samples further by vacuum distillation, retaining the first 20% to boil over for vapor pressure measurements. They compared their measurements with those reported by Hieber and Woerner[23]. The latter data were consistently lower, and the conclusion was that the hydrazine samples used by Hieber and Woerner contained more water.

Chang and Gokcen reported experimental measurements of vapor pressure over the temperature range from 3° to 52°C. Their data are somewhat higher than those reported by Scott et al and Hieber and Woerner in this temperature interval. They suggested that their data are the most accurate, because they believed that their test samples were more pure than those used by the other investigators. The data of Pannetier and Mignotte, obtained over the range from about 84° to 133°C, were extrapolated to cover the temperature range in which Chang and Gokcen made their measurements. The extrapolated values were lower, and Chang and Gokcen attribute this fact to the possibility that the samples used by Pannetier and Mignotte contained a significant amount of water.

4.2.2 Mixtures

A considerable amount of the data for hydrazine-UDMH mixtures, which are needed to compute the properties of Aerozine-50, are missing or are controversial. The latter applies especially to previous measurements of phase equilibria.

Chang and Gokcen[9] studied the liquid-vapor phase equilibria for

mixtures of UDMH and hydrazine in the temperature range from 0° to 20°C. The compositions of the co-existing phases were determined from measurements of the refractive index of samples of the liquid and condensed samples of the vapor. In a separate set of experiments, the vapor pressures over liquid mixtures of known composition were measured with a mercury manometer.

Pannetier and Mignotte[10] reported isobaric data for liquid-vapor phase equilibria of mixtures in the pressure range from 250 to 760 mm. Phase compositions were determined from measurements of refractive index. The temperature range corresponding to these data was approximately 35° to 112°C.

Chang and Gokcen made a graphical comparison of their pressure-composition data obtained at 20°C and a set of data which they obtained by extrapolating the data of Pannetier and Mignotte to a temperature of 20°C. There was considerable deviation between the two sets of data.

However, both sets of data were shown to be thermodynamically inconsistent by means of a criterion derived from the Gibbs-Duhem equation by Scatchard and Raymond[11]. In this test, the dew point pressure is calculated from the measured compositions of the equilibrium phases and is compared to the measured pressures. The calculation is made assuming ideal vapor behavior and negligible molar volume of the liquid compared to that of the vapor. These assumptions are reasonable because of the low pressures involved. Since the test applies to data obtained at constant temperatures, the isobaric data was converted to isothermal form by cross-plotting. There are several possible explanations for the inconsistency of these data. The test samples used by the investigators may have decomposed due to catalysis or chemical reaction with the confining vessel or with mercury in the manometers. The samples may have undergone spontaneous, thermal decomposition particularly in the high temperature region in which Pannetier and Mignotte made their measurements.

Another set of P-x-y vapor-liquid equilibria data have been reported by Liberto[14], without reference to the source or to the experimental conditions under which it was obtained.

The temperatures and compositions of the condensed phases along the

curves PTP-II to PTP-I and PTP-I to QP (see Figure 3.1) have been determined[12,14]. The data reported by McMillan[13] are probably the most reliable, because these investigators prepared their test mixtures from very pure hydrazine and UDMH. They report a eutectic at 94 mole per cent UDMH which melted at 124°K (point QP, Figure 3.1.). On the other hand, no measurements of the vapor pressure of the compositions along the curves PTP-II to PTP-I and PTP-I to QP have been reported.

Data for the density of propellant-grade Aerozine-50 liquid have been reported by Aerojet[12] for the temperature range from 0° to 160°F. Since these data are averages for various liquid mixtures containing amounts of impurities within the limits of use specifications, they exhibit considerable scatter.

4.3 NEEDED EXPERIMENTAL MEASUREMENTS

The overall objective of this program was to provide a set of consistent data for the thermophysical properties of Aerozine-50, which would have sufficient accuracy for most engineering calculations. From the foregoing discussion, it is apparent that the existing thermal data, including ideal-gas enthalpy and entropy, condensed phase heat capacities, and heats of vaporization and fusion, are adequate for this purpose.

Thus sufficient data exist to compute the properties of the vapor phase, V(A-50), if ideal gas behavior or the adequacy of the equation of state, (3.1), may be assumed. However, sufficiently reliable data evidently are not available to define the properties of the two-phase and the condensed phase regions, including their boundaries. Crucial for this are accurate vapor-liquid data necessary to develop correlation of the liquid phase activity coefficients which, as shown in Sections 3.2.4, 3.2.3 and 3.2.5 are used to help define the thermophysical properties in these regions.

Accordingly, a program of experimental measurements was planned and executed. These measurements consisted of (1) the vapor pressure of the pure components, especially at the higher temperatures, for the purpose of checking existing data, (2) the liquid-vapor equilibria, (3) the density of

liquid mixtures for the purpose of checking existing data and providing additional data needed to derive the values of the activity coefficients, and (4) P-V-T-y data for the purpose of verifying the adequacy of the proposed equation of state.

Table 4.3 lists these experimental measurements and the range of values for the variables considered. The procedures and results of the experiments are discussed in the following two sections.

TABLE 4.3 - Experimental Measurements

Region	Measurement	Range of Adjusted Variables
Mixtures:		
Vapor	P vs V,T,y	T: 242°F y: 0.5, 0.4, 0.2 weight-fraction, nominal V: Adjusted to obtain pressures from 0.1 to 2.5 atm.
Liquid	density vs t, x	T: 40° to 200°F x: 0.2, 0.4, and 0.5 weight-fraction UDMH, nominal
Liquid-vapor	P vs x, T	T: 100, 175 and 242°F. x: 0.05, to 0.5 weight-fraction UDMH, nominal
Pure Components:		
Liquid-vapor	P vs T	T: 80 to 242°F.

5.0 EXPERIMENTAL INVESTIGATION

The experimental apparatus and procedures employed to obtain the additional data discussed in Section 4.3 are discussed in the following subsections.

5.1 PURIFICATION OF COMPONENTS

As indicated in section 4.0, the components must be quite pure in order to obtain meaningful data. Consequently, the vacuum distillation apparatus shown in Figure 5-1 was constructed for the purpose of purifying the hydrazine and UDMH used in all of the experiments.

In operation, the system was purged with ultra-pure nitrogen, and then the pressure was lowered enough to draw a charge into the boiler through the filling line. A trap to collect the product was immersed in a bath whose temperature was slightly higher than the freezing point of the product. A "light-ends" trap was immersed in a liquid nitrogen bath and accordingly only the permanent gases left the system through the vacuum pump.

To perform the distillation, the boiler was immersed in a warm water bath and the pressure of the system was lowered until boiling occurred. During the distillation, the temperature of the warm water bath and the cold bath were carefully maintained to minimize the need for regulating pressure.

Gas-chromatographic analyses indicated that a single distillation produced a significant reduction in the concentration of impurities, including water and amines. Also, as discussed in section 5.4.1, measurements of the vapor pressure of the distillates indicated that further distillation was not required.

5.2 DECOMPOSITION STUDIES

As indicated in Section 4.0, both hydrazine and UDMH are susceptible to homogeneous and heterogeneous decomposition. Therefore, a series of three decomposition tests were performed for the purpose of determining the compatibility of the following selected materials of construction with liquid and vapor Aerozine-50: (1) 304 stainless-steel; (2) 316 stainless-steel; (3) 416 stainless-steel;

13752

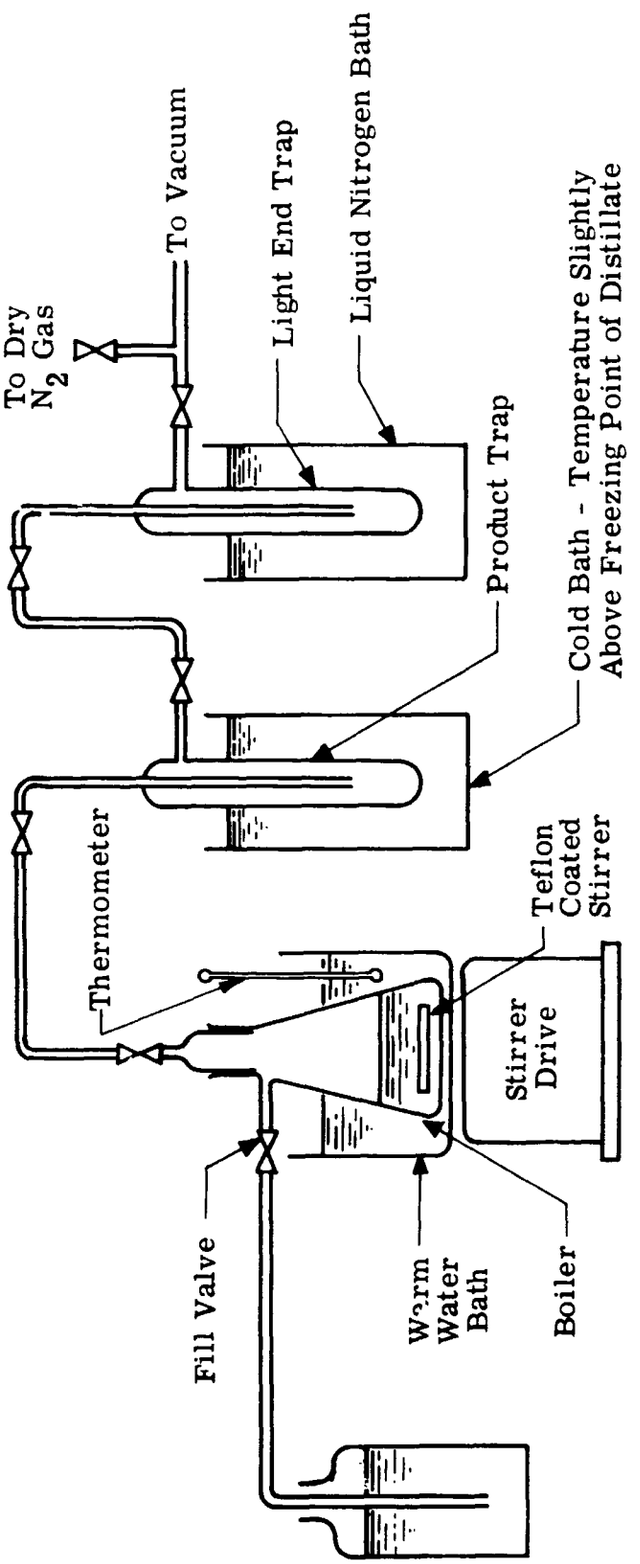

Figure 5.1. Vacuum Distillation Apparatus for Purifying Hydrazine and UDMH.

(4) Pyrex glass; (5) TFE-Teflon; (6) 6061-T6 aluminum.

Two significant results of these tests were: (1) decomposition causes a negligible alteration in the chemical composition of the liquid phase, but it causes a significant deviation of the vapor pressure; (2) all of the materials tested are compatible with purified mixtures of UDMH and hydrazine (liquid and vapor) at temperatures up to 240°F, provided that all surfaces exposed to the mixtures are thoroughly cleaned and then soaked in a mixture of the liquids for approximately 48 hours.

On the basis of these results, it was concluded that the proposed P-V-T and liquid-vapor equilibria experiments were feasible if performed in an apparatus constructed from the materials listed above.

The apparatus for performing the compatibility experiments is shown in Figure 5.2. It consisted of a stainless steel pressure vessel (30 cc volume) that was outfitted with a fill line for charging the vessel with the test liquid and a pressure tap which connected the vapor space of the vessel to a pressure sensor. To perform a test, the evacuated vessel, containing samples of the candidate materials of construction, was charged with approximately 15 cc of a liquid mixture of hydrazine and UDMH. The contents of the vessel then were heated to a predetermined temperature by means of an electrical heating mantle which was wrapped around the vessel. The temperature, measured by a thermocouple affixed to the outer wall of the vessel, was maintained at the desired level for periods of two to seven hours. At the end of the heating period, the mantle was removed, and the vessel and its contents were allowed to cool to room temperature. The temperature and pressure of the vessel were recorded at regular time intervals before, during and after the heating period.

For the first two series of tests, the mixtures were prepared by mixing equal volumes of unpurified, commercially available liquids. The pressure in the vessel was measured with a Bourdon-tube gage. During both tests, the vessel was heated to 300°F and was maintained at that temperature for over two hours. The pressure at room temperature (80°F) was significantly

13764

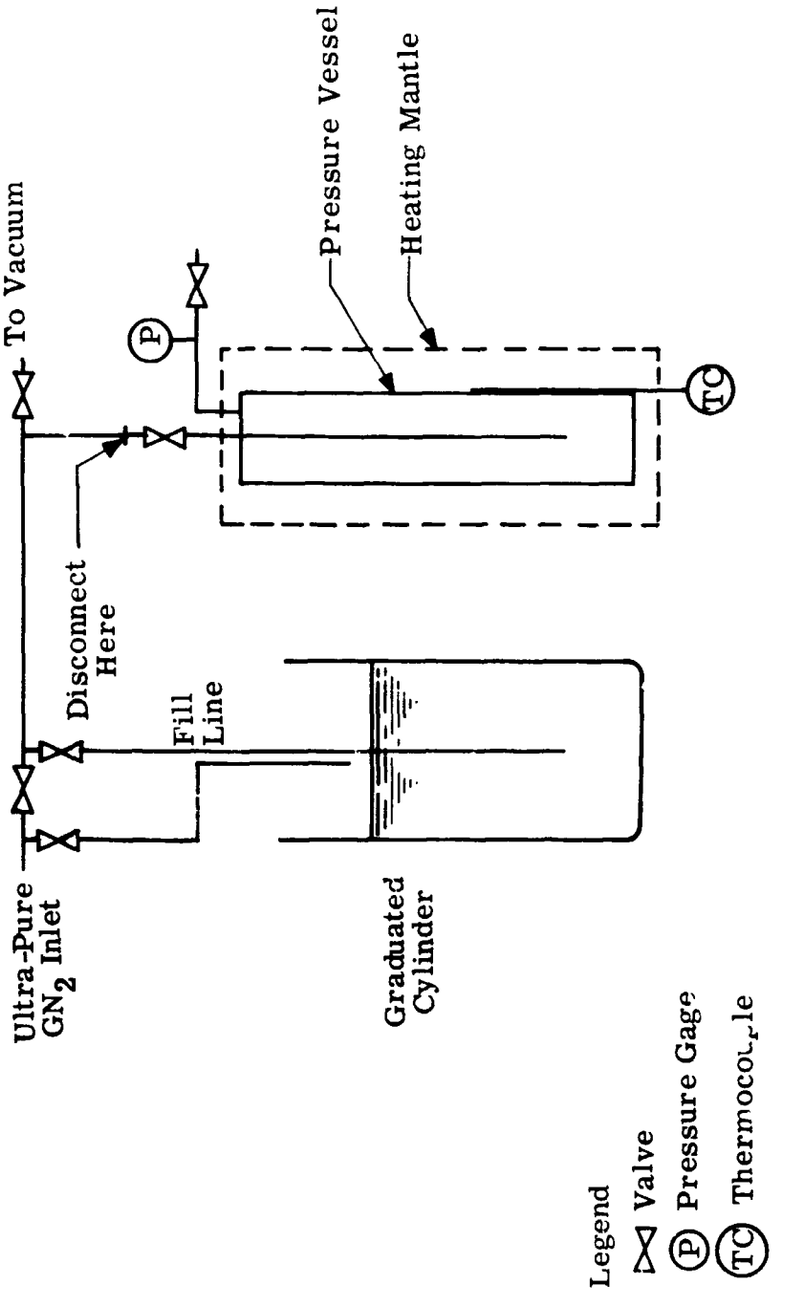

Figure 5.2. Apparatus for Compatibility Determinations.

higher after the heating period than before. Gas-chromatographic analysis of samples of the liquid used for the first test indicated that there were significant increases in the relative amounts of some of the impurities originally in the liquid before it was heated, but the absolute increases were quite small. No new chemical species were detected after the heating process.

The results of these tests indicated that decomposition causes a negligible change in the chemical composition of the liquid phase, but it causes a significant change in the vapor pressure. Consequently, it was decided to use pressure measurements as an indication of the occurrence of decomposition during subsequent tests. Therefore, the Bourdon-tube pressure gage was replaced with a variable reluctance-type pressure transducer which had better pressure resolution.

There are several possible reasons for the occurrence of decomposition during these two tests. (1) The material sample, vessel, valves, etc. had not been exposed previously to the liquids. It is conceivable that the decomposition occurred heterogeneously, involving catalysis or reaction with the samples or vessel, or with contaminates adsorbed on the exposed surfaces. If this were true, then it might have been possible to passivate the surfaces by exposing them to hydrazine-UDMH mixtures for a long period of time. (2) The liquid mixture had not been purified; one of the impurities might have caused or accelerated the decomposition reactions. (3) Spontaneous, thermal decomposition occurred. In this case, there is no practical remedy.

For the third series of tests, procedures were modified slightly to eliminate, or at least to minimize, the suspected causes of decomposition. In order to passivate the materials, the vessel and samples were soaked for about two days in a freshly prepared liquid mixture and then dried thoroughly and stored in a pure nitrogen atmosphere. The liquid mixture (composition approximately that of Aerozine-50),used in these tests, was purified by a single distillation at a reduced pressure.

After introducing the samples and filling with the liquid mixture, the vessel was allowed to stand at room temperature for seven hours. The

pressure in the vessel was virtually constant for the entire period. Then the heating mantle was installed, and the vessel was heated to 127°F. The pressure increased at first, and then it became constant. The temperature was maintained at 127°F for two hours after the pressure had reached a nearly stationary value. Then the vessel was allowed to cool to room temperature, and the equilibrium pressure was recorded. This value agreed closely with the value at room temperature prior to the heating period, which indicates that significant reaction had not occurred during the test.

The vessel was then heated to 201°F and was maintained at this temperature for about two hours after the pressure had reached a constant value. As before, the vessel was cooled to room temperature, and the equilibrium pressure was recorded. Again there was no significant difference between the values obtained before and after heating the liquid.

Finally, the vessel was heated until the pressure became constant at about 45 psia, corresponding to a temperature of 240°F, and was maintained at this temperature for over three hours. Again, after the vessel had cooled to room temperature, the pressure agreed closely with the value prior to heating.

After this last test the liquid was transferred to a glass sample bottle that had been purged with nitrogen. The liquid was quite clear and exhibited no visible evidence of reaction. The material samples, valves, vessel, and transducer diaphragm were examined visually also. There was no apparent change in color or luster as a result of the last test.

5.3 LIQUID DENSITY MEASUREMENTS

A pycnometric technique was employed to measure liquid densities. The apparatus is shown in Figure 5.3. The procedure involved determining the weight of liquid required to fill a vessel of known volume at a particular temperature. Prior to performing the measurements, the volume of the vessel was measured by determining the weight of water it would contain at various temperatures within the range over which density measurements were to be made.

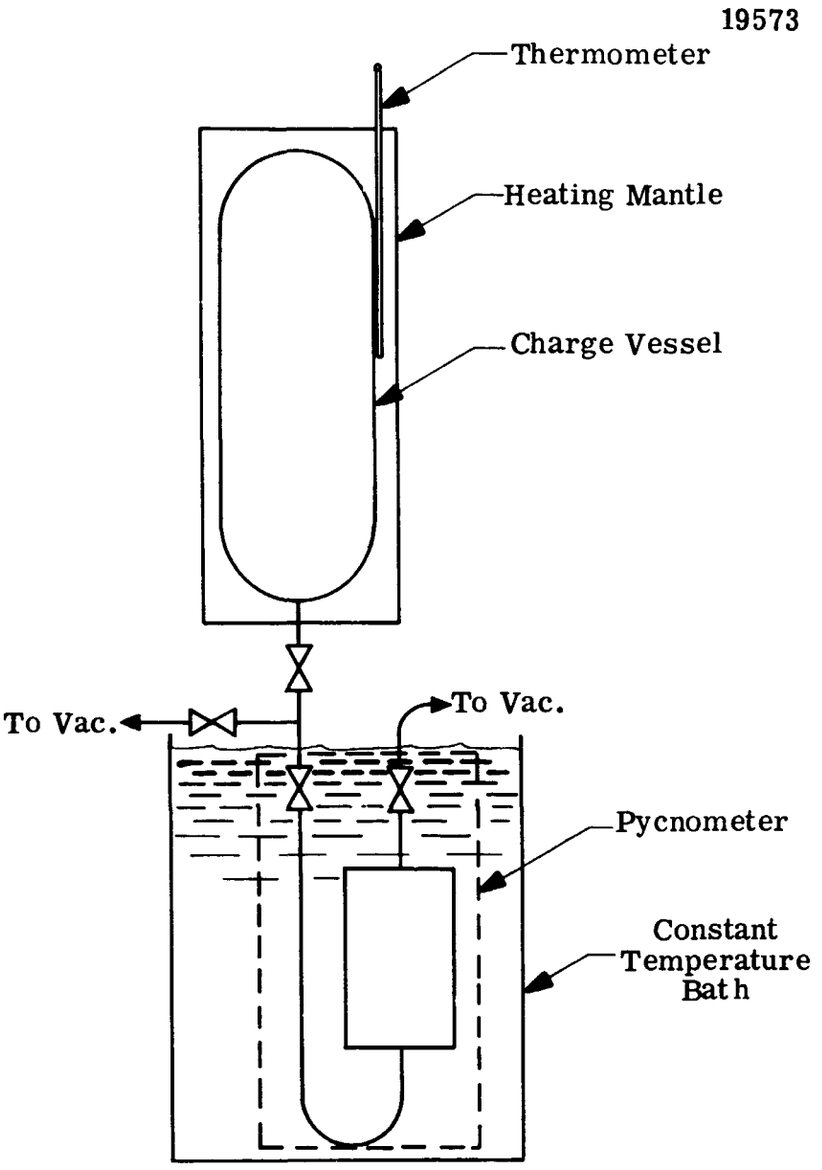

Figure 5.3. Apparatus for Determination of Liquid Density.

In order to assure that the pycnometer filled completely, it was evacuated prior to loading, and the charge vessel was heated to such a temperature that the system pressure was greater than one atmosphere and significantly higher than the vapor pressure of the liquid in the pycnometer. After filling, the pycnometer was soaked at bath temperature for several hours to allow for thermal equilibrium to be achieved. During this period, the fill line remained open, and the charge vessel was maintained at its higher temperature. After the soaking interval, the pycnometer inlet valve was closed, and the vessel was removed from the system, dried, and allowed to cool to room temperature. Then it was weighed on an analytic balance (±.5 milligram).

5.4 APPARATUS FOR P-V-T, LIQUID-VAPOR EQUILIBRIA AND PURE COMPONENT VAPOR PRESSURE MEASUREMENTS

The experiments to determine P-V-T properties and vapor-liquid equilibria were performed in an apparatus consisting of a constant volume cell, a constant temperature bath, and sample traps. The arrangement of these components, together with the associated instrumentation for the experiments, are shown in Figures 5.4 through 5.9.

The constant volume cell (Figures 5.8 and 5.9) was a thick-wall vessel constructed from 6061-T6 aluminum and had a Pyrex window at one end to permit visual observation of the phases present. In order to insure the establishment of equilibrium, the contents of the cell were stirred by a flat, magnetically driven paddle, which revolved about the horizontal (long) axis and swept the entire volume of the cell. The sampling valves were built into the walls of the cell in order to minimize the unstirred spaces between the interior of the cell and the valve seats.

The pressure of the contents of the cell was measured with a variable reluctance-type transducer which had a maximum resolution of about 0.057 torr. The transducer was mounted on the outer surface of the cell and was connected to the vapor space in the cell through a small-diameter port drilled through the wall.

The transducer was calibrated directly with standard pressure gages such as a McLeod-type vacuum gage, Bourdon-tube pressure gages, open-end U-tube

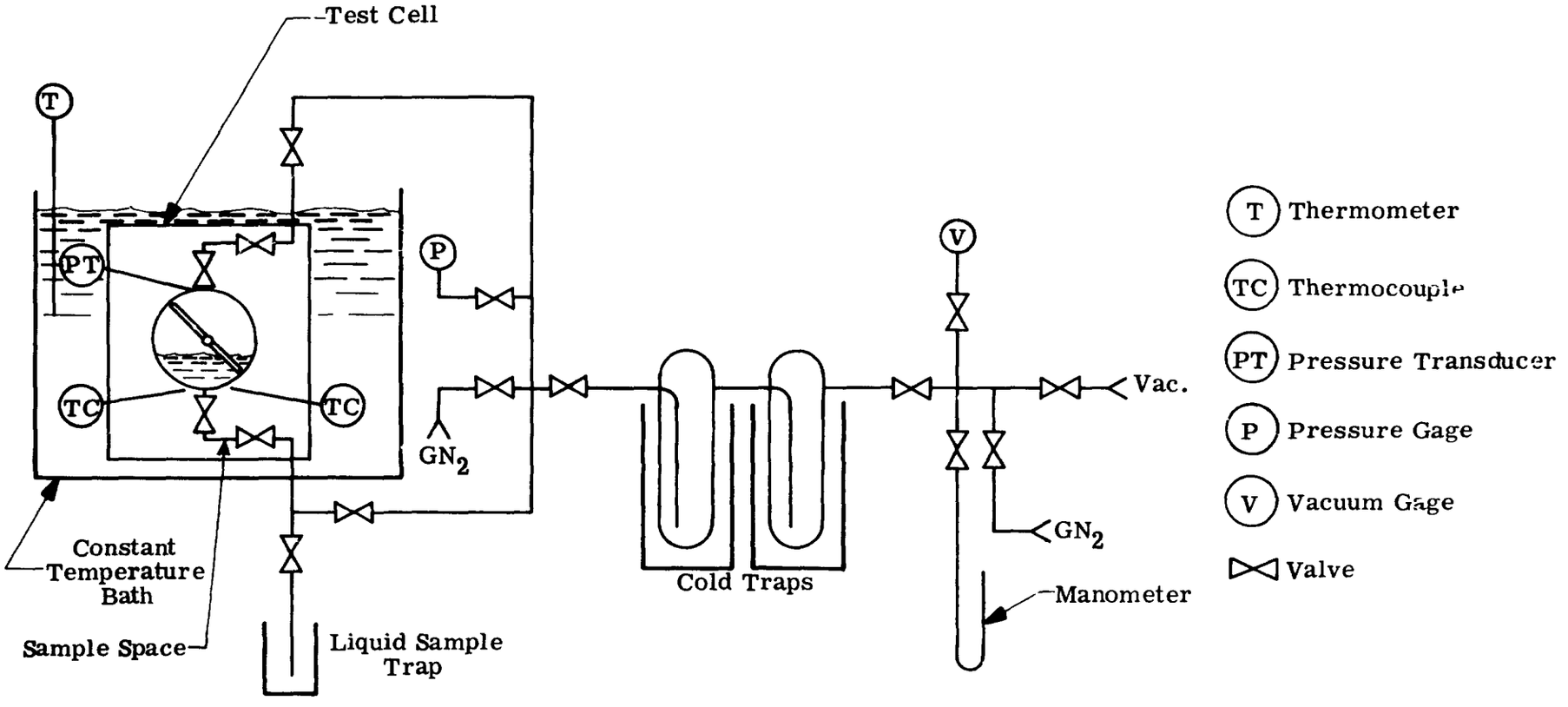

Figure 5.4. Schematic Diagram of the Apparatus for P-V-T and Equilibrium Experiments.

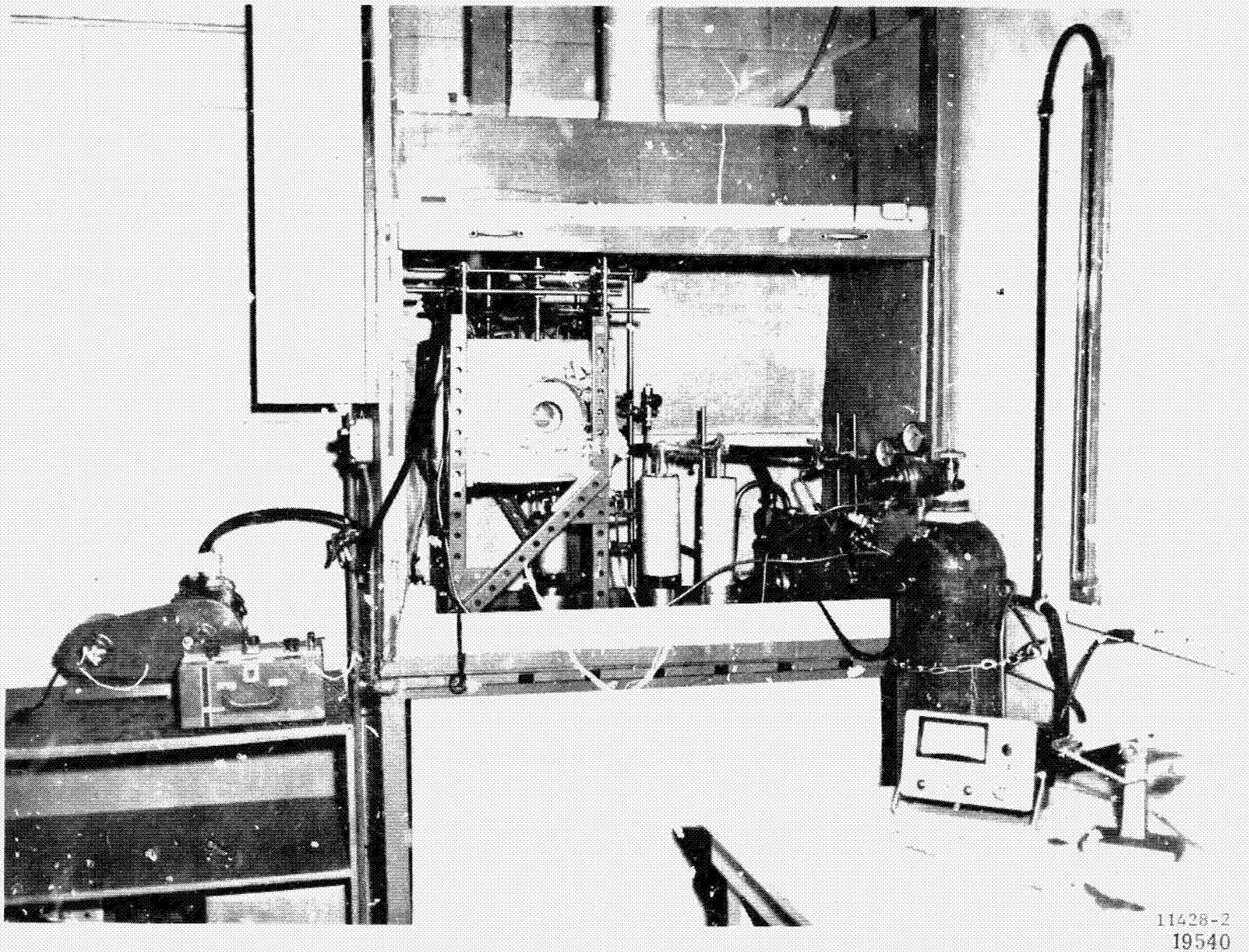

11428-2
19540

Figure 5.5. Overall View of Apparatus.

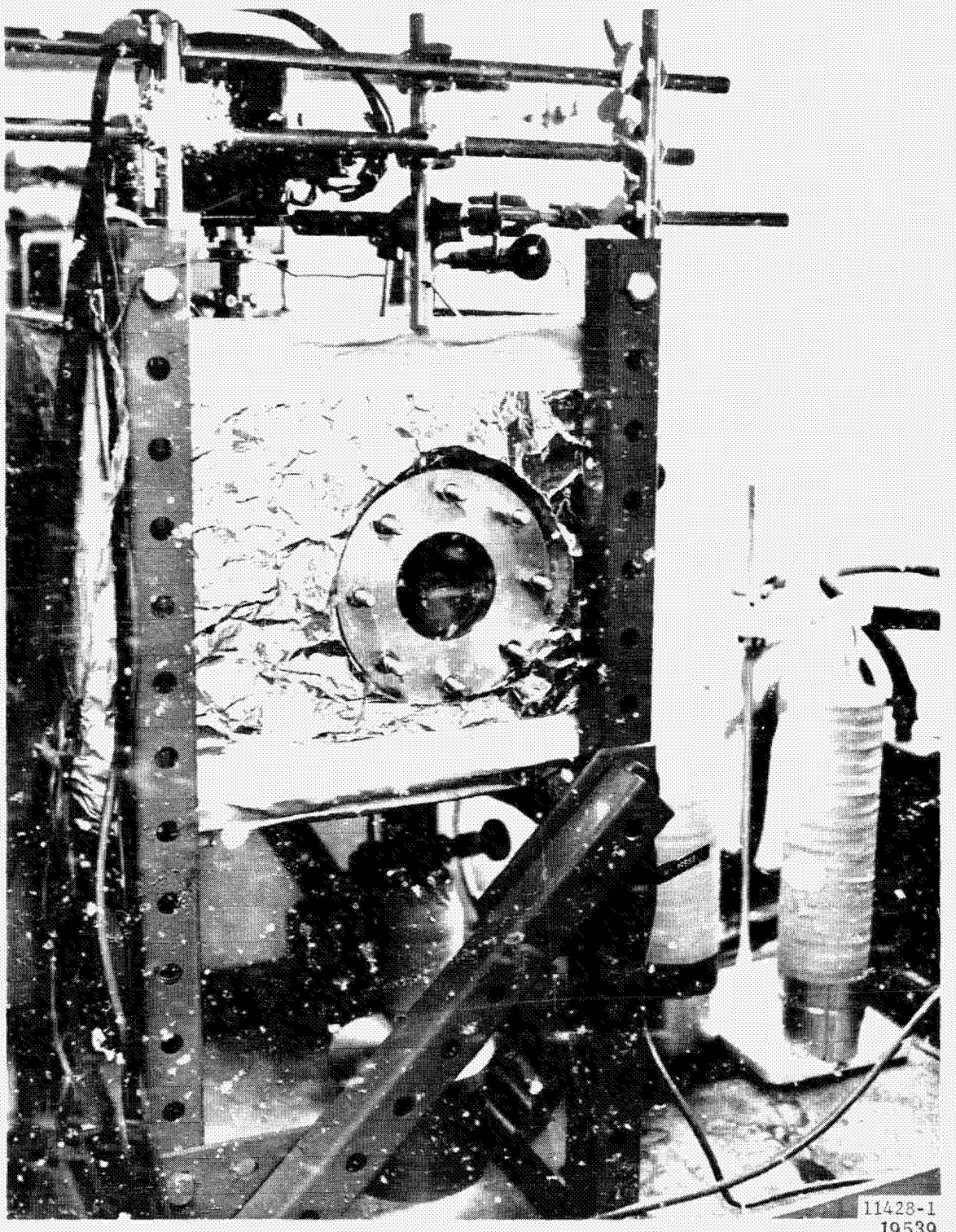

Figure 5-7. Constant Temperature Bath Containing Test Cell.

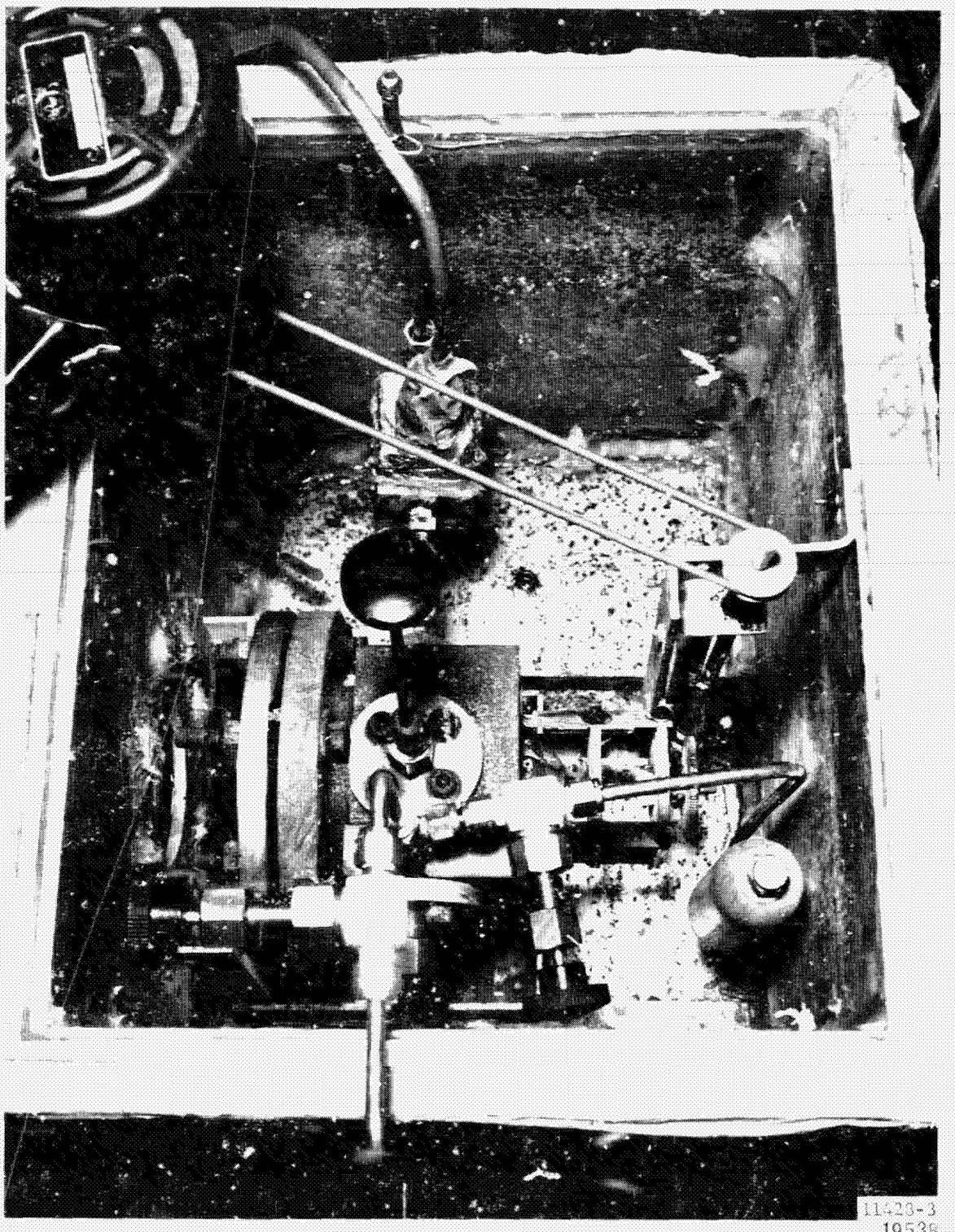

11423-3
19538

Figure .7. Arrangement of Components in Constant Temperature Bath.

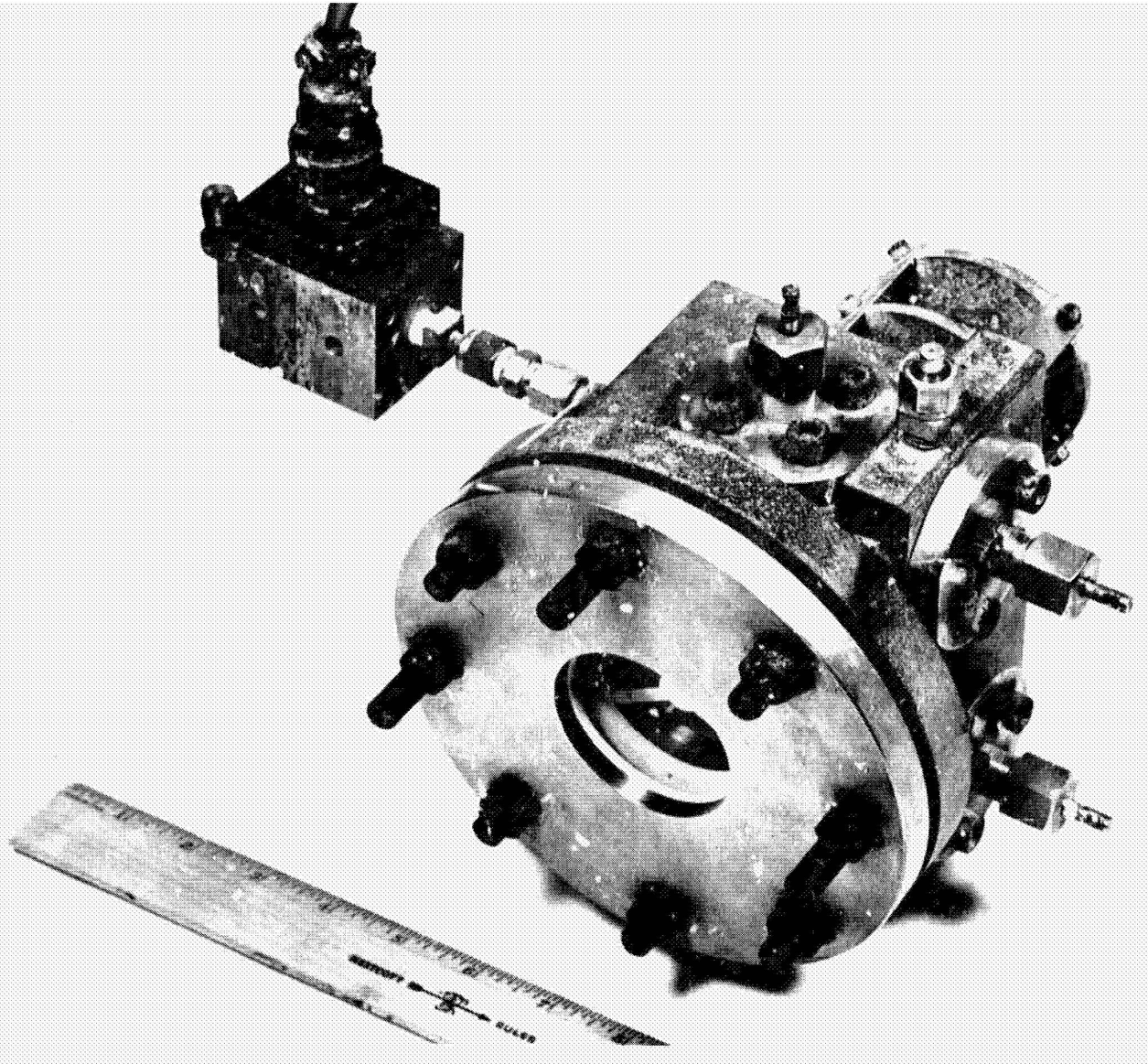

11428-7
19537

Figure 5.8. Test Cell.

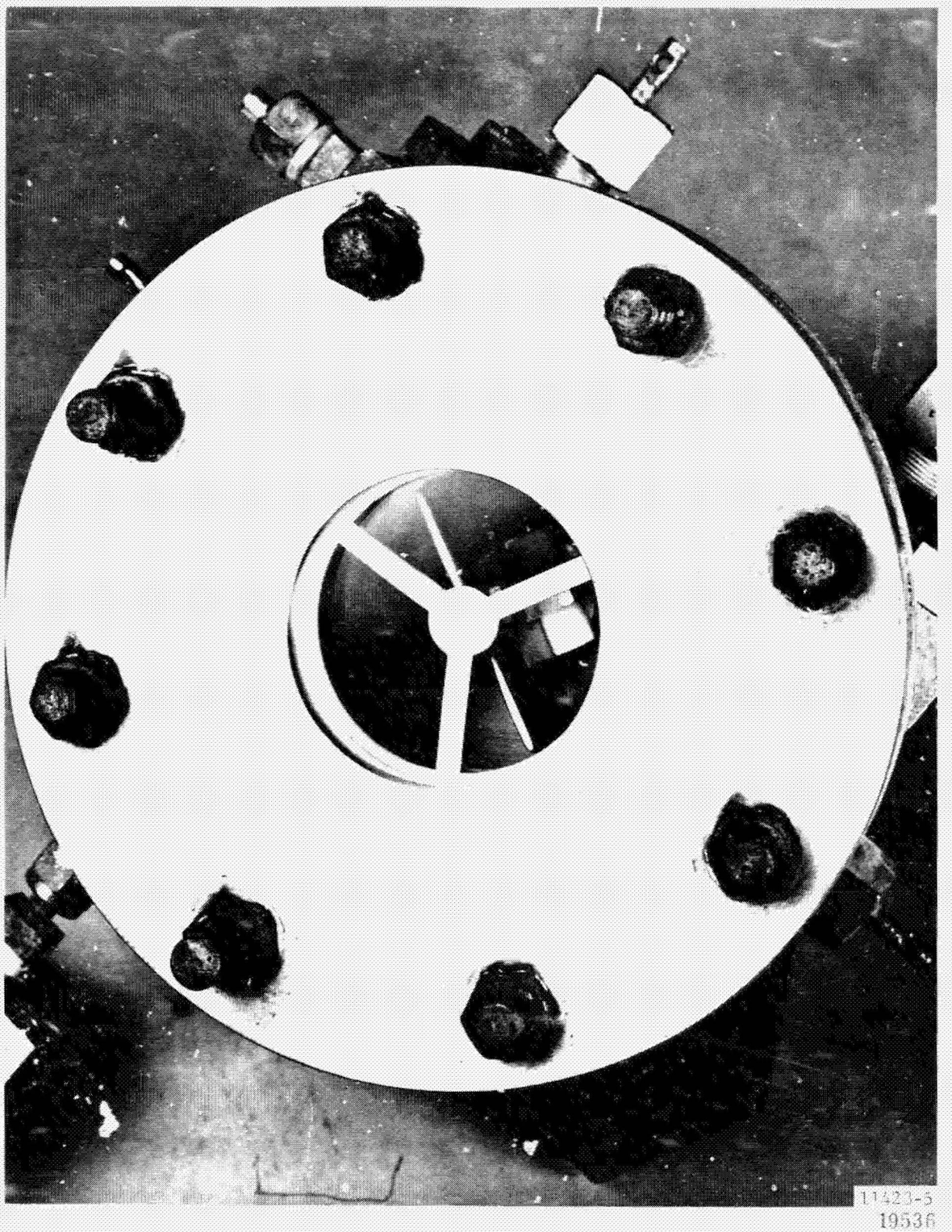

Figure 5.9. View of Test Cell Showing Magnetically Driven Paddle.

manometers, etc. Calibrations were performed both before and after each experiment.

The temperature of the cell was controlled by immersing it in a thermostated bath whose temperature was measured with standard thermometers. Two thermocouples, which were imbedded in the thickest portions of the wall of the cell, with their beads located very near the inner surface, were used to check the establishment of thermal equilibrium throughout the cell.

Considerable caution was exercised to prevent contamination or decomposition of the liquid samples from their contact with the apparatis. Prior to assembling the system, all surfaces which would be in contact with the samples were thoroughly cleaned. After assembly and leak testing, the system was evacuated and heated to induce outgassing. Then the test cell, sampling lines, etc. were passivated by filling with liquid A-50 and allowing to soak overnight.

After the bulk of the liquid was removed, the apparatus was vacuum dried. From this point on, the interior surfaces of the test cell and immediate connecting lines were exposed only to purified liquids and vapors, or to ultra-pure nitrogen. In cases where the removal or installation of components in the system was required during an experiment, the critical areas of the system were valved off, and then the fittings and connecting lines which might have been exposed to air were evacuated for a considerable length of time before the system valves were reopened.

5.5 PROCEDURES FOR VAPOR PRESSURE, P-V-T, AND LIQUID-VAPOR EQUILIBRIA EXPERIMENTS

5.5.1 Vapor Pressure of Pure Components

Approximately 50 cc of freshly distilled liquid was drawn into the evacuated cell. The bath temperature was adjusted to the desired value, the system was allowed to equilibrate, and the steady-state temperature and pressure were recorded. In order to test for the presence of significant amounts of liquid or vapor phase impurities, the pressure was determined again after a portion of the sample was boiled away by momentarily opening the vapor

space to the vacuum system. The values of vapor pressure obtained before and after the boil-off agreed closely for measurements with both liquid species, indicating that the purity of the distilled liquids were satisfactory for use in the P-V-T and liquid-vapor equilibria experiments.

5.5.2 P-V-T Experiments

Approximately one cc of liquid mixture of known composition was transferred into a small charge vessel that was subsequently attached to the upper sample port of the equilibrium cell. After the transducer had been calibrated, the cell and all connecting passages were evacuated. Then the lower sampling valves were closed and all upper valves were opened (cf. Figure 5.4.) The vessel containing the test sample was heated by means of an air gun, and the cell was kept at a relatively low temperature by adding ice to the bath medium. As a result, the sample distilled out of the charge vessel into the cell where it condensed.

After the transfer had been completed, the charge vessel was replaced by a larger vessel, of known volume, immersed in the bath fluid. This "expansion volume" and associated connecting lines were evacuated.

The bath was heated to the desired temperature and held at that level until the thermocouples imbedded in the cell wall and the pressure transducer indicated that equilibrium had been reached. The temperature and pressure of the cell were recorded. Next, the cell was opened to the expansion volume, and the cell pressure was recorded after equilibrium had been reached. Then the valves were closed, and the expansion volume was re-evacuated. By repeating this expansion process several times, data were obtained of the form: (cell pressure) vs (volume fraction of initial charge). As indicated in section 6, these data were used to calculate the constants of the equation of state.

The volume of the expansion vessel was determined by weighing the distilled water it would contain at a known temperature. The volume of the upper passages of the cell was calculated from the known dimensions of the ports, valve cavities, etc. These two volumes, the vessel and the cell

passages, constituted the expansion volume.

The volume of the test cell (confined by the two inner valves) was determined by pressurizing the cell with nitrogen, and then allowing this gas to expand into the initially evacuated expansion volume. Since the expansion volume, the temperature, and the pressure before and after the expansion process were known, the volume of the cell could be calculated.

5.5.3 Liquid-Vapor Equilibria

The expansion vessel used for the P-V-T experiments was partially filled with freshly distilled UDMH and then re-installed at the upper part of the test cell. About 30 cc of hydrazine was distilled into the evacuated cell through the lower sample port. The bath temperature was adjusted to the desired level, and the system was allowed to reach equilibrium. The temperature and pressure of the test cell were recorded. In order to assure that the system was free of non-condensibles, a small amount of the liquid was boiled away by momentarily opening the upper valves of the cell, and pumping away some of the vapors. The system was allowed to re-equilibrate, and again the pressure and temperature were recorded. This was repeated until reproducible values of pressure and temperature were obtained, but ordinarily only one boil-off was required. The final set of data served as a check on the pure component vapor pressure data obtained previously during a separate set of experiments (see Section 5.5.1.)

After the check for permanent gases had been completed, a sufficient quantity of UDMH was admitted to the cell through the upper port to raise the pressure to a pre-selected value. The system was allowed to equilibrate as indicated by a constant pressure reading. Again, some of the liquid was boiled off, this time to remove any gases that may have been dissolved in the UDMH. After equilibrium had been re-established, the bath temperature and cell pressure were recorded. A sample of the liquid phase was collected in the previously evacuated passage between the two lower sampling valves. The sample vessel was evacuated and then cooled with liquid nitrogen. The outer sampling valve was opened, and the sample was allowed to distill, totally,

into the vessel where it solidified. After the transfer was complete, the vessel was pressurized to one atmosphere with ultra-pure nitrogen gas, removed from the system, and then capped. The UDMH addition, partial boil-off, pressure measurement, and sampling were repeated several times at constant temperature until the vapor pressure of the liquid was that of Aerozine-50 (based on literature data). The samples of liquids were analyzed by means of gas chromatography.

6.0 ANALYSIS AND DISCUSSION OF DATA

6.1 DENSITY

The data for the density of liquid mixtures are presented graphically in Figure 6.1. The solid curves in this figure were calculated from density data for the pure components assuming that the solutions were ideal (volume change of mixing equals zero). The following formula for the density of a mixture was used:

$$\rho = \frac{1}{\frac{x_h}{\rho_h} + \frac{x_u}{\rho_u}} \tag{6.1}$$

For the pure component values, the following correlations of the literature data (checked by experiment) were used:

$$\rho_h = 1.026 - 8.3406 \times 10^{-4} t - 1.2122 \times 10^{-6} t^2 + 3.1171 \times 10^{-9} t^3, \tag{6.2}$$

and

$$\rho_u = 0.814 - 1.011 \times 10^{-3} t, \tag{6.3}$$

where t is temperature in °C.

The maximum deviation of the data from the theoretical curves is approximately 2%, which is nearly the limit of repeatability of the experimental measurements. This accuracy should be sufficient for most design calculations.

6.2 VAPOR PRESSURE OF PURE COMPONENTS

Figure 6.2 presents the data for the vapor pressure of hydrazine and UDMH. Both sets of data were fitted by the method of least squares to the simplified form of the integrated Clausius-Clapeyron equation. The resulting expressions are :

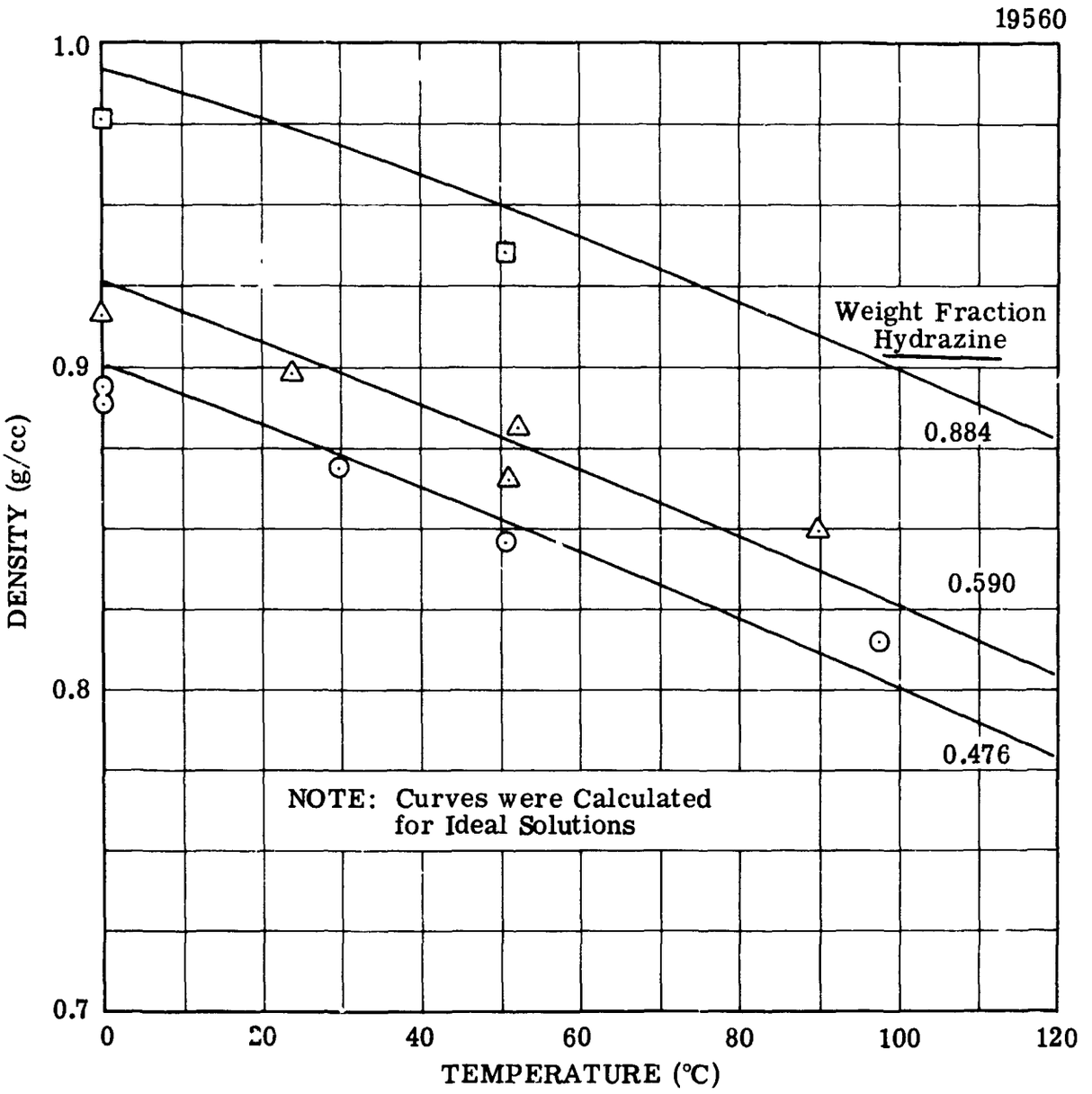

Figure 6.1. Data for Density of Liquids.

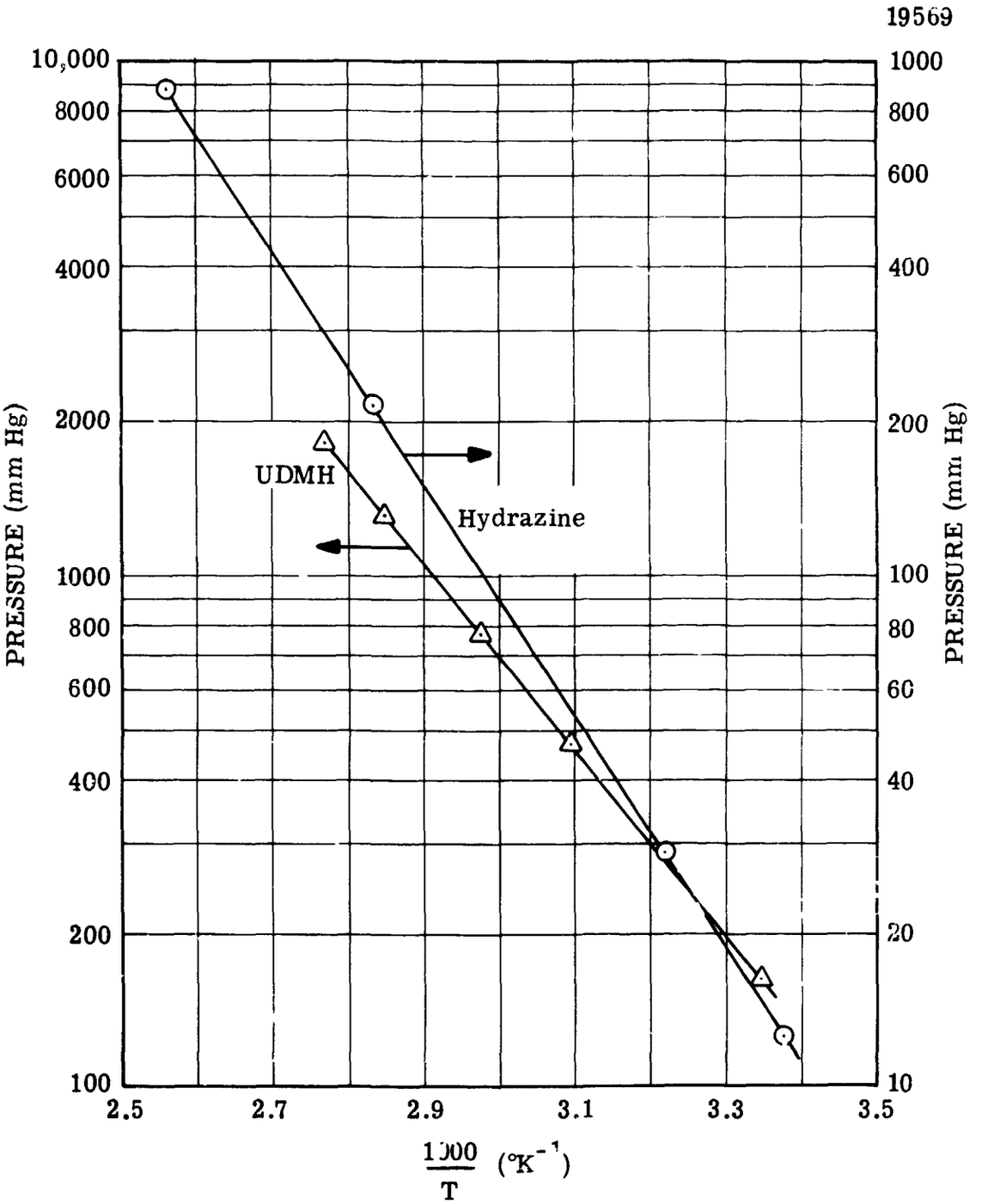

Figure 6.2. Vapor Pressure of Pure Components.

for hydrazine,

$$\log_{10} P_h' = 8.9288 - \frac{2320.2}{T} \; ; \qquad (6.4)$$

for UDMH,

$$\log_{10} P_u' = 8.2611 - \frac{1807.6}{T} \qquad (6.5)$$

Tables 6.1 and 6.2 compare the values of vapor pressure calculated from equations (6.4) and (6.5) with values calculated from correlating expressions given in the literature. For hydrazine, the data of Scott et al[7] are in closest agreement with the present work, and for UDMH, the data of Pannetier and Mignotte[10] are in closest agreement.

As discussed in Section 4.0, there are two primary reasons for discrepancies between sets of vapor pressure data reported by different investigators: impurity of test samples and chemical decomposition. The degree of purity of the liquids employed in these measurements was shown to be quite high (Section 5.0), and considerable preliminary experimentation was performed for the purpose of selecting suitable materials of construction and limits of operation to avoid significant decomposition in both the liquid and the vapor phases. As a result, the vapor pressure data obtained are considered to be quite reliable.

6.3 P-V-T

As indicated in Section 5.0, the P-V-T data were obtained in the form: (pressure) vs (volume fraction of initial cell charge) at constant temperature. These data yielded the constants of the equation of state for gaseous mixtures, as described in the following paragraphs.

The number of moles of vapor originally in the cell, N_0, is given by:

$$N_0 = m/M,$$

where m is the mass of the vapor and M is its molecular weight. (for a

TABLE 6.1. Comparison of Data for Vapor Pressure of Hydrazine

Temperature °C	This Work	Scott et al[7]	Chang and Gokcen[9]	ICT[27]	Hieber and Woener[23]	Pannetier and Mignotte[10]
0	2.74	2.75	2.94	2.81	2.67	2.84
50	56.4	56.6	56.7	54.0	54.4	54.9
100	516.5	514.5	494.5	469.9	493.9	481.0
150	2802	2807	2585	2454	2663	2520

Pressure units: millimeters of mercury.

TABLE 6.2. Comparison of Data for Vapor Pressure of UDMH

Temperature °C	This Work	Pannetier and Mignotte[10]	Aston et al[8]	Chang and Gokcen[9]	Barger[28]
0	44.1	44.7	41.1	48.0	45.2
50	465.9	460.2	515.0	496.3	483.5
100	2616	2535	3278	2746	2739
150	9768	9331	13480	10040	10300

Pressure units: millimeters of mercury.

mixture, the molecular weight is the molar average of the molecular weights of the pure components.) After the first expansion, the number of moles, N_1 remaining in the cell is

$$N_1 = \left(\frac{m}{M}\right)\left(\frac{V_C}{V_C + V_E}\right),$$

where V_C is the volume of the cell, and V_E is the expansion volume.

After the second expansion, N_2 moles remain as given by:

$$N_2 = \left(\frac{m}{M}\right)\left(\frac{V_C}{V_C + V_E}\right)^2 .$$

In general, after k expansions:

$$N_k = \left(\frac{m}{M}\right)\varepsilon^k \qquad (6.6)$$

where $\varepsilon = V_C/(V_C + V_E)$, the volume fraction of the charge which remains in the cell after the expansion.

Now for moderate values of pressure the equation of state (equation 3.1) may be simplified, since V>>b. The equation becomes:

$$P = \frac{RT}{V} - \left(\frac{BRT}{V^2}\right), \qquad (6.7)$$

where

$$B = fb. \qquad (6.8)$$

The molar volume, V, may be replaced by the equivalent, V_C/N_k. Then equation (6.7) becomes after rearrangement:

$$\frac{P_k}{N_k} = \frac{RT}{V_C} - \left(\frac{BRT^2}{V_C}\right)N_k \quad . \qquad (6.9)$$

Equations (6.6) and (6.9) are combined and then rearranged to obtain:

$$\frac{P_k}{\varepsilon^k} = \left(\frac{m}{M}\right)\frac{RT}{V_C} - \frac{BRT}{V_C^2}\left(\frac{m}{M}\right)^2 \varepsilon^k . \qquad (6.10)$$

According to equation (6.10), for data obtained at constant temperature and composition, a plot of $\left(\frac{P_k}{\varepsilon^k}\right)$ vs ε^k should be a straight line with slope, S, given by:

$$S = -\left(\frac{m}{M}\right)^2 \frac{BRT}{V_C^2} \qquad (6.11)$$

and intercept, I, given by:

$$I = \left(\frac{m}{M}\right)\frac{RT}{V_C} . \qquad (6.12)$$

Then the constant B can be calculated from the following relationship which results from the combination of equations(6.11) and (6.12):

$$B = -\left(\frac{S}{I^2}\right) RT . \qquad (6.13)$$

The procedure for testing the validity of the equation of state (3.1) was as follows: (1) The experimental data were plotted in the manner just described to test for the predicted linearity and to calculate the value of B using equation (6.13). (2) Values of the constant, B, were calculated from equation (6.8), using the values of b and f, given by equations (3.2) and (3.3),respectively. (3) Both values of B were substituted into equation (6.7) to calculate values of pressure at various selected values of molar volume.

Figure 6.3 is a typical example of the experimental data plotted in the manner indicated above. The straight line was constructed by using

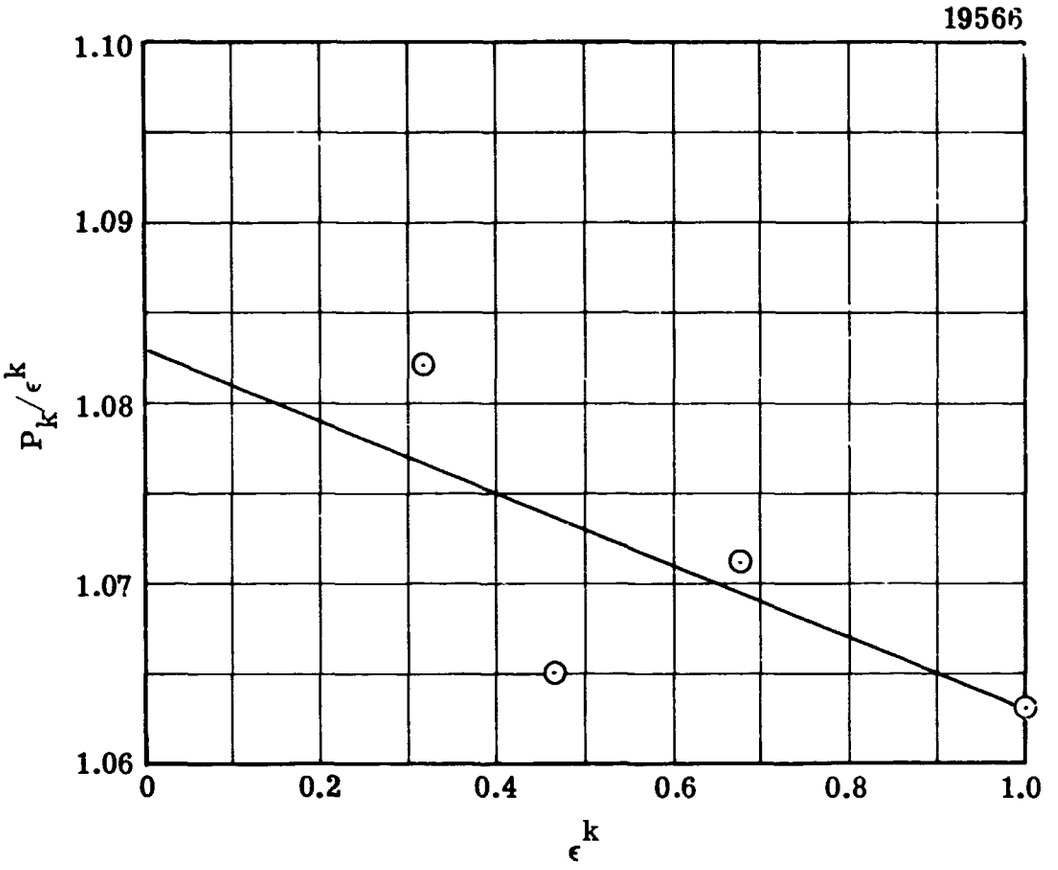

Figure 6.3. P-V-T Data for y_h = 0.567, T = 242.3°F.

the values of S and I obtained by fitting the data to equation (6.10) by the method of least squares. Ordinarily, the data deviated from the fitted curves by less than 1.5%, which is acceptable since this method of plotting the data emphasizes experimental error.

Table 6.3 compares the values of the constant B obtained from the data with those values calculated by means of equations (3.2),(3.3), and (6.8). The somewhat large deviations listed in the table are not particularly bothersome because, as shown later, the term containing B in the simplified equation of state (6.7) represents only a few per cent of the calculated pressure.

Table 6.4 compares values of pressure calculated by means of equation (6.7) using both the experimental and predicted values of B for a temperature of 390°K (242.3°F) and for a vapor composition of 56.74 weight per cent hydrazine. This particular data point was chosen for illustration because the highest relative deviation occurred between the two values of B. Even so, as indicated by the last column in the table, the agreement between the values of pressure is quite good. The reason for this lies with the form of the equation of state (6.7). The first term on the right hand side is identical to the ideal gas law. Then the second term may be regarded as a correction for non-ideality. Since only moderate pressures are under consideration, it is expected that rather small corrections for non-ideality are required. As a result, the second term of the equation should be rather small compared to the first, and consequently large relative errors in B have a very minor effect on the calculated values of pressure.

Further examination of Table 6.4 reveals that for pressures below approximately 0.5 atm, the ideal gas law is a suitable equation of state for hydrazine-UDMH mixtures. Note that at a pressure of 0.528 atm the ideal gas law predicts a value of 0.533 atm, a deviation of less than one per cent.

TABLE 6.3. Comparison Between Experimental and Predicted Values of B for 242.6°F

y_h (weight fraction)	B_{exp}	$B_{predicted}$	Deviation
0.2342	-514	-535	- 4
0.5674	-564	-461	22
0.5949	-366	-455	20
0.7818	-358	-416	-14

TABLE 6.4. Comparison of Calculated Values of Pressure Using Experimental Value of B with Corresponding Values Using Predicted Value of B

Molar Volume (cc/mole)	P_{ideal} (atm)	P_{exp} (atm)	P_{theor} (atm)	Deviation (Per cent)
10,000	3.200	3.020	3.052	-1.1
20,000	1.600	1.555	1.563	-0.5
30,000	1.067	1.047	1.051	-0.4
32,003	1.000	0.982	0.986	-0.4
40,000	0.800	0.789	0.791	-0.2
60,000	0.533	0.528	0.529	-0.2

Temperature: 390°K

Vapor Composition: 56.74% by weight hydrazine

$$\text{Deviation} \equiv \frac{100\ (P_{exp} - P_{theor})}{P_{theor}}$$

In conclusion, the P-V-T experiments have shown that the originally proposed equation of state for the vapor phase, the Redlich-Kwong equation, is suitable for application to the hydrazine-UDMH system for pressures up to approximately three atmospheres. Also, the simpler ideal gas law is adequate for pressures up to approximately 0.5 atm.

6.4 LIQUID-VAPOR EQUILIBRIA

Figures 6.4, 6.5 and 6.6 present the experimental P-x isotherms. The curves for the liquid were drawn through the data points by hand. The solid curves for the vapor were calculated with the aid of an IBM System 360 digital computer, from the P-x data, using the Gibbs-Duhem equation and the equation of state for the vapor. The method for doing this is developed in Appendix A.

The dashed curves for the vapor in these figures were calculated by assuming that the vapor was ideal and that the volume of the liquid was negligible compared to that of the vapor (as is commonly done for low pressures). The errors resulting from these assumptions, as shown in Figure 6.7, are rather significant and become larger at the higher pressures. Consequently, these two assumptions are not valid for this system, even at the moderate pressures at which these experiments were performed.

Values of the logarithm of the activity coefficients for both components in solution were calculated from the P-x-y data employing the relationships derived in Appendix B. The results are listed in Tables 6.5, 6.6, and 6.7.

Correlation of the activity coefficients was a difficult problem. The reason for this was that a correlation, which could extrapolate the data well outside the range of the measurements, was desired. Thus, a direct correlation using arbitrary polynomials is unsatisfactory, since such a technique is accurate only for interpolation. Accordingly, it was necessary first to extrapolate the data, using some reasonable theoretical basis. Subsequent to this, interpolative correlations then were developed.

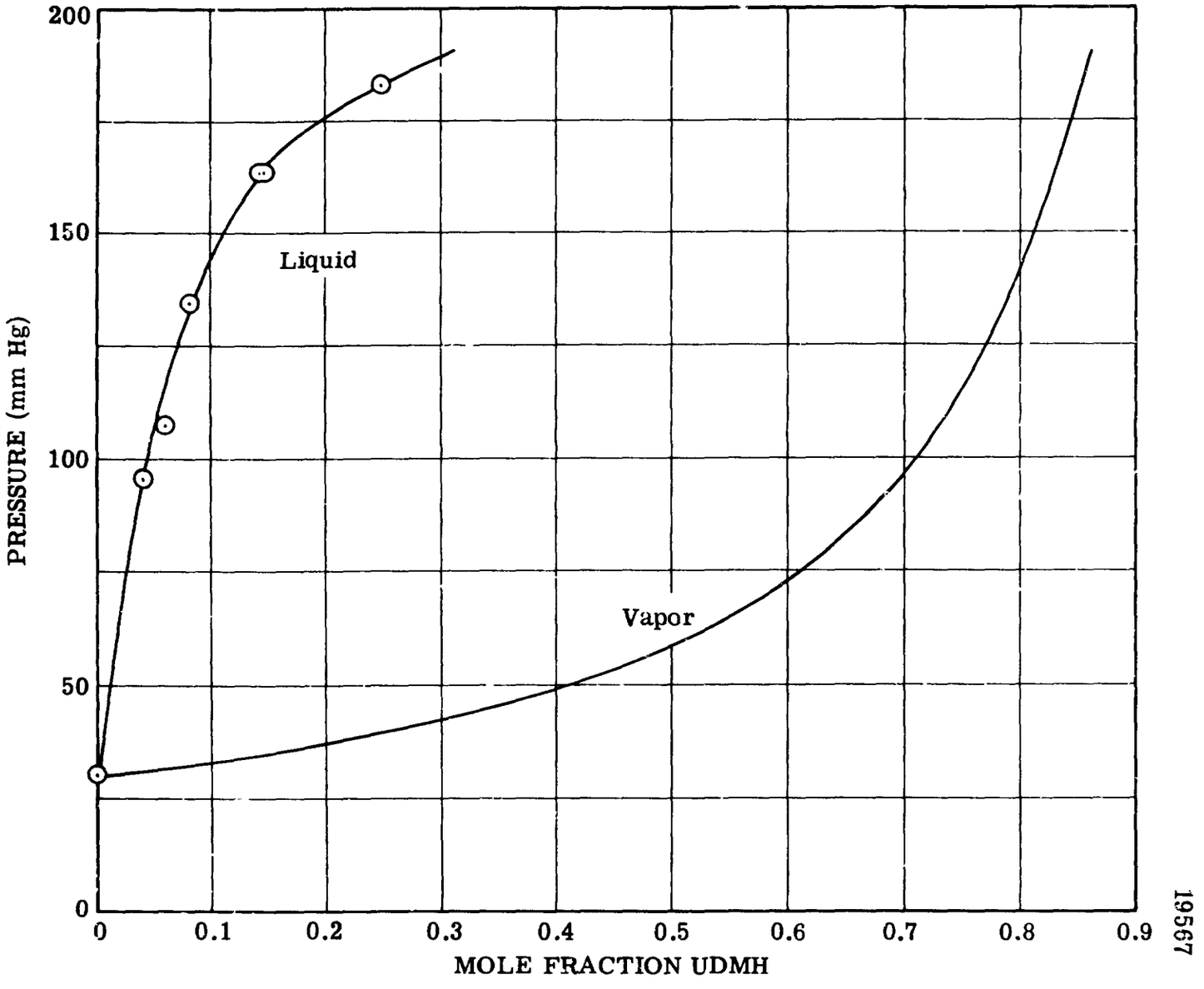

Figure 6.4. Liquid-Vapor Equilibria for 100.2°F.

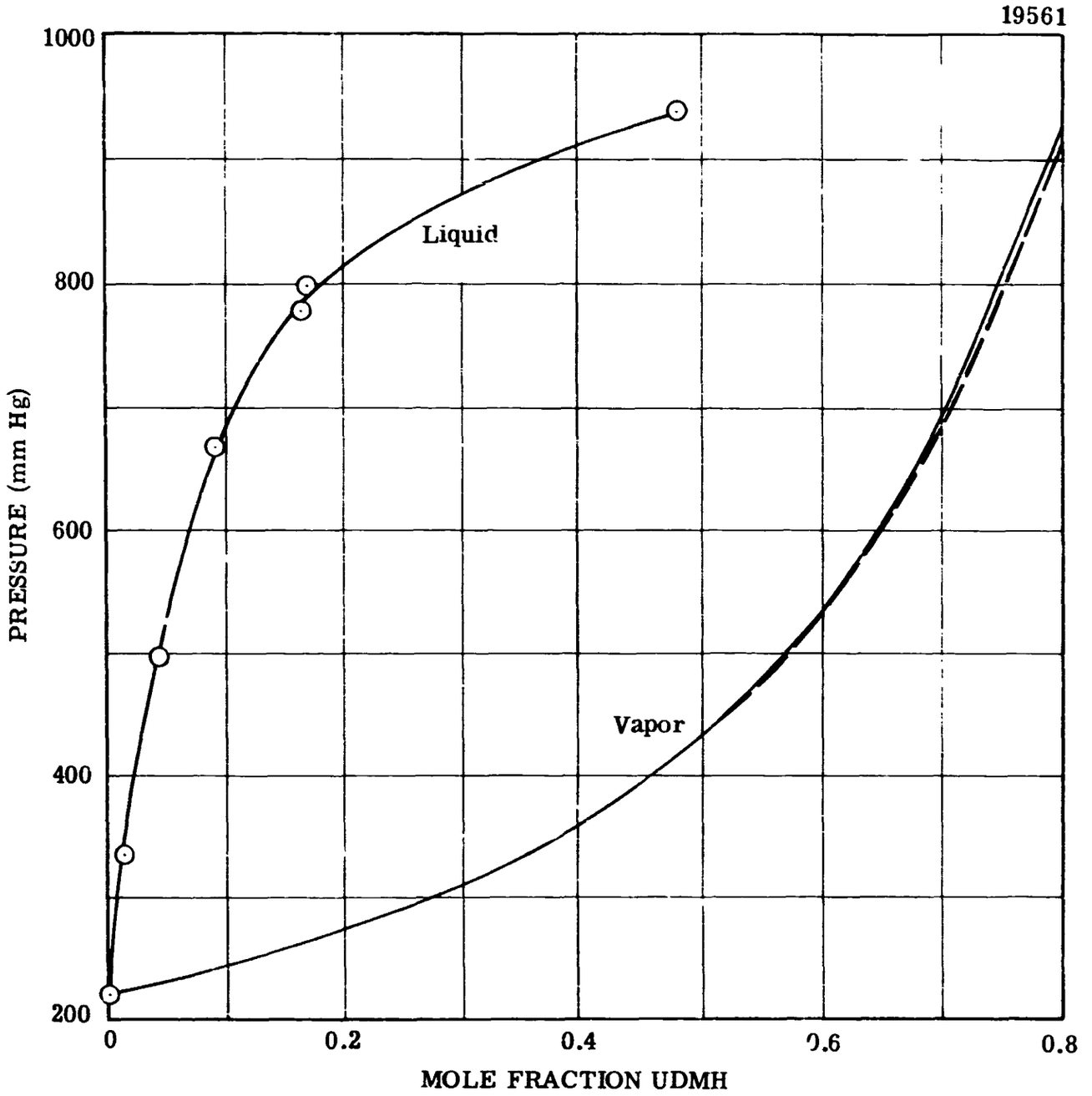

Figure 6.5. Liquid-Vapor Equilibria for 176.0°F.

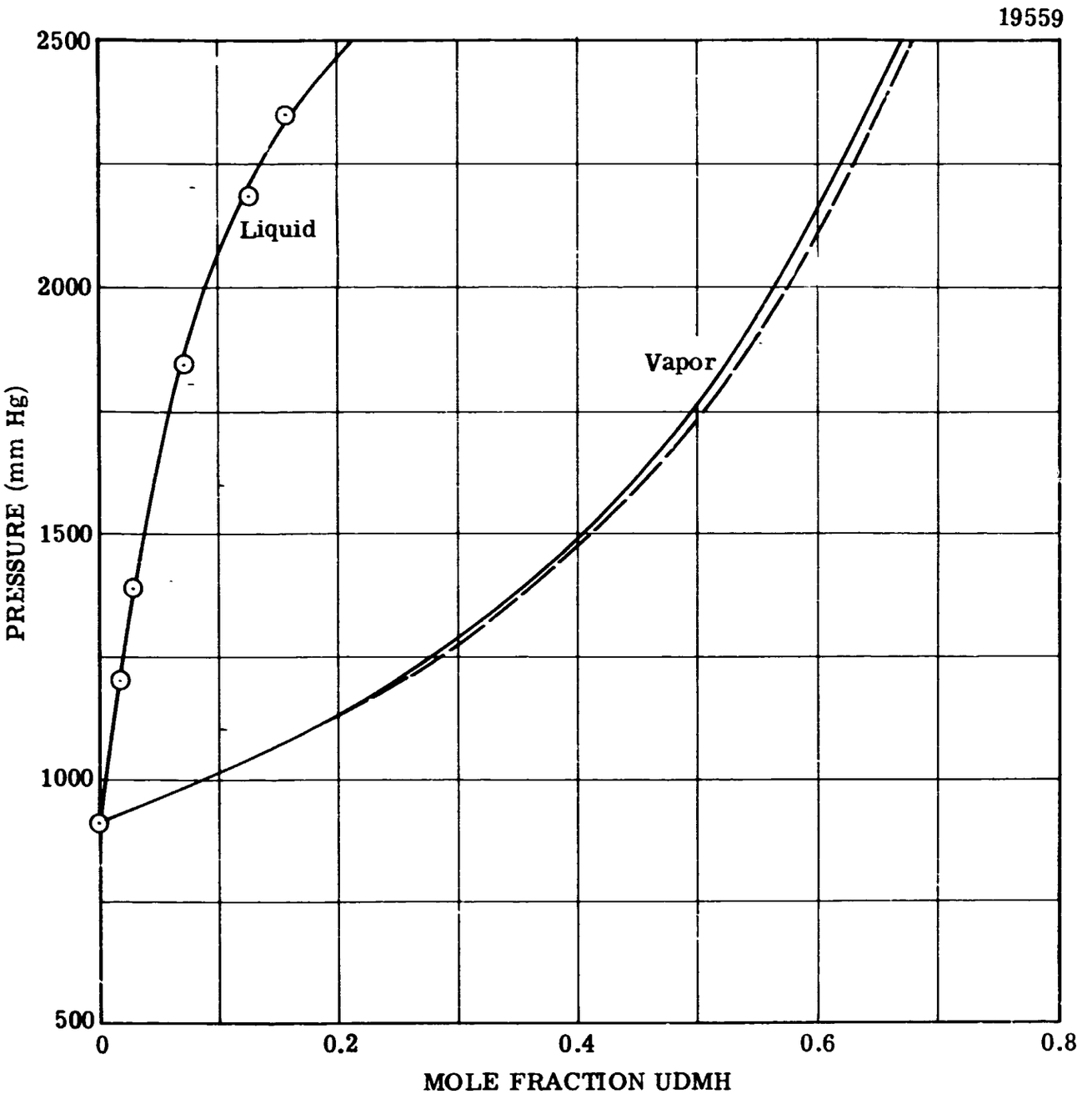

Figure 6.6. Liquid-Vapor Equilibria for 242.6°F.

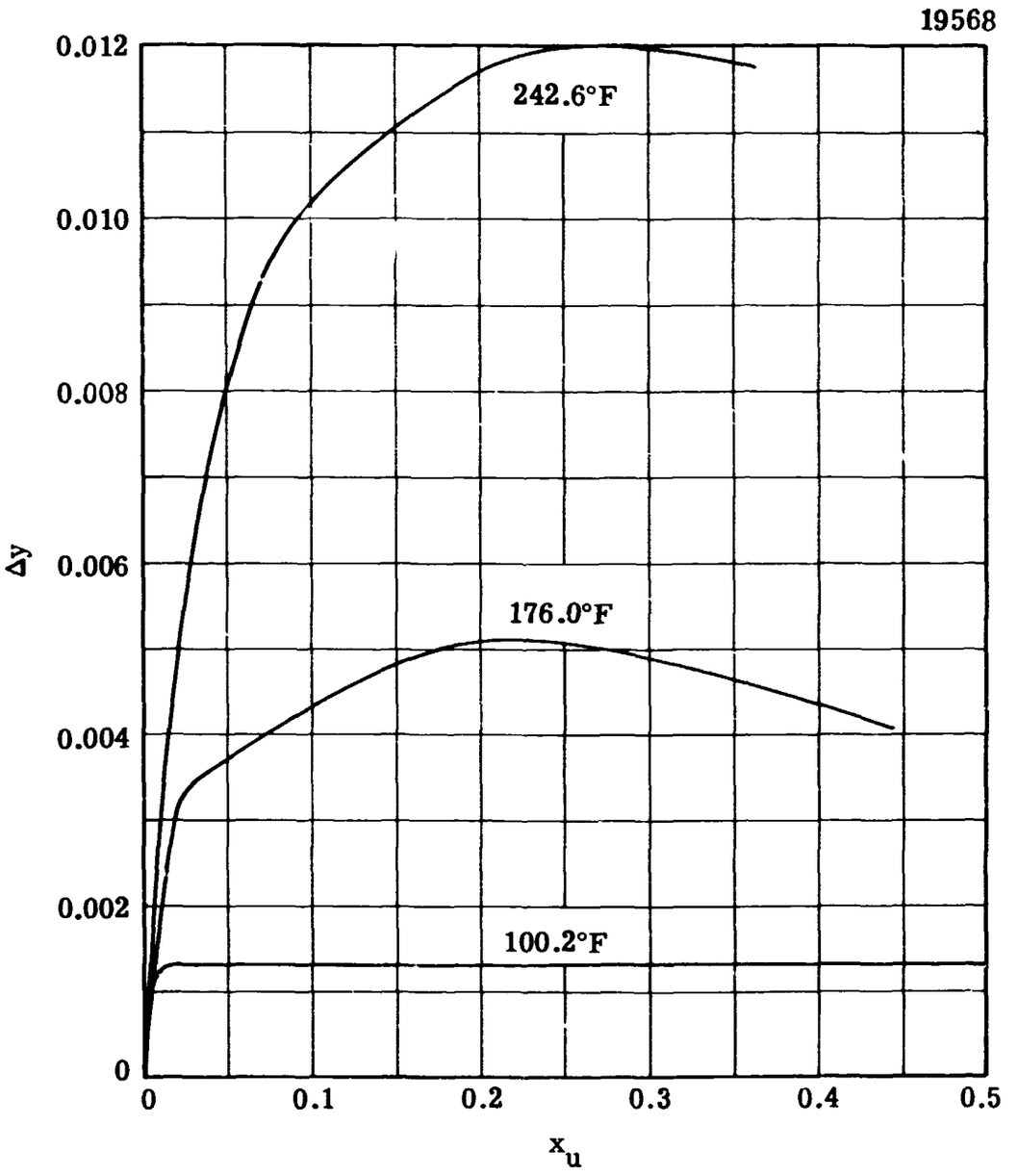

Figure 6.7. Errors Resulting from Assumption of Ideal Vapor and Negligible Liquid Volume.

TABLE 6.5. Liquid-Phase Activity Coefficients for Hydrazine-UDMH Mixtures at 100.2°F

Weight Fraction UDMH in Liquid	Weight Fraction UDMH in Vapor	$\ln\gamma_u$	$\ln\gamma_h$	Pressure (mm)
0.020	0.564	1.8992	0.0031	49.5
0.040	0.724	1.8956	0.0039	69.5
0.060	0.799	1.8848	0.0049	89.5
0.092	0.843	1.7283	0.0122	109.5
0.133	0 872	1.5641	0.023	129.5
0.187	0.893	1.3784	0.0432	149.5
0.271	0.909	1.1189	0.0857	169.5
0.446	0.922	0.6595	0.2225	189.5
0.675	0.936	0.2266	0.5219	209.5

TABLE 6.6. Liquid-Phase Activity Coefficients for Hydrazine-UDMH Mixtures at 176.0°F

Weight Fraction UDMH in Liquid	Weight Fraction UDMH in Vapor	$\ln\gamma_u$	$\ln\gamma_h$	Pressure (mm)
0.025	0.465	1.7142	0.0056	321.8
0.050	0.637	1.7033	0.0088	421.8
0.089	0.728	1.5141	0.0177	521.8
0.137	0.785	1.3464	0.0305	621.8
0.204	0.823	1.1383	0.0557	721.8
0.338	0.853	0.7470	0.1363	821.8
0.595	0.881	0.1956	0.3942	921.8

TABLE 6.7. Liquid-Phase Activity Coefficients for Hydrazine-UDMH Mixtures at 242.6°F

Weight Fraction UDMH in Liquid	Weight Fraction UDMH in Vapor	$\ln\gamma_u$	$\ln\gamma_h$	Pressure (mm)
0.022	0.299	1.4508	^ 0069	1110.7
0.044	0.463	1.4448	0.0110	1310.7
0.070	0.567	1.3749	0.0165	1510.7
0.101	0.638	1.2750	0.0250	1710.7
0.137	0.691	1.1755	0.0349	1910.7
0.185	0.732	1.0349	0.0519	2110.7
0.251	0.765	0.8534	0.0813	2310.7
0.347	0.794	0.6131	0.1390	2510.7
0.500	0.821	0.2878	0.2689	2710.7

The following procedure accomplished the extrapolation and is based upon theoretical expressions relating excess free energy of mixing to temperature and composition. Excess free energy of mixing is related to the activity coefficients by equation (3.19),

$$\frac{\Delta G^E}{RT} = x_1 \ln \gamma_1 + x_2 \ln \gamma_2. \qquad (3.19)$$

At constant temperature, this quantity may be expressed as a function of composition in the form of equation (3.18). A plot of $x_u\ x_h\ RT/\Delta G^E$ vs x_u, shown in Figure 6.8 for the data obtained, is linear and accordingly the data fit the equation

$$\frac{x_u\ x_h\ RT}{\Delta G^E} = S\ x_u + I\ . \qquad (6.13)$$

The constant S and I, are functions of temperature, alone. As will be shown later this means that the activity coefficients are related to liquid composition by the two-constant van Larr equation (which was originally derived assuming that van der Waals equation applies to both the components and the mixture, and that the excess entropy of mixing is zero.)

Basis for the temperature extrapolation derives from the differential equation at constant pressure and composition:

$$\frac{\partial(\Delta G^E/RT)}{\partial T} = -\frac{\Delta H}{RT^2}\ , \qquad (6.14)$$

where ΔH is the heat of mixing. If the heat capacities of the liquid components and the mixture may be assumed to be linear functions of temperature then the heat of mixing is given by the equation

$$\Delta H = a\ T + \frac{b}{2}\ T^2 + c\ . \qquad (6.15)$$

Integration of (6.14) using this equation for ΔH gives the equation

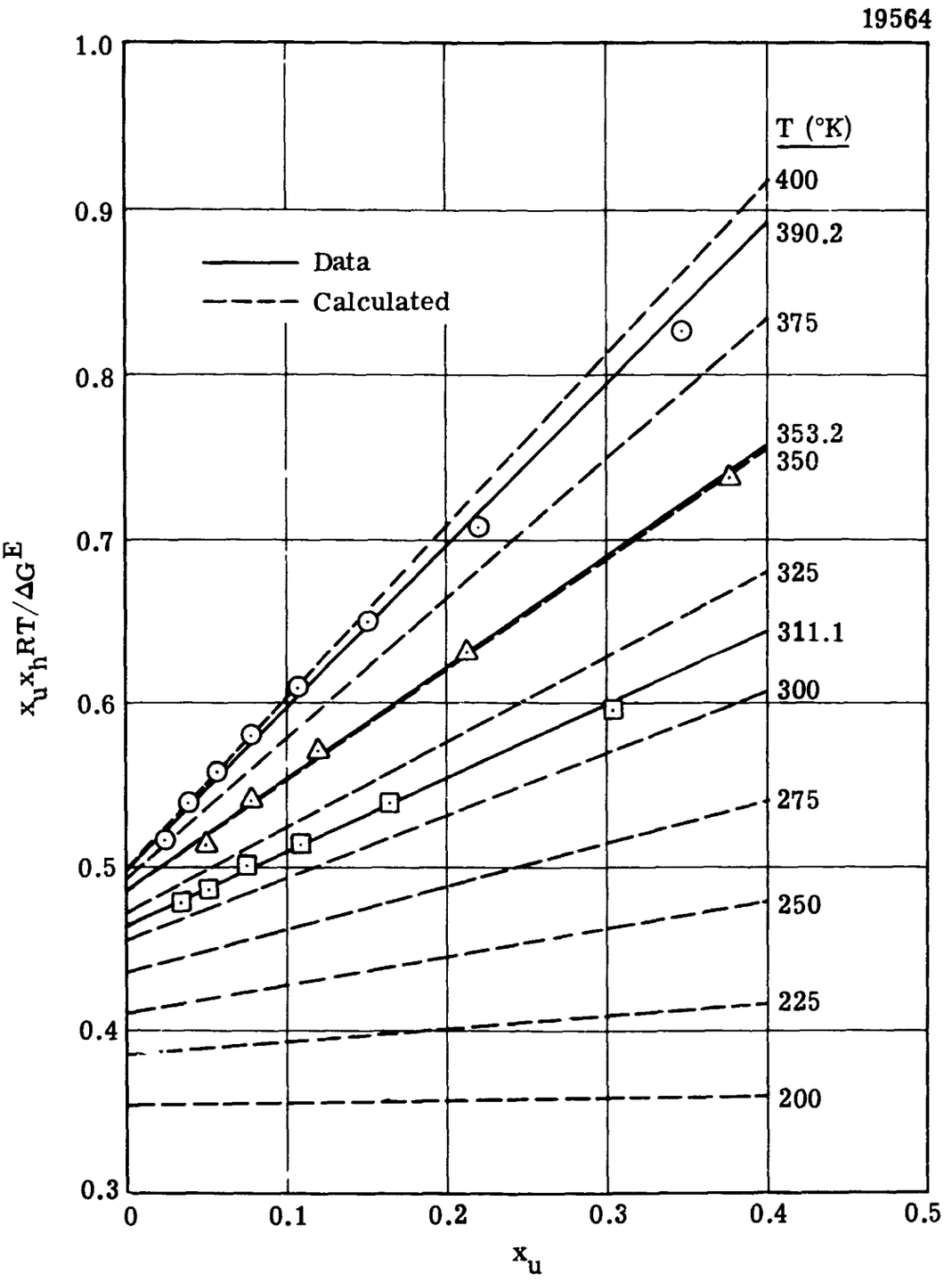

Figure 6.8. Concentration Dependency of Excess Free Energy of Mixing at Constant Temperature.

$$\frac{\Delta G^E}{RT} = -\frac{a \ln T}{R} - \frac{bT}{2R} + \frac{c}{RT} + \frac{d}{R}, \qquad (6.16)$$

where all the constants are independent of temperature but are functions of composition. Using the curves in Figure 6.8, plots of $(\Delta G^E/RT\ x_u\ x_h)$ vs $(1/T)$ were constructed for values of constant x_u, as shown in Figure 6.9. The curves are essentially linear. Thus ΔH is independent of temperature $(a = b = o)$ and equation (6.16) may be reduced to the equation

$$\frac{\Delta G^E}{x_u x_h RT} = \frac{A}{T} + B, \qquad (6.17)$$

where $A = \frac{c}{R\ x_u x_h}$ and $B = \frac{d}{R\ x_u x_h}$. The constants, A and B, were evaluated for selected values of x_u (cf. Figure 6.9). These then were used to calculate additional data (values of $\frac{x_u x_h RT}{\Delta G^E}$) in order to cover the entire range of temperature and composition which is of interest.

This extrapolated data also was plotted in Figure 6.8. The slope and intercept of the lines give the values of S and I, respectively, of equation (6.13) at the temperature indicated for each curve. Correlation of S and I with temperature gave the following formulas:

$$S = 0.01075 + 0.21725\Theta + 0.058375\ \Theta(\Theta-1) + 0.0042083\ \Theta(\Theta-1)(\Theta-2), \qquad (6.18)$$

where $\Theta = 0.015(T - 200)$, and

$$I = -2.98505 \times 10^{-5}T^2 + 2.51003 \times 10^{-2}T - 2.840 \times 10^{-2}. \qquad (6.19)$$

The activity coefficients are most easily computed from the derivatives of equation (3.19) with respect to composition (applying the Gibbs-Duhem relation). This yields the equation,

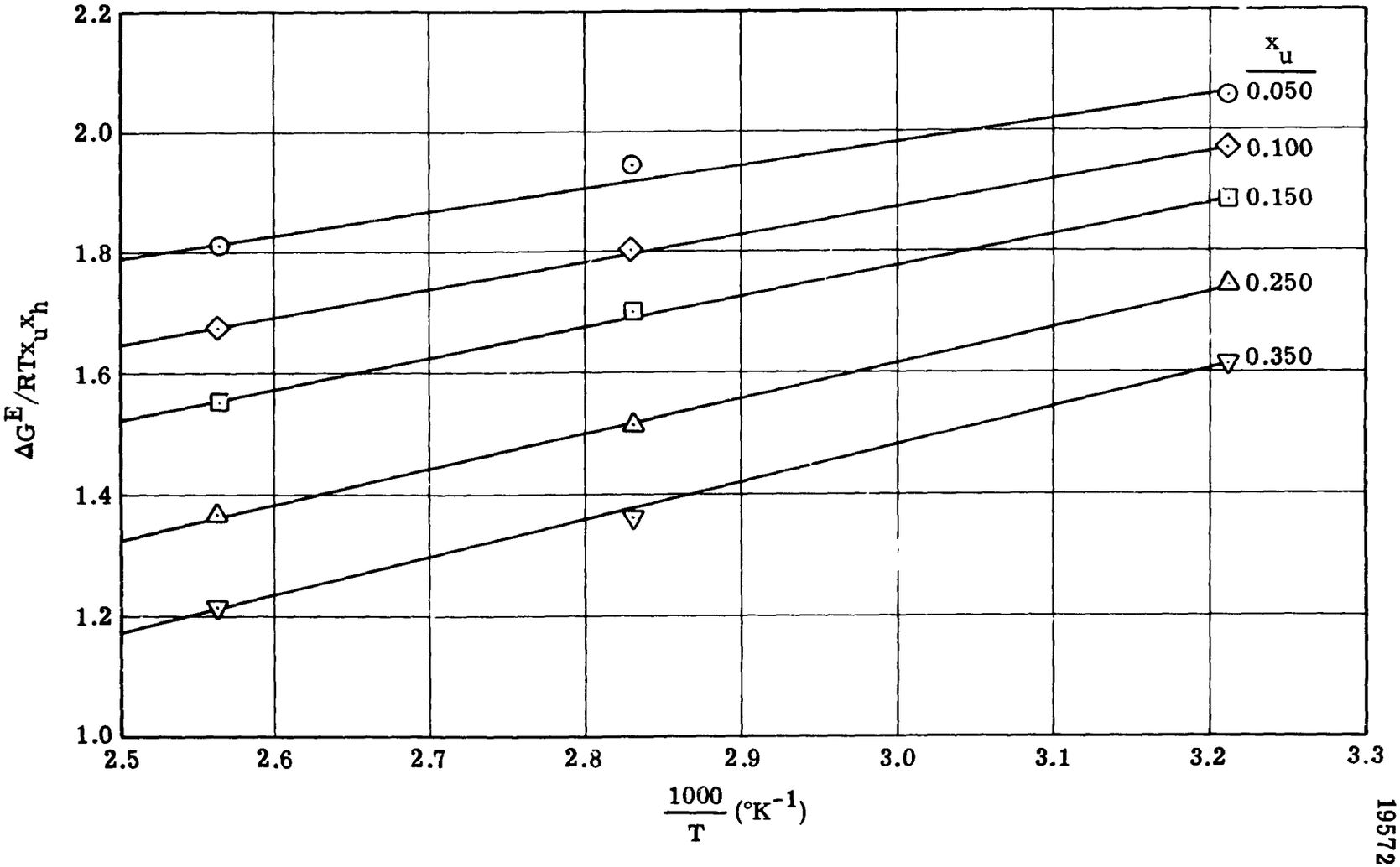

Figure 6.9. Temperature Dependency of Excess Free Energy of Mixing at Constant Composition.

$$\ln \gamma_u = \frac{\Delta G^E}{RT} + x_h \frac{d(\Delta G^E/RT)}{d x_u}, \tag{6.20}$$

for the activity coefficient of UDMH and a similar equation for hydrazine:

$$\ln \gamma_h = \frac{\Delta G^E}{RT} - x_u \frac{d(\Delta G^E/RT)}{d x_u} . \tag{6.21}$$

Eliminating $\frac{\Delta G^E}{RT}$ and its derivative between these equations and equation (6.13) gives the equations:

$$\ln \gamma_u = \frac{(1 - x_u)^2 I}{(S x_u + I)^2}, \tag{6.22}$$

and

$$\ln \gamma_h = \frac{x_u^2 (S + I)}{(S x_u + I)^2}, \tag{6.23}$$

which are identical to equations (3.21) and (3.22) with UDMH and hydrazine being components 1 and 2, respectively.

Equations (6.18), (6.19), (6.22) and (6.23) comprise the desired correlation of the activity coefficients. The procedure for calculating values of γ_u and γ_h for a given temperature and composition is (1) the computation of S and I from equations (6.18) and (6.19), and (2) the substitution of these values into equations (6.22) and (6.23). The procedure, when given some other pair of intensive variables, requires an iterative process using the same equations.

Figures 6.10, 6.11 and 6.12 compare the P-x and P-y curves derived from the experimental data with the curves which were calculated fro values of ln γ that were predicted by the correlations. (See Appendix B for the derivation of the relationships that were required for this calculation.) In all cases, the predicted P-y curves were virtually identical with the curves that were obtained directly from the data. For the P-x curves, the average deviation in pressure was approximately 2%. The maximum deviation, approximately

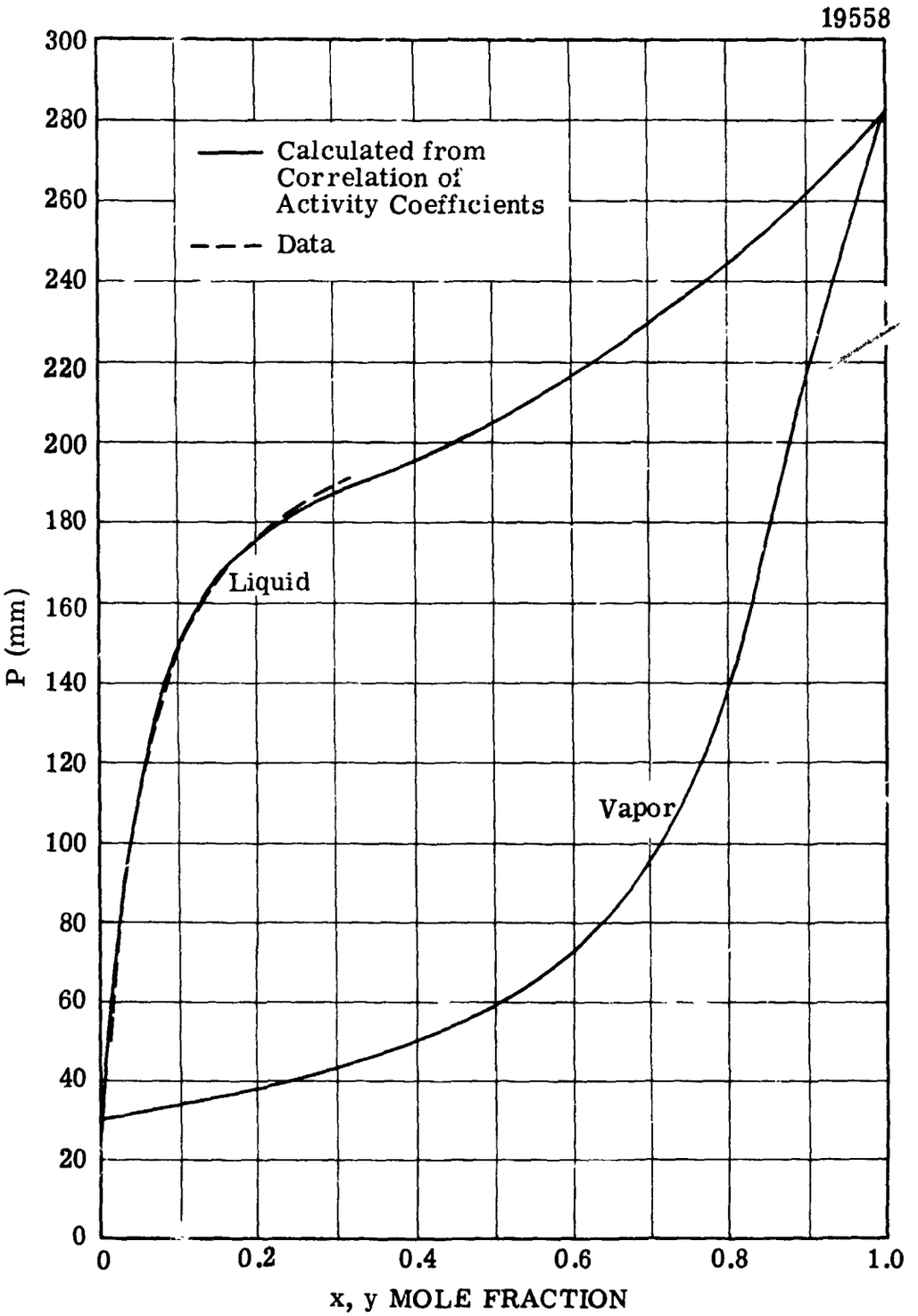

Figure 6.10. Calculated P, x, y Curves for 100.2°F.

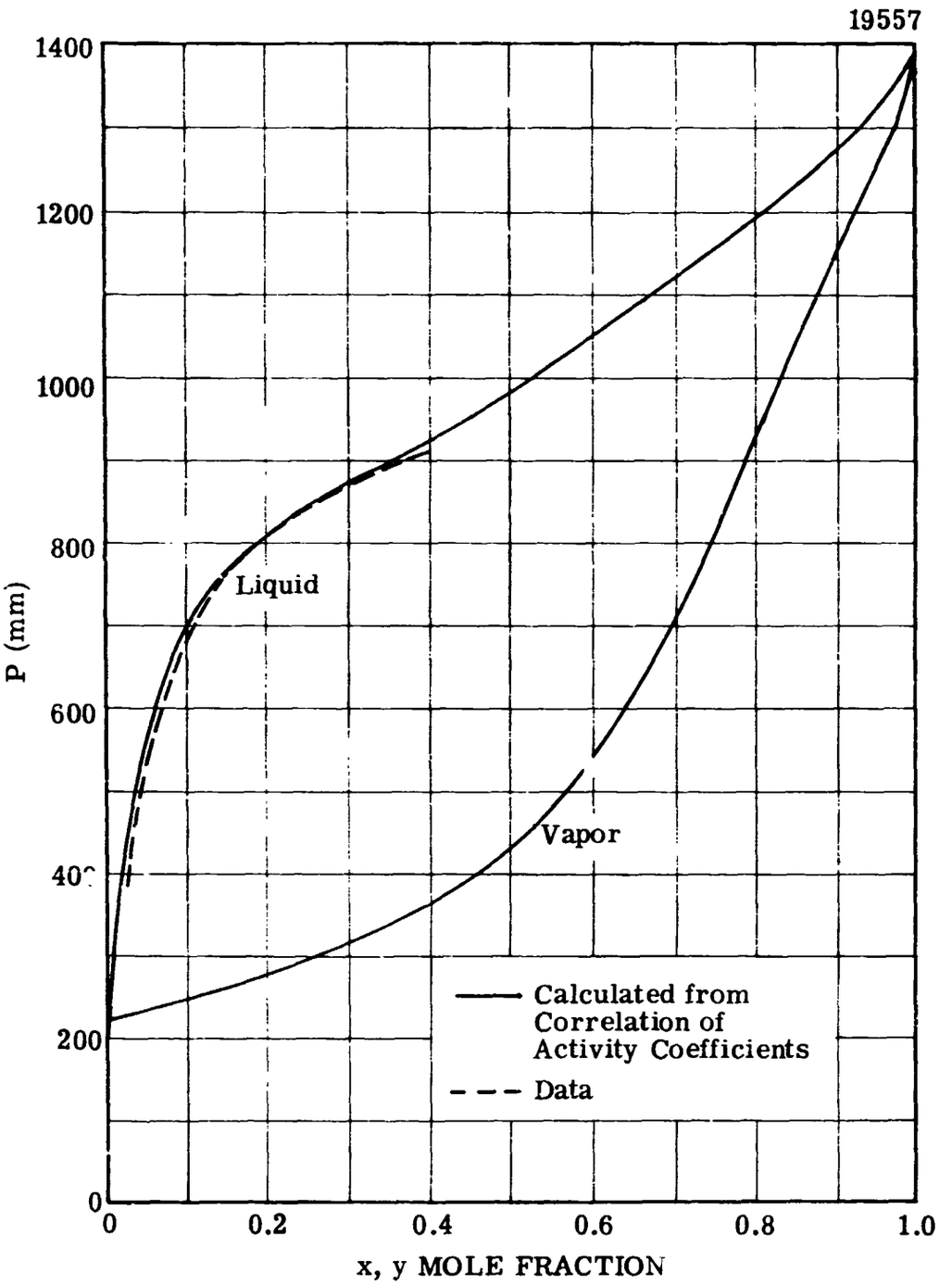

Figure 6.11. Calculated P, x, y Curves for 176°F.

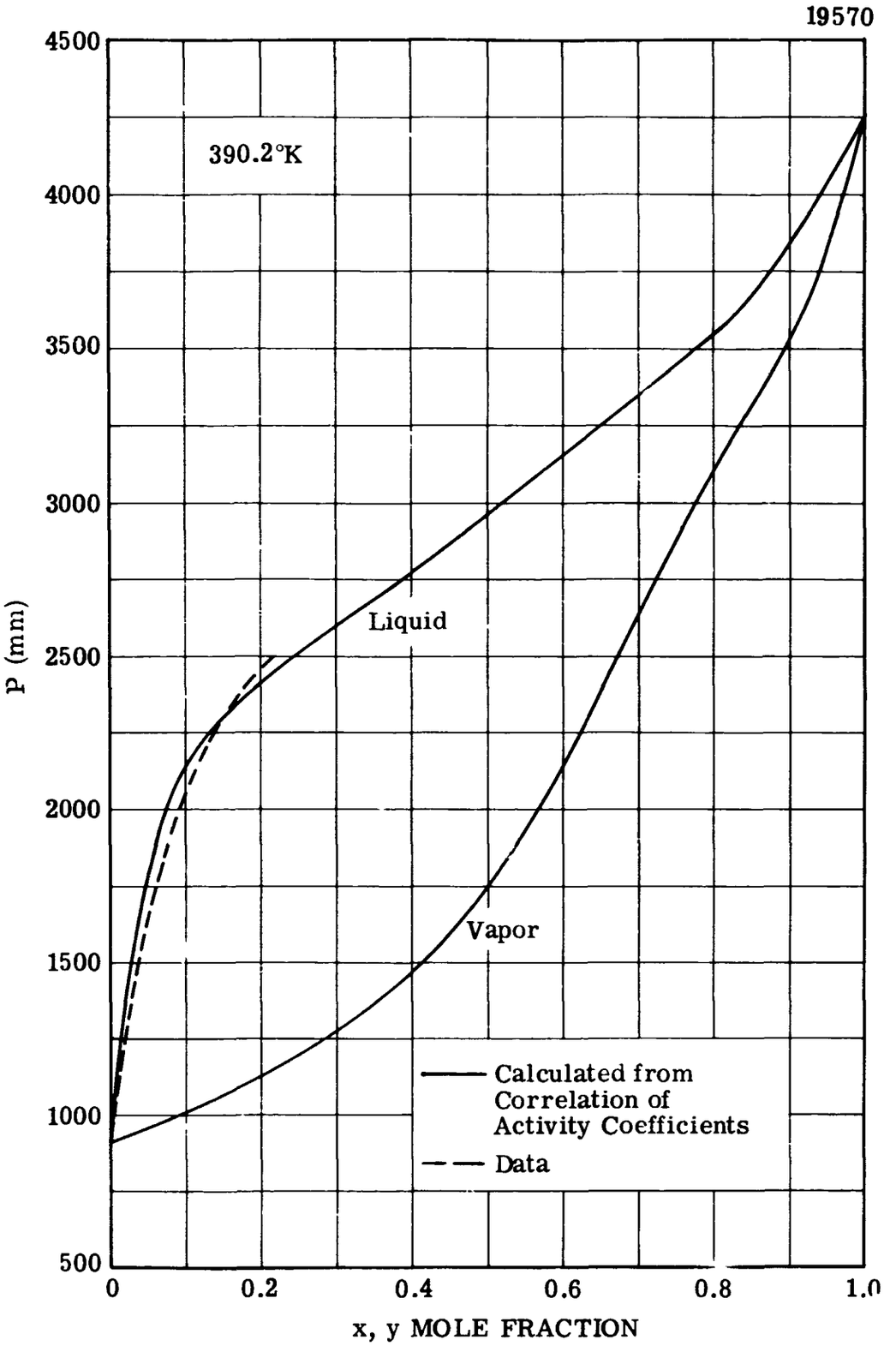

Figure 6.12. Calculated P, x, y Curves for 242.6°F.

8%, occurred for the 390.2°K isotherm at x_U=0.05. This kind of agreement is acceptable considering that the correlations are based on so few data.

Figures 6.13, 6.14, 6.15, and 6.16 compare curves for experimental P-x-y data reported in the literature with curves which were calculated from the correlations as discussed above. The data of Chang and Gokcen, Figures 6.13, 6.14 and 6.15, exhibit considerably higher values of pressure than the calculated data, particularly at higher values of x_U. The data of Pannetier and Mignotte, Figure 6.16, show somewhat better agreement. Since these data were obtained by cross-plotting a family of iosbaric T-x-y curves which were drawn on a very compressed coordinate system in the publication, the curve shown may not be an accurate representation.

The data obtained in this program are to be preferred to the literature data for the following reasons: As discussed in Section 4.0, the literature data are of questionable accuracy because of the possibility of decomposition; which, in part, would explain their lack of thermodynamic consistency. On the other hand, the data developed in this work are necessarily consistent, because the vapor compositions were calculated from P-x data by employing the Gibbs-Duhem equation and a reliable equation of state. In addition, it was shown that decomposition and impurities did not occur to a significant extent during the experimental measurements.

As indicated in Section 3.0, the entropy and enthalpy of mixing may be evaluated assuming that the mixtures are "regular" solutions. The following analysis and discussion shows that this assumption for UDMH-hydrazine mixtures is acceptable for most purposes.

Equation(6.17)may be rewritten thusly:

$$\Delta G^E = c + dT \qquad (6.24)$$

The excess free energy of mixing, ΔS^E, is related to ΔG^E according to

$$\Delta S^E = - \frac{\partial \Delta G^E}{\partial T} \quad . \qquad (6.25)$$

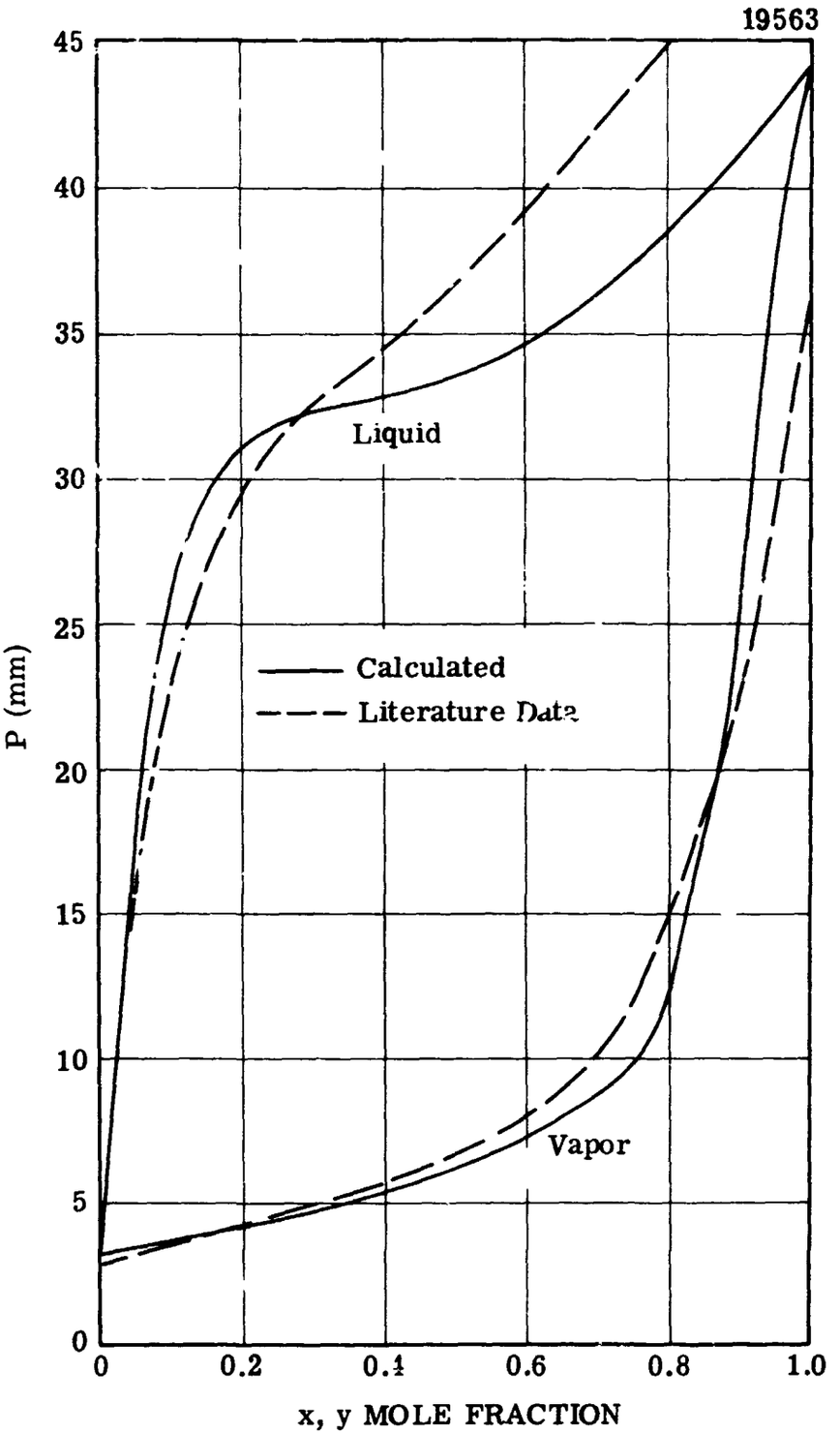

Figure 6.13. Comparison of Calculated P, x, y Curves with Experimental Data of Chang and Gokcen for 273.2°K.

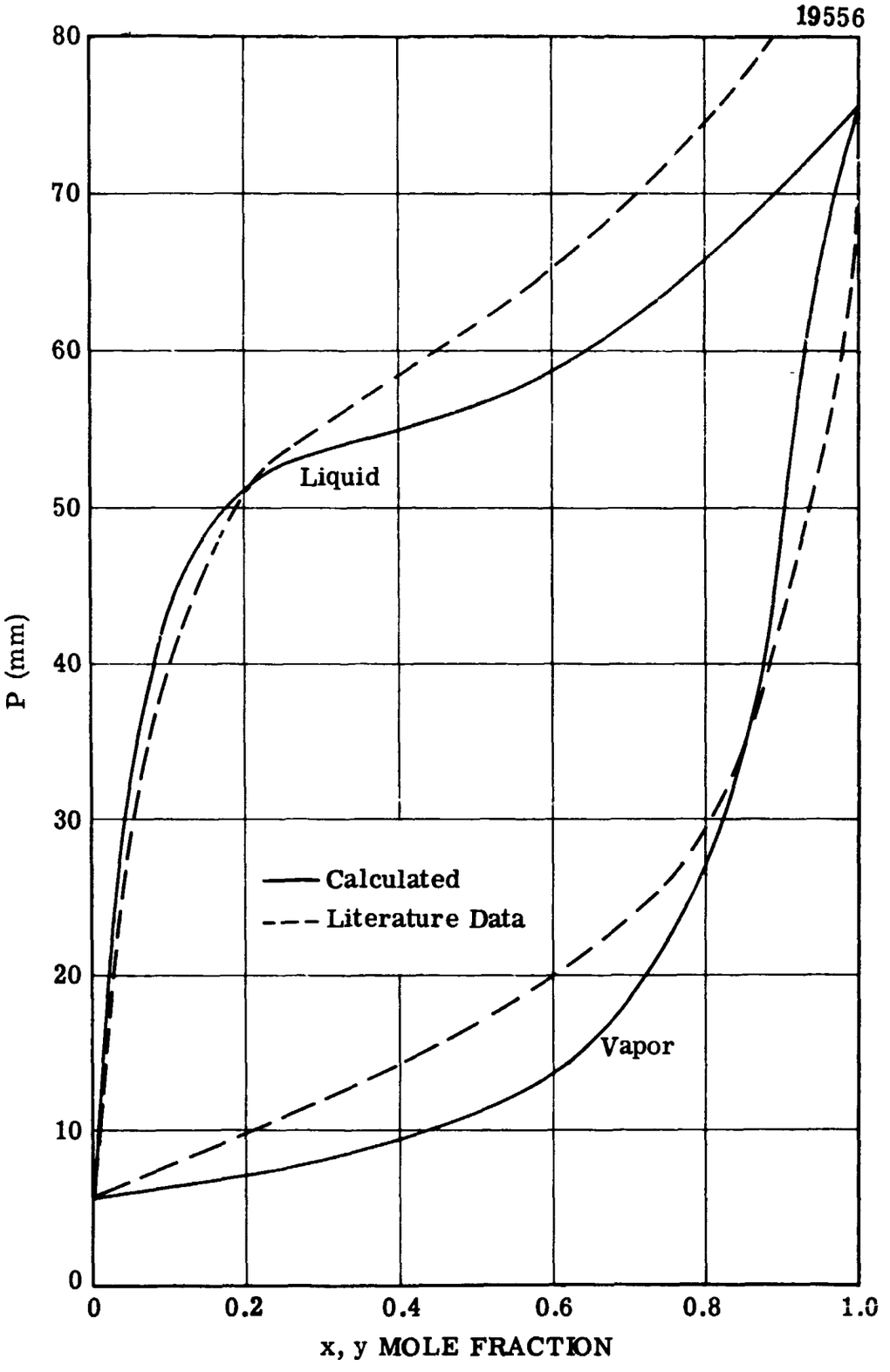

Figure 6.14. Comparison of Calculated P, x, y Curves with Experimental Data of Chang and Gokcen for 283.2°K.

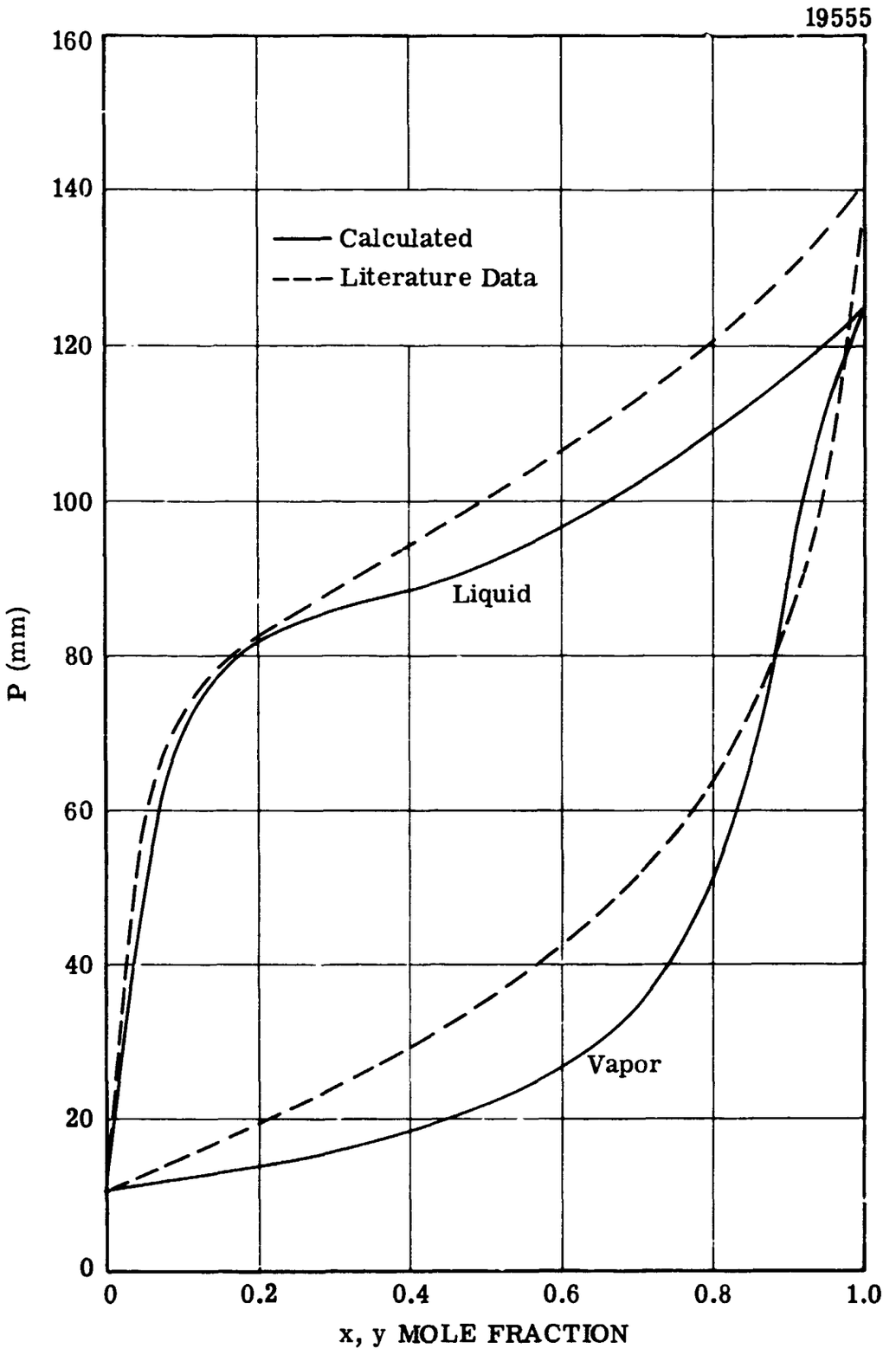

Figure 6.15. Comparison of Calculated P, x, y Curves with Experimental Data of Chang and Gokcen for 293.2°K.

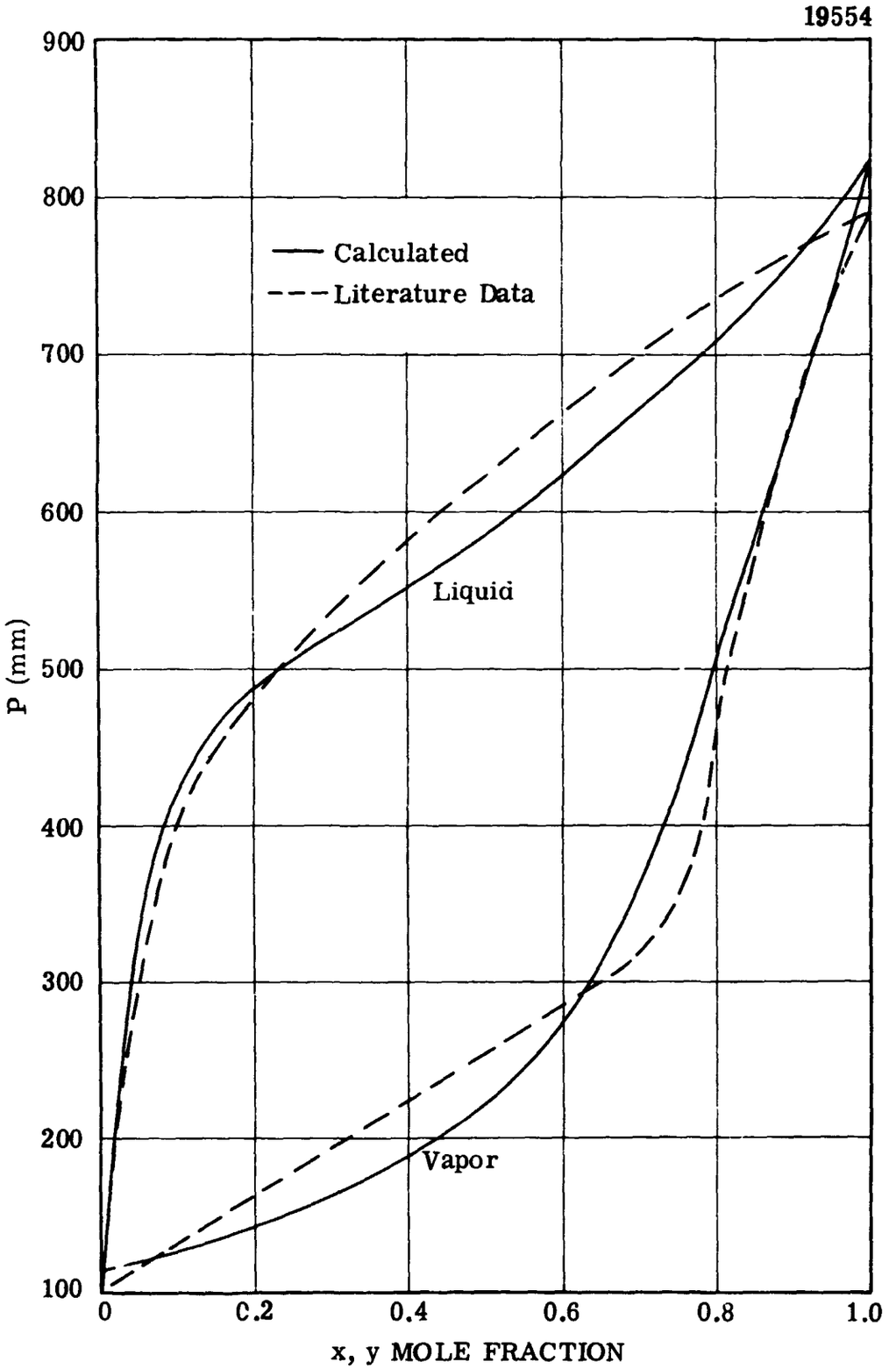

Figure 6.16. Comparison of Calculated P, x, y Curves with Experimental Data of Pannetier and Mignotte for 338.2°K.

Then,

$$\Delta S^E = -d.$$

The total entropy change of mixing, is given by:

$$\Delta S = \Delta S^{id} + \Delta S^E, \tag{6.26}$$

where

$$\Delta S^{id} = -R\sum_i x_i \ln x_i, \tag{6.27}$$

Recalling that $B = d/R\ x_u\ x_h$, the excess entropy of mixing is simply

$$\Delta S^E = -BR\ x_u\ x_h \tag{6.28}$$

and equation (6.26) for hydrazine-UDMH mixtures becomes,

$$\Delta S = -R(x_u \ln x_u + x_h \ln x_h) - BRx_u\ x_h \tag{6.29}$$

Figure 6.17 shows curves for ΔS^{id}, ΔS^E, and ΔS versus x_u which were computed by employing equations (6.27, (6.28), and (6.29), respectively. The figure shows that the quantity ΔS^{id} contributes far more to the value of ΔS than does ΔS^E. Considering that ΔS represents only a few per cent of the value of the absolute entropy, it is quite reasonable to neglect ΔS^E, i.e., assume that

$$\Delta S = \Delta S^{id}.$$

This is equivalent to assuming that the quantity d in equation (6.24) is zero. Then $\Delta G^E = c = \Delta H$, i.e., the heat of mixing is independent of temperature. These two conditions, $\Delta S^E = 0$ and ΔH independent of temperature, define a regular solution.

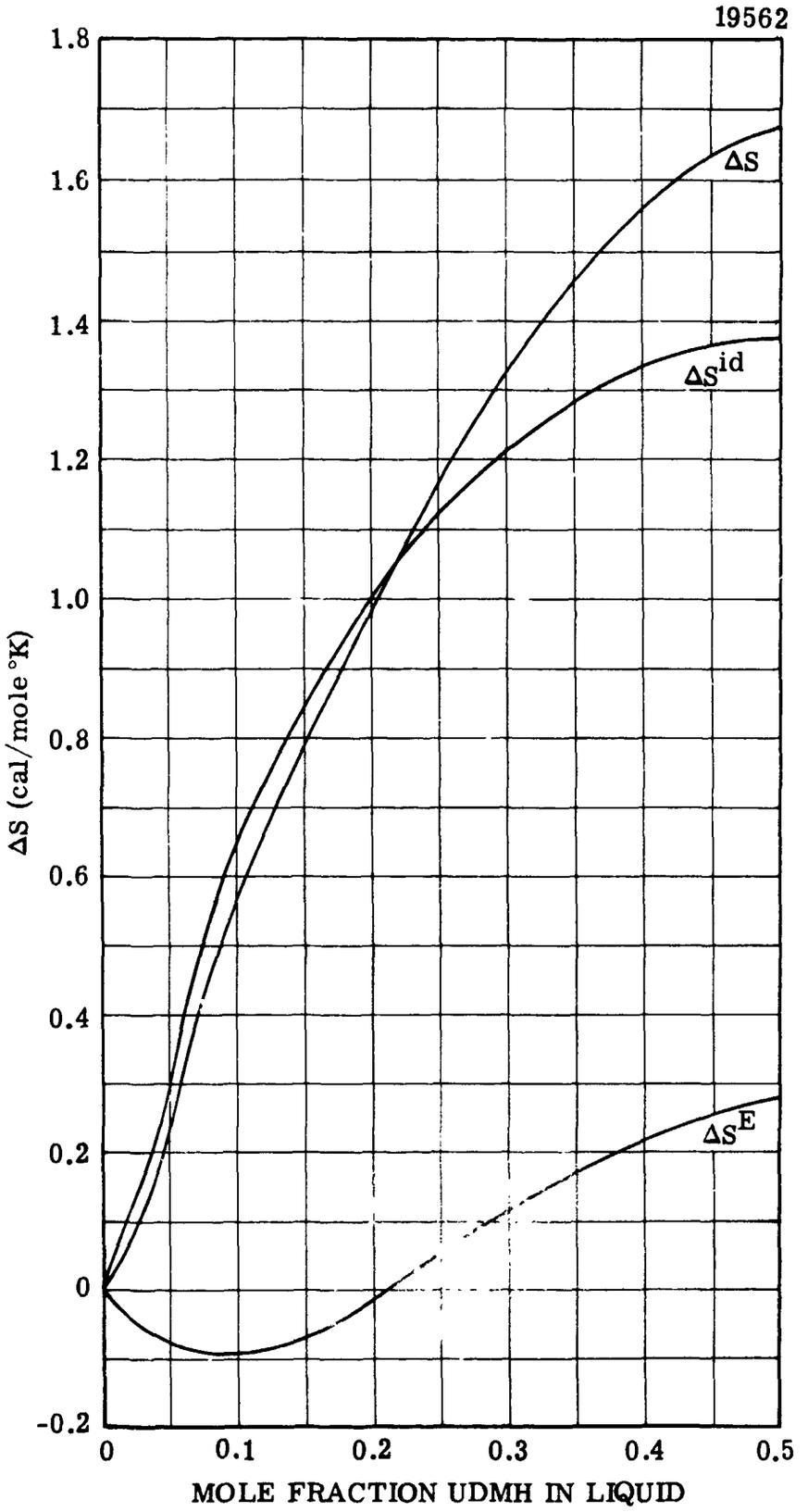

Figure 6.17. Entropy Change of Mixing for Hydrazine-UDMH Mixtures.

7.0 DISCUSSION OF CHARTS AND TABLES

The phase diagram, temperature-entropy diagram, and pressure-enthalpy diagram for Aerozine-50 are shown in Figures 7.1 through 7.3. Tables of properties for all of the regions and boundaries of these diagrams are presented in Appendix D. The techniques employed for the purpose of obtaining the information necessary for constructing these curves and tables of properties are summarized in Table 7.1. The following paragraphs discuss the significant features of the curves and explain the format of the tables.

7.1 PHASE DIAGRAM

Figure 7.1 exhibits all of the features of a general P-T diagram for a binary system as discussed in Section 3.0.The values of P and T and the compositions of the phases at various points of intersection of the phase boundaries are given in Table 7.2. The determination of the points QP and PTPI was discussed in Section 3.0. Point PTP2 was located by determining, graphically, the point of intersection of the S_h-V, L-V boundary with the dew point curve.

A somewhat unique characteristic of the Aerozine-50 diagram is the shape of the boundary between the L-V and S_h-V regions. This curve exhibits a pressure maximum (.561 psia) located between the two pseudo-triple points. Consequently, if liquid Aerozine-50 at a pressure of 0.53 psia, for example, were heated isobarically, an equilibrium vapor phase would appear at a temperature of about 26°F. At a slightly higher temperature, about 28°F, the liquid phase would disappear, and solid hydrazine would form. Continuing the heating process, the solid phase would disappear, and the liquid phase would reappear at a temperature of approximately 33°F. After a temperature of about 86°F had been reached, the Aerozine-50 would be entirely vaporized.

The dashed curve in Figure 7.1 was constructed from vapor pressure data for Aerozine-50 propellant reported in the literature[12,14]. As the figure shows, the literature data are from 0.2 to two psia higher than the data obtained during this work. A likely reason for this discrepancy is

TABLE 7.1. Summary of Techniques for Obtaining Data and Calculating Values of Enthalpy and Entropy

Region	Variable	How Determined
Vapor	P, V, T	Measured and correlated by Redlich-Kwong equation of state (3.1).
	H	Calculated by means of equation (3.5).
	S	Calculated by means of equation (3.6).
Liquid-Vapor	P	Measured.
	x	Measured.
	y	Calculated from Gibbs-Duhem equation, together with data for P and x. (See Appendix A).
	γ	Calculated by equation (3.15). Correlated as function of liquid phase composition by equations (6.22) and (6.23). For correlation with temperature, the constants in these equations were represented by equations (6.18) and (6.19).
	Bubble point	Measured.
	Dew point	Calculated using the correlations for activity coefficients, equations (3 20) and (3.21) and the fact that $y_h = 0.652$.
	H	Calculated by equations (3.9) and (3.11) for the liquid and equation (3.5) for the vapor.
	S	Calculated by equations (3.10) and (3.12) for the liquid and equation (3.6) for the vapor.

TABLE 7.1 - (Continued)

Region	Variable	How Determined
Liquid	γ	Calculated by equations (6.22) and (6.23).
	H	Calculated by equations (3.9) and (3.11).
	S	Calculated by equations (3.10) and (3.12).
Solid-Vapor	Dew point curve	Calculated by equation (3.24).
	P vs y,T	Calculated by equation (3.23).
	Solid-liquid, Solid-vapor boundary	Calculated by equation (3.25) together with published freezing-composition data.
	Liquid-vapor, Solid-vapor boundary	Calculated by equation (3.25) together with published freezing-composition data.
	Solid, Solid-vapor boundary	Pressure estimated to be sum of vapor pressures of solid hydrazine and solid UDMH.
	H	Calculated by equation (3.29) for the solid and (3.7) for the vapor.
	S	Calculated by equation (3.30) for the solid and (3.8) for the vapor.

TABLE 7.1 - (Continued)

Region	Variable	How Determined
Solid-liquid	x	Literature Data, Reference 13.
	H	Calculated by equations (3.9) and (3.10) for the liquid and equation (3.27) for the solid.
	S	Calculated by equations (3.11) and (3.12) for the liquid and equation (3.28) for the solid.
Solid	Composition of S_{II}	Published data, Reference 13.
	H	Calculated by equation (3.29).
	S	Calculated by equation (3.30).

TABLE 7.2. Quadruple and Pseudo-triple Points for Aerozine-50 Phase Diagram

Point	Pressure (psia)	Temperature (°F)	Phases present and Composition
PTP1	.492	23.6	L, x = 0.500 V, y = 0.961 S_h
PTP2	.093	34.38	L, x = .0078 V, y = .5000 S_h
QP	.0116	74.49	L, x = .967 V, y = .994 S_e, x = .967 S_h

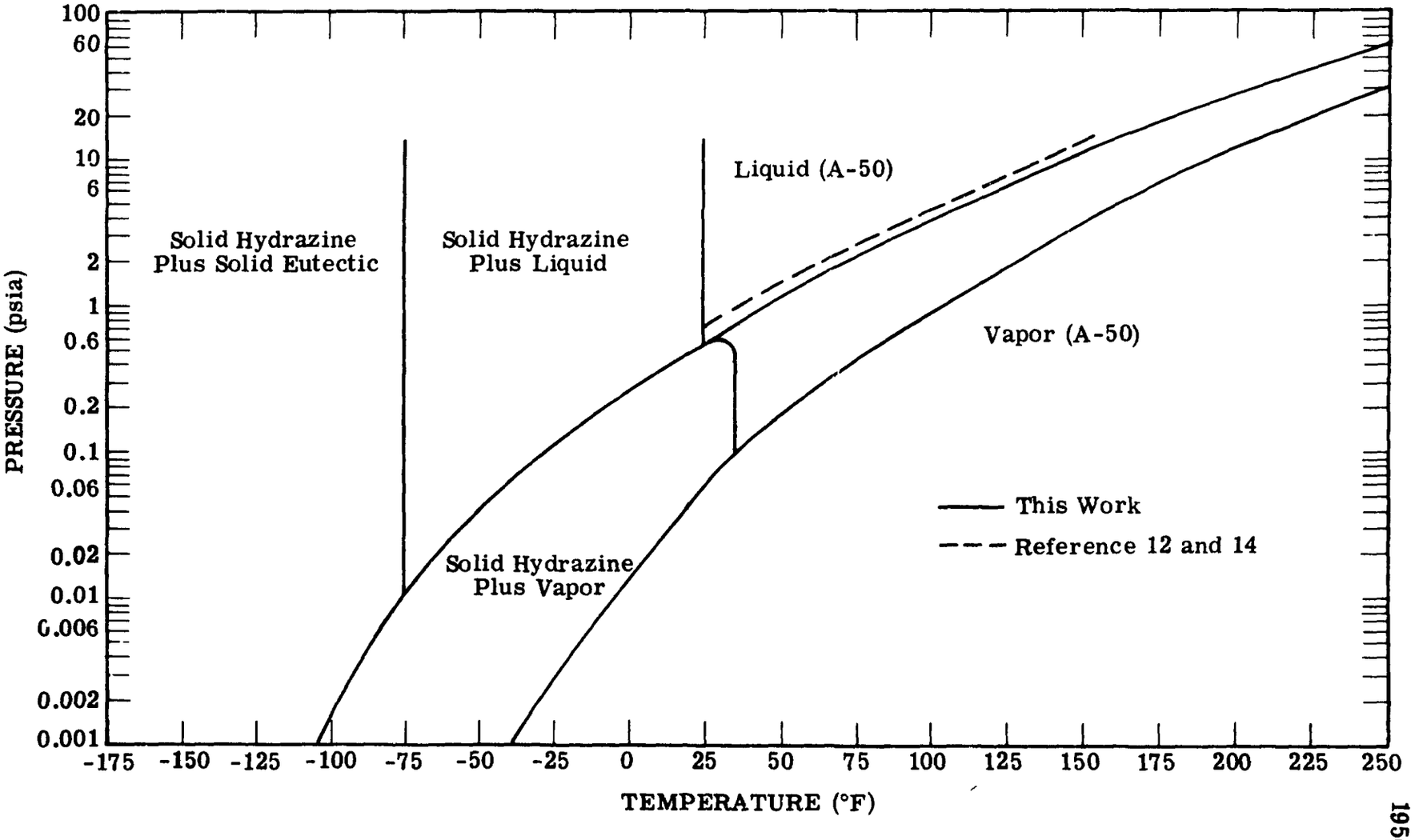

Figure 7.1. Phase Diagram for Aerozine-50.

dissolved nitrogen in the propellant. Assuming that the test samples for the measurements with the propellant were obtained from standard shipping containers in which the liquid is covered with a dry nitrogen blanket, it is likely that these samples were saturated with the gas at a pressure of approximately one atmosphere. The high values of vapor pressure would result if the samples were not thoroughly degassed before the measurements were made. For example, at 68°F rough calculations using some recent data[26] for the solubility of nitrogen in hydrazine and UDMH show that the difference in pressure between the literature and present curves would result if 14% of the nitrogen contained in the initially saturated sample were released into the vapor space (50% ullage) during the measurements.

7.2 THERMODYNAMIC CHARTS

As for the phase diagram, the thermodynamic charts, Figures 7.2 and 7.3, have 4 two-phase and two single-phase regions. On the T-S diagram, the liquid-vapor region is bounded on the sides and above by curves for the dew-and bubble-points (which bend towards each other at high temperatures and join at the critical point) and on the bottom by the curve connecting the two pseudo-triple points. On the P-H diagram, the vapor region is above and the liquid region is below the envelope, and the critical points are to the right.

The boundary between the liquid and solid-liquid region proceeds isothermally to the left on the T-S diagram and isobarically to the right on the P-H diagram. This results from the fact that within the pressure range of these diagrams, the properties of the condensed phases are independent of pressure; and, therefore, the boundaries are isotherms as shown in Figure 7.1.

The boundary between the solid and solid-liquid regions represents the coexistence of three phases (solid hydrazine, S_h, solid entectic, S_e, and liquid, L) while the point QP represents four equilibrium phases(S_h, S_e, L and vapor, V). On the T-S diagram, the boundary appears as an isothermal line, while on the P-H diagram, the boundary appears as an isothermal region.

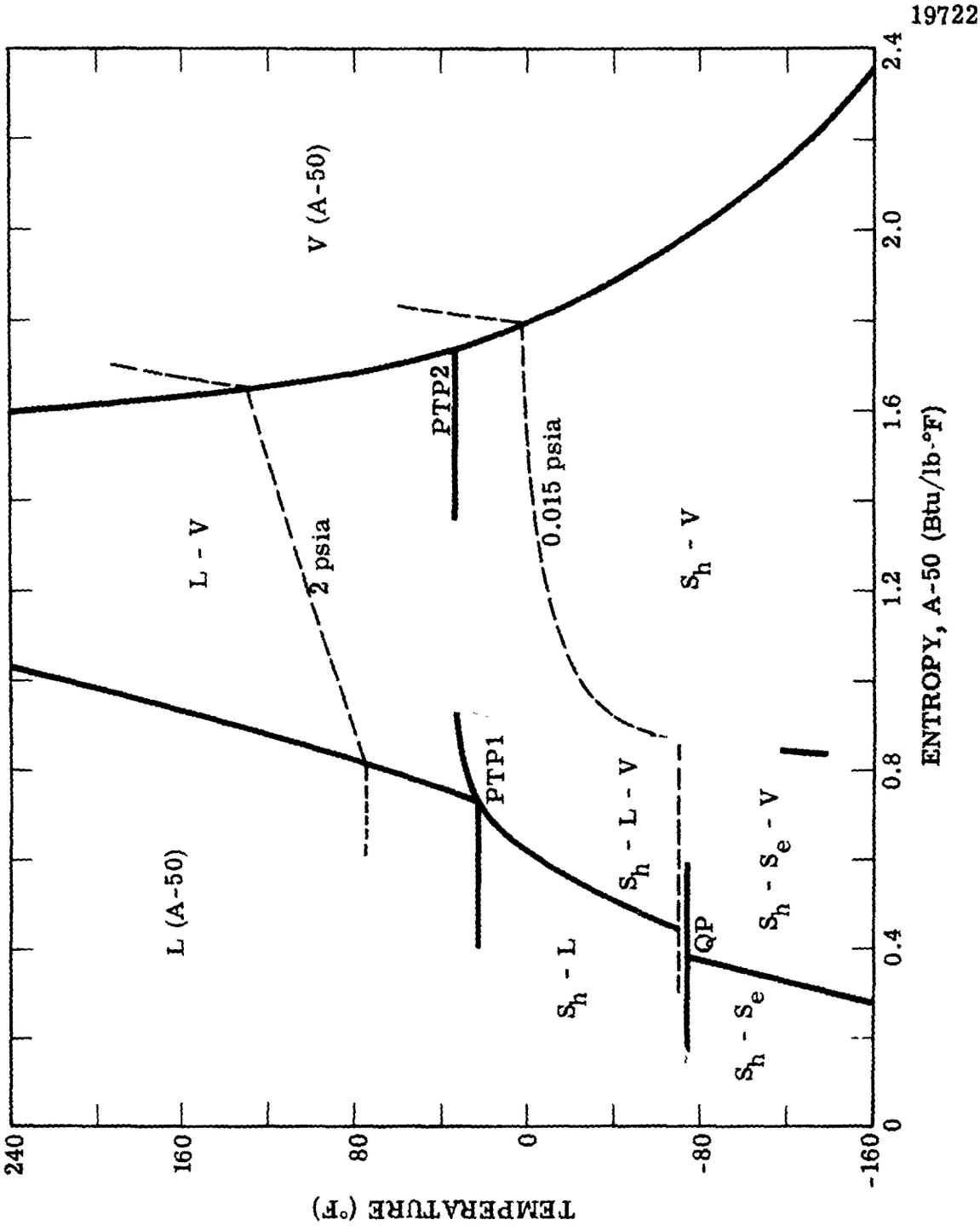

Figure 7.2. Temperature - Entropy Diagram for Aerozine -50.

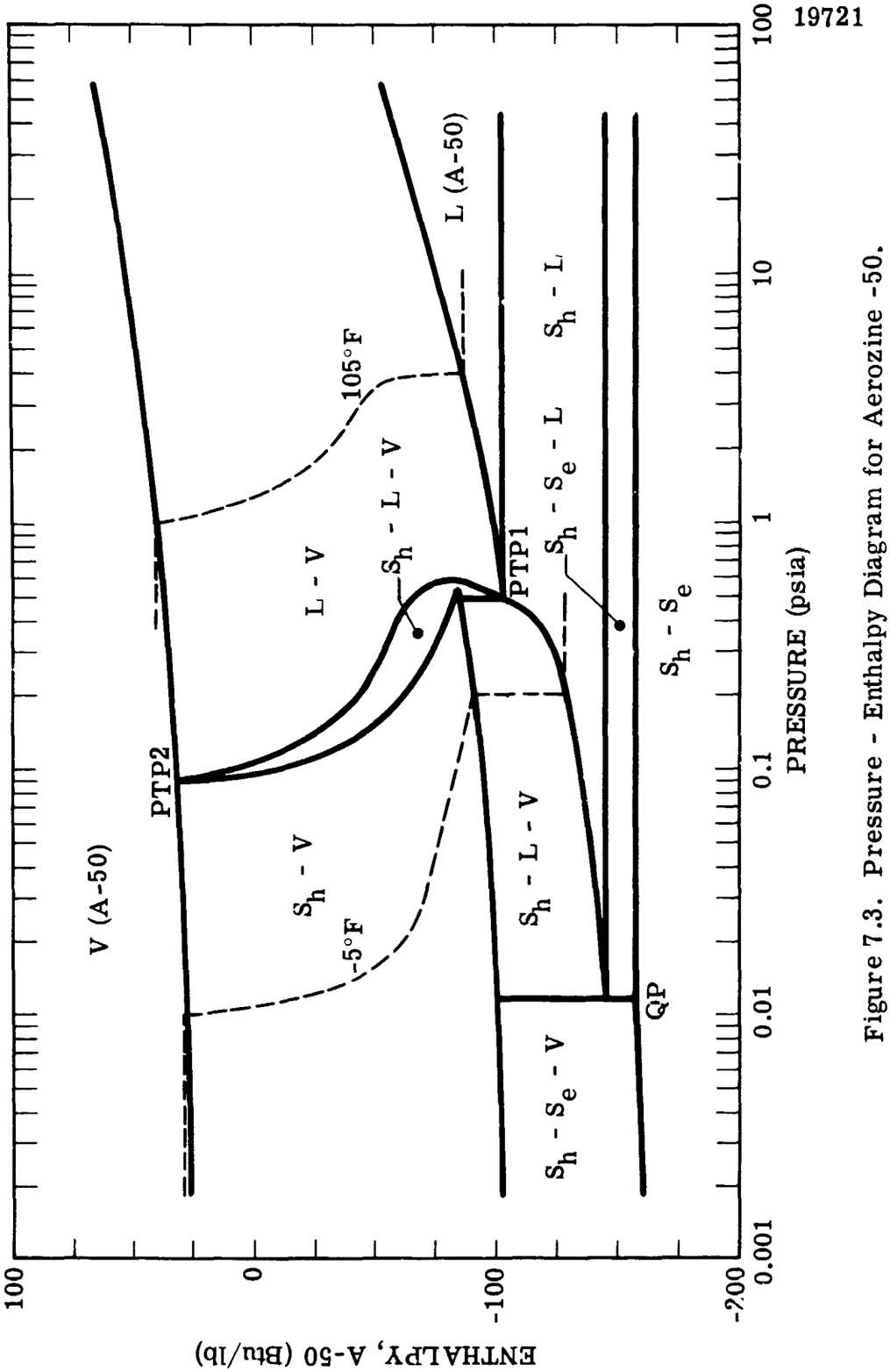

Figure 7.3. Pressure - Enthalpy Diagram for Aerozine -50.

The discontinuity at QP results from the appearance of the solid eutectic and represents its entropy or enthalpy of fusion.

The boundaries which separate the S_h-V region from the L-V, S_e-S_h, and S_h-L regions on the P-T diagram each appear as three-phase regions on the thermodynamic charts. This results from the enthalpy or entropy changes of phase transition which occur at these boundaries. For example, the region labeled S_h-S_e-V which separates the S_h-V and S_h-S_e regions on the T-S and P-H diagrams represents the enthalpy or entropy of sublimation of UDMH.

7.3 TABLES OF PROPERTIES

Tables were constructed for all of the regions and boundaries of the phase diagram. For the condensed phase regions, values are listed at various temperatures along the S-V or L-V boundary only, since there is no pressure dependency within these regions. For the L-V and S_h-V regions, values are listed at various temperatures for the bordering condensed phase and vapor boundaries and for various values of pressure within the regions. For the vapor region, property values are listed for various temperatures along the dew point curve, and for temperatures in the superheat region.

The following units apply for all of the tables:

Pressure: psia
Temperature: degrees Fahrenheit
Volume: cubic feet/lb of phase(1)
Enthalpy: BTu/lb of phase(1)
Entropy: BTu/°F-lb of phase(1)
Composition: Weight fraction UDMH.

---

(1) For the L-V and S_h-V regions, additional tables were constructed in which the values of volume, enthalpy, and entropy were calculated for a total system mass of one pound and composition equal to 50 percent UDMH.

8.0 RECOMMENDATIONS

In order to obtain values of the thermodynamic properties for use in the analysis of high pressure and high temperature processes (such as occur in rocket engine combustion chambers), there is a need for extending the range of the data obtained in this program. Additional P-V-T data should be obtained for pressures above three atmospheres in order to test the reliability of the modified Redlich-Kwong equation at high pressures or, if necessary, in order to choose or derive a more suitable equation of state. More data for liquid-vapor equilibria should be obtained both within the range of temperatures employed in this work as well as at higher temperatures in order to more firmly establish the activity coefficient correlations. Also, for higher pressures, the variation of the density of the liquids with pressure must be determined.

Prior to performing experiments to obtain data at higher temperatures, there must be additional decomposition experiments. Homogeneous decomposition will be a more serious problem at high temperatures; and, consequently, a set of limits for the measurements should be established.

In addition to data for mixtures, the vapor pressure data for the pure components must be extended to high temperatures and pressures, also.

APPENDIX A

CALCULATIONS OF y FROM P-x DATA

The following form of the Gibbs-Duhem equation is valid for a binary system at variable temperature or pressure, whether the system is in equilibrium or not:

$$\frac{V}{RT}\,dP + \frac{(H^{id} - H)}{RH^2 dT}\,dT = x_1 d(\ln \hat{f}_1) + x_2 \ln \hat{f}_2) \qquad \text{(A-1)}$$

Equation (A-1) can be written for the vapor and liquid phases in equilibrium in which case the pressure, temperature, and fugacities in both phases are equal. Combining the two relationships yields:

$$\frac{V^V - V^L}{RT}\,dP - \frac{(H^V - H^L) - (y_1 - x_1)(H_1^{id} - H_2^{id})}{RT^2}$$

$$= (y_1 - x_1)\, d\left(\ln \frac{\hat{f}_1}{\hat{f}_2}\right) \qquad \text{(A-2)}$$

Equation (A-2) is combined with the definition of the activity coefficient in the vapor phase,

$$\gamma_i^V \equiv \frac{\hat{f}_i}{y_i f_i^V} \quad , \qquad \text{(A-3)}$$

(in which the standard state is the pure component at the pressure and temperature of the solution) together with the following relationships for f_i^V:

$$d(\ln f_i^V) = \frac{V_i}{RT}\,dP + \frac{H_i^{id} - H_i}{RT^2}\,dT$$

The result is :

$$\psi dP + \Omega dT = (y_1 - x_1) d \left(\ln \frac{\gamma_1^v}{\gamma_2^v} \right) + \frac{y_1 - x_1}{y_1(1-y_1)} dy_1 \qquad \text{(A-4)}$$

where

$$\Psi \equiv \frac{\Delta V^v + x_1 V_1^v + x_2 V_2^v - V^L}{RT}$$

$$\Omega \equiv \frac{-(\Delta H^v + x_1 H_1^v + x_2^v - H^L}{RT^2} \quad ,$$

and

$$\Delta V^v = V^v - y_1 V_1^v - y_2 V_2^v \quad .$$

Equation (A-4) is a general relationship for a binary system in which two phases exist in equilibrium.

The special case of constant temperature is of primary interest here. For dT = 0, equation (A-4) reduces to:

$$\psi dP = (y_1 - x_1) d \left(\ln \frac{\gamma_1^v}{\gamma_2^v} \right) + \frac{y_1 - x_1}{y_1(1-y_1)} dy_1 \qquad \text{(A-5)}$$

Equation (A-5) may be integrated if phase equilibrium data and P-V-T data or equations of state are available for the coexisting phases. The following paragraphs explain the combination of equation (A-5) with the modified Redlich-Kwong equation of state for the vapors, experimental P-x data, and correlations for the density of liquids.

In terms of fugacity coefficients, equation (A-3) becomes:

$$\gamma_i = \frac{\hat{\phi}_i}{\phi_i} ,$$

or, in logarithmic form,

$$\ln \gamma_i = \ln \hat{\phi}_1 - \ln \phi_i . \qquad \text{(A-6)}$$

Using this relationship the logarithm of the ratio of activity coefficients in equation (A-5) may be written:

$$\ln \frac{\gamma_1^V}{\gamma_2^V} = \ln \hat{\phi}_1 - \ln \hat{\phi}_2 - \ln \phi_1 + \ln \phi_2 \qquad \text{(A-7)}$$

The fugacity coefficients for the components in the vapor solution, $\hat{\phi}_i$, may be related to the fugacity coefficient for the vapor according to:

$$\ln \hat{\phi}_1 = \ln\phi + y_2 \left(\frac{\partial \ln\phi}{\partial y_1} - \frac{\partial \ln\phi}{\partial y_2} \right)$$

$$\ln \hat{\phi}_2 = \ln\phi + y_1 \left(\frac{\partial \ln\phi}{\partial y_2} - \frac{\partial \ln\phi}{\partial y_1} \right)$$

Combining these relationships with equation (A-7) yields:

$$\ln \frac{\gamma_1^V}{\gamma_2^V} = \left(\frac{\partial \ln\phi}{\partial y_1} \right)_{y_2,V} - \left(\frac{\partial \ln\phi}{\partial y_2} \right)_{y_1,V} - \ln\phi_1 + \ln\phi_2 \qquad \text{(A-8)}$$

The quantities $\ln\phi$, $\ln\phi_1$ and $\ln\phi_2$ are evaluated by means of the following

equation which is applicable for pure components or mixtures of constant composition:

$$\ln\phi = -\frac{1}{RT}\int_0^P\left(\frac{RT}{P} - V\right)dP$$

or rewritten,

$$\ln\phi = -\int_0^P\frac{dP}{P} + \frac{1}{RT}\int_0^P VdP \qquad \text{(A-9)}$$

The second integral can be evaluated by employing P-V-T data or, more conveniently, an equation of state. Wilson's modification of the Redlich-Kwong equation will be used here, i.e.:

$$P = \frac{RT}{V-b} - \frac{RTfb}{V(V+b)} \qquad \text{(A-10)}$$

where

$f = y_1f_1 + y_2f_2$, and

$b = y_1b_1 + y_2b_2$.

By differentiating equation (A-10) with respect to V, for constant y there results:

$$dP = RT\left[-\frac{1}{(V-b)^2} + \frac{2fb}{V(V+b)^2} + \frac{fb^2}{[V(V+b)]^2}\right]dV. \qquad \text{(A-11)}$$

Combining equations (A-9) and (A-11) and integrating gives

$$\ln\phi = \ln\left[1 - \frac{fb(V-b)}{V(V+b)}\right] + \frac{b}{V-b} - \frac{fb}{V+b} - f\ln\left(\frac{V+b}{V}\right) \qquad \text{(A-12)}$$

The partial derivatives in equation (A-8) are evaluated by differentiating equation (A-12). Combining the resulting expressions with equation (9) gives:

$$\ln \frac{\gamma_1^v}{\gamma_2^v} = - \frac{(f\Delta b + b\Delta f)V - 3fb\Delta b - b^2\Delta f}{V[V + (1+f)b] - fb^2} + \frac{\Delta b}{V-b} + \frac{b\Delta b}{(V-b)^2} -$$

$$\frac{2f\Delta b + b\Delta f}{V + b} + \frac{fb\Delta b}{(V + b)^2} - \Delta f \ln\left(\frac{V + b}{V}\right) + \ln \frac{\phi_2}{\phi_1} \qquad \text{(A-13)}$$

where $\Delta b \equiv b_1 - b_2$, and $\Delta f \equiv f_1 - f_2$.

Since the quantity, $\ln \frac{\gamma_1^v}{\gamma_2^v}$, is a function of both V and y, then

$$d\left(\ln \frac{\gamma_1}{\gamma_2}\right) = \left[\frac{\partial\left(\ln \frac{\gamma_1^v}{\gamma_2^v}\right)}{\partial y}\right]_V dy + \left[\frac{\partial\left(\ln \frac{\gamma_1^v}{\gamma_2^v}\right)}{\partial V}\right]_y dV \qquad \text{(A-14)}$$

Expressions for the partial derivatives are derived by differentiating equation (A-13). The results are:

$$\frac{\partial\left(\ln \frac{\gamma_1^v}{\gamma_2^v}\right)}{\partial y} \equiv d_{1y} = - \frac{Dd_{ny} - Nd_{Dy}}{D^2} + \frac{2\Delta b^2}{(V-b)^2} + \frac{2b\Delta b}{(V-b)^3}$$

$$- \frac{4\Delta f\Delta b}{(V+b)} - \frac{f\Delta b^2}{(V+b)^2} - \frac{2fb\Delta b^2}{(V+b)^3} \qquad \text{(A-15)}$$

$$\frac{\partial\left(\ln \frac{\gamma_1^v}{\gamma_2^v}\right)}{\partial V} \equiv d_{1V} = -\frac{Dd_{NV} - Nd_{DV}}{D^2} - \frac{\Delta b}{(V-b)^2} - \frac{2b\Delta b}{(V-b)^3}$$

$$+ \frac{b\Delta f}{V(V+b)} + \frac{2f\Delta b+b\Delta f}{(V+b)^2} - \frac{2fb\Delta b}{(V+b)^3} \qquad \text{(A-16)}$$

where $d_{Ny} = \Delta b\Delta f(2V-5b)-3f\Delta b^2$

$d_{Dy} = \Delta b[V(1+f)-2fb]+b\Delta f(V-b)$

$d_{NV} = f\Delta b+b\Delta f$

$d_{DV} = 2V+b(1+f)$

$D = V[V+(1+f)b]-fb^2$

$N = V(f\Delta b+b\Delta f) - b(3f\Delta b+b\Delta f)$

Equation (A-14), written in terms of the notation defined by equations (A-15) and (A-16), becomes:

$$d \ln\left(\frac{\gamma_1^v}{\gamma_2^v}\right) = d_{1y}\, dy + d_{1V} dV \qquad \text{(A-17)}$$

The differential, dP, in equation (A-5) is evaluated from the equation of state, equation (A-10). Since the total pressure is a function of volume and composition at constant temperature; then,

$$dP = \left(\frac{\partial P}{\partial y}\right)_V dy + \left(\frac{\partial P}{\partial V}\right)_y dV \qquad \text{(A-18)}$$

Differentiation of equation (A-10) gives for the first term in equation (A-18):

$$\left(\frac{\partial P}{\partial y}\right)_V \equiv d_{Py} = -RT\left[\frac{\Delta b}{(V-b)^2} + \frac{f\Delta b+b\Delta f}{V(V+b)} - \frac{fb\Delta b}{V(V+b)^2}\right] . \qquad \text{(A-19)}$$

For the second term,

$$\left(\frac{\partial P}{\partial V}\right)_y \equiv d_{PV} = RT\left[-\frac{1}{(V-b)^2} + \frac{2fb}{V(V+b)^2} + \frac{fb^2}{[V(V+b)]^2}\right] \qquad \text{(A-20)}$$

Equation (A-18), rewritten in terms of the notation defined by equations (A-19) and (A-20), becomes:

$$dp = d_{Py}\, dy + d_{PV}\, dV. \qquad \text{(A-21)}$$

Equations (A-17) and (A-21) are substituted into equation (A-5) to obtain

$$\frac{dy}{dV} = \frac{\psi d_{pV} - (y-x)d_{lV}}{\psi d_{Py} - (y-x)d_{ly} + \frac{y-x}{y(1-y)}} \qquad \text{(A-22)}$$

Equation (A-22) can be combined with experimental P-x and liquid phase density data and integrated numerically to obtain y by employing the Runge-Kutta method.

APPENDIX B

EXPRESSIONS FOR ACTIVITY COEFFICIENTS AS FUNCTIONS OF PRESSURE AND PHASE COMPOSITIONS

The activity coefficient, γ_i, defined for the standard state as the pure component at the pressure and temperature of the solution and in the same physical state is:

$$\gamma_i = \frac{\hat{f}_i}{x_i f_i} \quad , \tag{B-1}$$

where $\hat{f}_i$ is the fugacity of component i in the solution of mole fraction x_i, and f_i is the fugacity of pure i in the standard state.[22]

For the case of liquid-vapor equilibria:

$$\hat{f}_i^L = \hat{f}_i^V \quad ; \tag{B-2}$$

then,

$$\gamma_i^L \, x_i \, f_i^L = \gamma_i^V \, y_i \, f_i^V \, . \tag{B-3}$$

Multiplying equation (B-3) by P and rearranging gives:

$$\gamma_i^L = \frac{y_i}{x_i} \left(\frac{f_i^V/P}{f_i^L/P} \right) \gamma_i^V \quad , \tag{B-4}$$

Taking the logarithm yields:

$$\ln \gamma_i^L = \ln \left(\frac{y_i}{x_i} \right) + \ln \left(\frac{\phi_i^V}{\phi_i^L} \right) + \ln \gamma_i^V \, , \tag{B-5}$$

where $\phi_i = f_i/P$.

Writing equation (B-1) for the vapor and multiplying by P, there results:

$$\gamma_i^V = \frac{(\hat{f}_i^V / y_i)P}{f_i^V / P} \quad .$$

Taking the logarithm and substituting for the fugacity coefficients gives:

$$\ln \gamma_i^V = \ln \hat{\phi}_i^V - \ln \phi_i^V \qquad \text{(B-6)}$$

From the general properties of a partial molar quantity (see reference 22), it may be shown that:

$$\ln \hat{\phi}_i^V = \ln \phi + \frac{\partial \ln \phi^V}{\partial y_i} - \Sigma_i \left(y_i \frac{\partial \ln \phi^V}{\partial y_i} \right) . \qquad \text{(B-7)}$$

For a binary system, equations (B-5), (B-6) and (B-7) are combined to obtain for component (1):

$$\ln \gamma_1^L = \ln \frac{y_1}{x_1} - \ln \phi_1^L + \ln \phi^V + y_2 \left(\frac{\partial \ln \phi^V}{\partial y_1} - \frac{\partial \ln \phi^V}{\partial y_2} \right); \qquad \text{(B-8)}$$

and, for component (2)

$$\ln \gamma_2^L = \ln \frac{y_2}{x_2} - \ln \phi_2^L + \ln \phi^V - y_1 \left(\frac{\partial \ln \phi^V}{\partial y_1} \quad \frac{\partial \ln \phi^V}{\partial y_2} \right). \qquad \text{(B-9)}$$

The terms $\ln \phi_1^L$ and $\ln \phi_2^L$ involve the fugacities of the components in the standard state, i.e. liquid at the pressure and temperature of the solution. In terms of pure component vapor pressures and liquid volumes,

$$\ln \phi_i^L = \ln \phi_i' + \frac{1}{RT} \int_{P_i'}^{P} \left(V_i^L - \frac{RT}{P} \right) dP \ . \qquad \text{(B-10)}$$

The term involving the integral is the difference between the value of $\ln \phi_i^L$ evaluated at P and the value at P_i'. Assuming that the liquid volume is independent of pressure, equation (B-10) becomes for the two components:

$$\ln \phi_1^L = \ln \phi_1' + \frac{V_1^L}{RT} (P - P_1') - \ln \frac{P}{P_1'} \qquad \text{(B-11)}$$

$$\ln \phi_2^L = \ln \phi_2' + \frac{V_2^L}{RT} (P - P_2') - \ln \frac{P}{P_2'} \qquad \text{(B-12)}$$

Combining equation (B-11) with (B-8) and equation (B-12) with (B-9) gives:

$$\ln \gamma_i^L = \ln \frac{y_1 P}{x_1 P_1'} - \ln \phi_1' - \frac{V_1^2}{RT} (P - P_1') + \ln \phi^V$$

$$+ y_2 \left(\frac{\partial \ln \phi^V}{\partial y_1} - \frac{\partial \ln \phi^V}{\partial y_2} \right) \ ; \qquad \text{(B-13)}$$

and,

$$\ln \gamma_2^L = \ln \frac{y_2 P}{x_2 P_2'} - \ln \phi_2' - \frac{V_2^L}{RT} (P - P_2') + \ln \phi^V$$

$$- y_1 \left(\frac{\partial \ln \phi^V}{\partial y_1} - \frac{\partial \ln \phi^V}{\partial y_2} \right) \ . \qquad \text{(B-14)}$$

Values of $\ln \phi_1'$, $\ln \phi_2'$, and $\ln \phi^V$ are obtained from equation (A-12). The difference in partial derivatives is evaluated by rearranging equation (A-8), i.e.,

$$\left(\frac{\partial \ln \phi^V}{\partial y_1} - \frac{\partial \ln \phi^V}{\partial y_2}\right) = \ln \frac{\gamma_1^V}{\gamma_2^V} + \ln \phi_1^V - \ln \phi_2^V \qquad \text{(B-15)}$$

The quantity, $\ln \frac{\gamma_1^V}{\gamma_2^V}$, is given by equation (A-13).

Equations (B-13) and (B-14) may be used to calculate values of γ_1^L and γ_2^L from phase equilibria data. The process involves converting the P-x-y data to V-x-y form by means of the equation of state, evaluating the terms involving ϕ^V, ϕ_1', and ϕ_2', and then substituting directly into the above relationships.

As discussed in Sections 3.0 and 5.0, values of γ_1^L, and γ_2^L can be correlated with liquid composition. Then the two equations may be solved simultaneously to calculate y and P from x-T data (calculation of bubble point curve), or to calculate x and P from y-T (calculation of dew point curve), or to calculate x and y from P-T data (calculations within the L-V region of the phase diagram, Figure 3.1).

APPENDIX C

DERIVATION OF FXPRESSIONS FOR ENTHALPY AND ENTROPY OF VAPOR PHASE

Since the internal energy, U and the entropy, S, may be expressed in terms of V and T at constant composition; i.e.,

$$U = f_u(V,T),$$

and

$$S = f_s(V,T),$$

then
$$dU = \left(\frac{\partial U}{\partial T}\right)_V dT + \left(\frac{\partial U}{\partial V}\right)_T dV. \tag{C-1}$$

and

$$dS = \left(\frac{\partial S}{\partial T}\right)_V dT + \left(\frac{\partial S}{\partial V}\right)_T dV. \tag{C-2}$$

Further, from the first and second laws of thermodynamics,

$$dU = TdS - PdV. \tag{C-3}$$

From the definition of enthalpy,

$$dH = dU + PdV + VdP. \tag{C-4}$$

By definition,

$$C_V \equiv \left(\frac{\partial U}{\partial T}\right)_V . \tag{C-5}$$

Dividing equation (C-3) by dT at constant volume, there results:

$$\left(\frac{\partial U}{\partial T}\right)_V = T\left(\frac{\partial S}{\partial T}\right)_V . \tag{C-6}$$

Combining equations (C-5) and (C-6) gives:

$$\left(\frac{\partial S}{\partial T}\right)_V = \frac{C_V}{T} . \qquad (6\text{-}7)$$

Dividing equation (C-3) by dV at constant T gives:

$$\left(\frac{\partial U}{\partial V}\right)_T = T\left(\frac{\partial S}{\partial V}\right)_T - P. \qquad (C\text{-}8)$$

The following Maxwell relationship applies:

$$\left(\frac{\partial S}{\partial V}\right)_T = \left(\frac{\partial P}{\partial T}\right)_V . \qquad (C\text{-}9)$$

Combining equations (C-8) and (C-9) gives:

$$\left(\frac{\partial U}{\partial V}\right)_T = T\left(\frac{\partial P}{\partial T}\right)_V - P. \qquad (C\text{-}10).$$

Combining equations (C-1), (C-5), and (C-10) yields:

$$dU = C_V dT + \left[T\left(\frac{\partial P}{\partial T}\right)_V - P\right]_T dV. \qquad (C\text{-}11)$$

Equations (C-4) and (C-11) are combined to obtain:

$$dH = C_V dT + d(pV) + \left[T\left(\frac{\partial P}{\partial T}\right)_V - P\right]_T dV, \qquad (C\text{-}12)$$

Integrating equation (C-12) at constant temperature gives:

$$H_T - H_T^* = \int_{P^*}^{P} d(pV) + \int_{P^*}^{P} \left[T\left(\frac{\partial P}{\partial T}\right)_V - P\right] dV,$$

where p* is a low pressure approaching zero such that the vapor is ideal. Evaluating the first integrals gives:

$$H_T = H_T^{id} + PV - RT + \int_{\infty}^{V} \left[T\left(\frac{\partial P}{\partial T}\right)_V - P\right]_T dV \ . \qquad \text{(C-13)}$$

The quantity H_{Ti}^{id}, for a pure component, may be evaluated from C_{pi}^{id} data, since

$$dH_{Ti}^{id} = \int_{T_D}^{T} (C_p^{id}) dT,$$

where T_D is the datum plane temperature. A convenient choice for the datum plane is:

$$H_{Ti}^{id} \equiv 0 \text{ for } T_D = 0.$$

Then H_{Ti}^{id} is given by:

$$H_{Ti}^{id} = \int_{0}^{T} (C_p^{id}) dT.$$

For a mixture,

$$H_T^{id} = y_1 H_{T1}^{id} + y_2 H_{T2}^{id} \ .$$

The integral in equation (C-13) can be evaluated analytically by employing an equation of state; viz,

$$P = \frac{RT}{V-b} - \frac{RTfb}{V(V+b)} \ , \qquad \text{(C-14)}$$

where the variable f is a function of T.

Differentiation with respect to T at constant V gives:

$$\left(\frac{\partial P}{\partial T}\right)_V = \frac{R}{V-b} - \frac{Rb}{V(V+b)}\left(T\frac{df}{dT} + f\right). \qquad (C\text{-}15)$$

For a pure component,

$$f_i \equiv 4.934\ (1.57+1.62\omega_i)\ \frac{Tci}{T}\ ; \qquad (C\text{-}16)$$

Then

$$\frac{df_i}{dT} = -\ 4.934\ (1.57 + 1.62\omega_i)\ \frac{T_{ci}}{T^2}\ . \qquad (C\text{-}17)$$

Since , for a mixture,

$$f = \sum_i y_i f_i,$$

then,

$$\frac{df}{dT} = \sum_i \left(y_i \frac{df_i}{dt}\right). \qquad (C\text{-}18)$$

Let, by definition,

$$F \equiv T^2\ \frac{df}{dT}\ . \qquad (C\text{-}19)$$

Then the integral in equation (C-13) becomes:

$$\int_\infty^V \left[P - T\left(\frac{\partial P}{\partial T}\right)_V\right]_T dV = -RF\ln\left(\frac{V+b}{V}\right). \qquad (C\text{-}20)$$

Combining equations (C-14) and (C-20) with equation (C-13) gives

$$H_T = H_T^{id} - RT + \frac{RTV}{V-b} - \frac{RTfb}{V+b} - RF\ln\left(\frac{V+b}{V}\right)\ ; \qquad (C\text{-}21)$$

where, for a binary system,

$$F = -4.934 \left[y_1 \ (1.57+1.62\omega_1)T_{C1} + y_2(1.57 + 1.62\omega_2)T_{C2} \right].$$

Equations (C-7) and (C-9) are combined with equation (C-2) to obtain

$$dS = \frac{C_v}{T} dT + \left(\frac{\partial P}{\partial T}\right)_V dV \ . \qquad \text{(C-22)}$$

Writing equation (C-22) for constant temperature and both adding and subtracting the quantity $(\frac{R}{P}dP)$ to the right hand side gives:

$$dS = - \frac{R}{P}dP + \frac{R}{P}dP + \left(\frac{\partial P}{\partial T}\right)_V dV \ . \qquad \text{(C-23)}$$

Equation (C-23) can be integrated at constant T from a low pressure, P*, at which the vapor is ideal to the system pressure P to obtain:

$$S_T = S^*_T - \int_{P*}^{P} \frac{R}{P}dP + \int_{P*}^{P} \frac{R}{P}dP + \int_{P*}^{P} \left(\frac{\partial P}{\partial T}\right)_V dV \ ; \qquad \text{(C-24)}$$

The quantity, S^*_T, is the absolute entropy of the vapor in the ideal gas state at system temperature and at the low pressure P*. For a pure component, it is related to the ideal gas entropy at unit fugacity (1 atm), $S^o_o(T)$, according to:

$$S^*_T = S^o_o(T) - \int_1^{P*} (\frac{R}{P})dP. \qquad \text{(C-25)}$$

Combining equations (C-24) and (C-25) gives:

$$S_T = S^{id}_T + \int_0^P \frac{R}{P}dP + \int_0^P \left(\frac{\partial P}{\partial T}\right)_V dV, \qquad \text{(C-26)}$$

where S^{id}_T is the entropy of the ideal vapor at the temperature and pressure of the system and is given by:

$$S_T^{id} = S_o^o (T) - R \ln P \ . \qquad (C\text{-}27)$$

For a component in a mixture

$$S_{Ti}^{id} = S_o^o (T)_i - R \ln (y_i P) \ .$$

Then for the mixture,

$$S_T^{id} = y_1 S_{T1}^{id} + y_2 S_{T2}^{id} \ .$$

Equations (C-15) and (C-25) are combined and then integrated to obtain:

$$S_T = S_T^{id} + R \ln \left[1 - \frac{fb(V-b)}{V(V+b)}\right] + RG \ln \left(\frac{V+b}{V}\right) \ ; \qquad (C\text{-}28)$$

where, for a pure component,

$$G = 4.934 \ (0.57 + 1.62\omega_i) \ ,$$

and for a binary mixture

$$G = - 4.934 \ [0.57 + 1.62(y_1\omega_1 + y_2\omega_2)].$$

Ordinarily, it is desirable to compute values of H_T and S_T at selected values of P. Therefore, corresponding values of V are calculated by trial and error solution of equation (C-14), and then the thermodynamic properties may be calculated by use of equations (C-21)and (C-28).

REFERENCES

1. Audrieth, L.F. and B.A. Ogg, "The Chemistry of Hydrazine", John Wiley and Sons, Inc., New York, 1951.

2. Gift, R.D., J.A. Simmons, J.M. Spurlock, J.P. Copeland, and J.M. Miller, "Study of Propellant Valve Leakage in a Vacuum" Atlantic Research Corporation, Final Report for Contract No. NAS9-4494, October 28, 1966.

3. McHale, E.T., B.E. Knox, and H.B. Palmer, "Tenth Symposium on Combustion", p. 341, The Combustion Institute, 1965.

4. Spakowski, A.E., "The Thermal Stability of Unsymmetrical Dimethylhydrazine," NASA Memo 12-13-58E (1958).

5. Hericks, J.A., G.H. Damon, and M.G. Zabetakis, "Determining the Safety Characteristics of Unsymmetrical Dimethylhydrazine," Bureau of Mines Rpt No RI 5635 (1960).

6. Eberstein, I.J. and I. Glassman, "Tenth Symposium on Combustion", p. 465, The Combustion Institute, 1965.

7. Scott, D.W., G.E. Oliver, M.E. Gross, W.N. Hubbard, and H.M. Huggman, Jour. Amer. Chem. Soc. 71 2293 (1949).

8. Aston, J.G., J.L. Wood, and T.P. Zolki, Jour. Amer. Chem. Soc. 75 6202 (1953); 77 (1955).

9. Chang, E.T. and N.A. Gokcen, "Thermodynamic Properties of Hydrazine, Unsymmetrical Dimethylhydrazine, and Their Mixtures." Aerospace Corp. Rept. No. ATN-64 (9228)-2(1964).

10. Pannetier, G. and P. Mignotte, Bull. Soc. Chim. France 1963, 694.

11. Scatchard, G. and C.L. Raymond, Jour. Amer. Chem. Soc. 60 No. 6, 1278 (1938).

12. "Storable Liquid Propellants for Titan II, Revision C", Aerojet-General Corp. Rpt. No. LRP 148, (June, 1961).

13. McMillan, J.A., Jour. Chem. Eng. Data. 12, No. 1, 39 (1967).

14. Liberto, R. R., "Titan II Storable Propellant Handbook", Bell Aerosystems Co. Rpt. No. 8182-933004 (March, 1962).

15. Eberstein, I.J. and I. Glassman, Prog. in Astro. and Rocketry, 2, 351 (1960).

16. Eberstein, I.J. and I. Glassman, "Consideration of Hydrazine Decomposition", Tech. Rpt. on Contract AF 18(600)-1527, Princeton University, Princeton, N.J. (1959).

17. Kant, A. and W. J. McMahon, "Thermal Decomposition of Hydrazine", Tech. Rpt. No. WAL TR 804/20, Watertown Arsenal Laboratories (Oct. 1959).

18. Wilson, G.M., Adv. in Cryogenic Eng. 11 392 (1966).

19. Pitzer, K.S., D.Z. Lippman, R.F. Curl, C.M. Higgins, and D.E. Patterson, Jour. Amer. Chem. Soc. 77, 3433 (1955).

20. Liberto, R.R. "Storable Propellant Data for the Titan II Program", Bell Aerosystems Co. Rpt. No. 8182-93302 (Nov. 1961).

21. Haws, J.L. and D.G. Harden, J. Spacecraft 2, No. 6, 972 (1965).

22. Van Ness, H.C., "Classical Thermodynamics of Non-Electrolyte Solutions", The MacMillan Co., N.Y. (1964).

23. Hieber, W., and A. Woerner, Z. Electrochem. 40, 252 (1934).

24. Gift, R.D., J.M. Spurlock, J.A. Simmons, and J.M. Miller, "Lunar Excursion Module Propulsion Systems Valve Actuating Tests", Atlantic Research Corporation, Final Rpt. for Contract No. NAS9-5937, July 29 1966.

25. Lawrence, R.W., "Handbook of the Properties of Unsym.-dimethylhydrazine and Monomethylhydrazine", Aerojet Rpt. No. 1293, Volumes I and II (May, 1958).

26. Chang, E.T., N.A. Gokcen, and T.M. Poston J Phys. Chem. 72, No. 2, 638 (1968).

27. "International Critical Tables", 3, 228, McGraw-Hill Book Co., New York (1928).

28. Barger, J N., et al, "Applications of Alkylhydrazines to Rocket Power Plants", Aerojet-General Corp. Rpt. No. 1293, Wright Air Development Center (1958).